PROTEIN AGGREGATION IN PERIPHERAL MYELIN PROTEIN 22 (PMP22)-ASSOCIATED NEUROPATHIES

By

JENNY FORTUN

A DISSERTATION PRESENTED TO THE GRADUATE SCHOOL
OF THE UNIVERSITY OF FLORIDA IN PARTIAL FULFILLMENT
OF THE REQUIREMENTS FOR THE DEGREE OF
DOCTOR OF PHILOSOPHY

UNIVERSITY OF FLORIDA

2005

I dedicate this work to my family for their encouragement, support and love.

ACKNOWLEDGMENTS

I would like to give special thanks to my mentor, Dr. Lucia Notterpek, who has been crucial for the development of this work as well as shaping my scientific and personal life. I greatly appreciate the invaluable assistance and guidance of Dr. William Dunn. My gratitude goes to the rest of the members of my committee as well, Dr. Gerry Shaw, Dr. Harry Nick and Dr. Susan Frost, for their guidance and helpful comments. To my peers in Dr. Notterpek's laboratory for their help and making these years very enjoyable, goes also my appreciation. I am thankful to Ms. Debbie Akin and the Electron Microscopy Facility at UF for their help as well as the National Institute of Health and Muscular Dystrophy Association funding agencies. I would also like to mention all my friends that have supported me at all times. Last but not least, I would like to thank God for guiding me and being the light than illuminates my path.

TABLE OF CONTENTS

LIST OF TABLES

LIST OF FIGURES

Abstract of Dissertation Presented to the Graduate School
of the University of Florida in Partial Fulfillment of the
Requirements for the Degree of Doctor of Philosophy

PROTEIN AGGREGATION IN PERIPHERAL MYELIN PROTEIN 22-ASSOCIATED NEUROPATHIES

By

Jenny Fortun

May 2005

Chair: Lucia Notterpek
Major Department: Neuroscience

Peripheral myelin protein 22 (PMP22) is a hydrophobic, tetraspan protein of unknown function that is expressed mainly by myelinating Schwann cells (SC). Duplication, point mutations and deletion of PMP22 are associated with clinically related but different forms of demyelinating peripheral neuropathies of various degrees of severity. Since the neuropathies associated with the duplication and the point mutation paradigms are more severe than the one due to a lack of PMP22, a toxic gain of function of the mutated or excess of PMP22 has been proposed. However, the nature of this toxic gain of function remains elusive so far. To study this, we have used the Trembler J (TrJ) mouse model of peripheral neuropathy that carries a point mutation in PMP22. In sciatic nerves of the TrJ mouse, PMP22 has a reduced turnover rate when compared to the normal or the heterozygous deficient-protein. In TrJ nerves, PMP22 accumulates in cytoplasmic aggregates that recruit molecular chaperones as well as components of the ubiquitin-proteasomal and autophagic-lysosomal pathways. The presence of such

aggregates in TrJ nerves correlates with reduced activity of the proteasomal pathway and accumulation of ubiquitinated substrates, including PMP22. Utilizing a pharmacological approach in cultured SC, we have shown that under permissive conditions, the aggregates are removed by an autophagic-dependent mechanism. In support of the involvement of autophagy in the TrJ nerves, autophagosomes are present in the SC cytoplasm and the localization and levels of autophagic components are altered. Furthermore, the formation of new aggresomes is hindered by enhancement of autophagy and molecular chaperones, suggesting that different cellular pathways cooperate to prevent the accumulation of misfolded/non-functional proteins in the cell. Based on these results, we propose that the formation of aggregates is a protective response of the SC by which the misfolded/unfunctional PMP22 is concentrated in a central location to be delivered by autophagy to lysosomes for degradation. However, with additional insults and aging, these degradation pathways become less efficient and aggregates could accumulate, which could contribute to SC dysfunction through sequestering essential SC components and affecting proteasome functioning.

CHAPTER 1
INTRODUCTION

Peripheral Myelin Protein 22

Peripheral myelin protein 22 (PMP22) is a 22 kDa, highly hydrophobic, integral membrane glycoprotein, expressed mainly by myelinating Schwann cells (SCs) (Snipes et al., 1992). In addition to SCs, its transcript has been found during embryogenesis and in the adult both in neuronal and nonneuronal tissues (Baechner et al., 1995; Parmantier et al., 1995; 1997; Notterpek et al., 2001; Roux et al., 2004). The exact function of PMP22 has not been elucidated. In the peripheral nervous system, PMP22 is largely confined to the compact portion of myelin (Snipes et al., 1992; Haney et al., 1996), where it is believed to have a role in myelin formation and maintenance (Adlkofer et al., 1995 and 1997; Huxley et al., 1996; D'Urso et al., 1999; Perea et al., 2001). Independent *in vitro* studies have suggested additional involvements of the protein in the regulation of cellular growth (Zoidl et al., 1995; 1997), apoptosis (Fabbretti et al., 1995; Brancolini et al., 2000), differentiation and migration of SCs (Niemann et al., 2000; Nobbio et al., 2004) as well as cellular adhesion (Suter and Snipes, 1995; Hasse et al., 2004).

Peripheral Myelin Protein 22-Associated Neuropathies

Different mutations in PMP22, including duplication, deletion and point mutations, have been identified in patients diagnosed with hereditary peripheral neuropathies. PMP22-associated neuropathies comprise a large and heterogeneous group of diseases mainly characterized by progressive demyelination and reduced nerve conduction velocities (NCV) (Young and Suter, 2001). The most common form of such neuropathies

is Charcot-Marie-Tooth disease (CMT) type1A (CMT1A), which is mainly associated with a 1.5-megabase duplication in the human chromosome 17, including the PMP22 locus (Lupski et al., 1991; Valentijn et al., 1992a; Matsunami et al., 1992; Timmerman et al., 1992). The main hallmark of CMT1A is demyelination and, consequently, a marked reduction in NCV together with slowly progressive distal muscular atrophy and weakness (Garcia, 1999). On the other hand, deletion of the same fragment or truncation of the protein results in a milder variant known as Hereditary Neuropathy with liability to Pressure Palsies (HNPP) (Chance et al., 1993). Patients diagnosed with HNPP exhibit a clinically heterogeneous recurrent focal neuropathy following minor nerve trauma that is characterized mainly by segmental demyelination and focal myelin thickening (tomacula) (Chance, 1999; Pareyson et al., 1996). Compared to CMT1A, the reduction in NCV in HNPP is lesser, and in general, the symptoms presented are not as severe (Gabreëls-Festen and Wetering, 1999).

Based on the observation that both deletion and duplication of PMP22 are associated with demyelinating peripheral neuropathies, it was proposed that these disorders were caused by a gene-dosage effect (Gabriel et al., 1997). Furthermore, mutations in other myelin proteins such as myelin protein zero (P0) and connexin 32 (Cx32) are associated with other types of related CMT, namely CMT1B and CMTX, respectively (Maier et al., 2002). These three proteins, PMP22, Cx32 and P0, are essential constituents of peripheral myelin. Therefore, it seems that the correct stoichiometry of these proteins in myelin is important for its formation and maintenance (Naef and Suter, 1998).

In addition to deletion and duplication, a variety of single point mutations in the PMP22 gene have been identified in a small percentage of CMT1A cases and in another type of related neuropathy, known as Dejerine-Sottas Syndrome (DSS) (Dejerine and Sotas, 1893). DSS is chronic motor and sensory neuropathy with early-onset, marked reduction in NCV and more severe clinical pathology than CMT1A. Overall, the phenotypes resulting from most point mutations are more critical than the duplication or the deletion paradigms (Gabreëls-Festen et al., 1995; 2002; Tyson et al., 1997; Boerkoel et al., 2002). Furthermore, the same mutations have been independently diagnosed as CMT1A and DSS, suggesting an overlap between these two types of neuropathies and the idea that additional factors may contribute to disease severity (Valentijn et al., 1992b; Navon et al., 1996; Ionasescu et al., 1997; Gabreëls-Festen, 2002). In this regard, independent studies using mouse models of the disease have suggested that secondary to the SC damage, the phenotype severity is influenced by impaired SC-neuronal interaction, aberrant expression and reorganization of axonal ion channels as well as pronounced damage to axonal cytoskeleton and transport (Sancho et al, 1999; Maier et al., 2002; Devaux and Scherer, 2005).

Mouse Models of PMP22-Associated Peripheral Neuropathies

Animal models have provided useful tools in understanding the molecular and cellular alterations of PMP22-associated neuropathies, since they display similar behavioral and histological abnormalities as human patients (Notterpek and Tolwani, 1999). Genetically engineered PMP22 overexpressor rats (Sereda et al., 1996; Niemann et al., 1999) and mice (Huxley et al., 1996; Robertson et al., 2002; Perea et al., 2001), as well as PMP22-deficient mice (Adkofer et al., 1995; Maycox et al., 1997), have been developed to study the effects of PMP22 dosage in CMT1A and HNPP, respectively.

These models have confirmed the importance of adequate levels of PMP22 for myelin formation and stability (Niemann *et al.,* 1999; Huxley *et al.,* 1996; 1998; Perea et al., 2001). In a conditional mouse model of PMP22 overexpression, the phenotype was corrected when the expression of the exogenous *pmp22* was abolished (Perea et al., 2001). Although this effect was dependent on subsequent regulation of the protein, it opened the possibility for therapeutic approaches to reverse CMT1A associated with the duplication of PMP22. Indeed, independent treatments with progesterone antagonists or ascorbic acid ameliorate the neuropathy associated with PMP22 overexpression in CMT1A models by a mechanism likely involving a reduction in the protein levels (Sereda et al., 2003; Passage et al., 2004). Yet, the implications of these results for neuropathies associated with point mutations are not clear.

Models to study the effects of point mutations in PMP22 include the naturally occurring Trembler (Tr) and Trembler J (TrJ) mice (Notterpek and Tolwani, 1999). In the Tr mouse, Glycine-150 is substituted by Aspartic acid (G150D), resulting in the introduction of a new negatively charged amino acid in the fourth transmembrane domain of PMP22 (Suter et al., 1992a). Likewise, the TrJ mouse carries a point mutation that substitutes Leucine for Proline at position 16 (L16P) , an α-helix breaking amino acid, in the middle of the first transmembrane segment of PMP22 (Suter et al., 1992b). These mutations give rise to similar, but not identical neuropathies that have been used to model CMT1A, as well as DSS (Suter et al., 1992b; Notterpek and Tolwani, 1999; Meekins et al., 2004). Notably, the same mutations have been identified in patients diagnosed with CMT1A or DSS, confirming the validity of such mouse models (Valentijn et al., 1992; Navon et al., 1996; Ionasescu et al., 1997; Gabreëls-Festen, 2002).

It is uncertain how different genetic alterations (duplication, point mutation or deletion) result in similar demyelinating neuropathies, or how similar these neuropathies really are (Snipes et al., 1999). Since animal models of PMP22 overexpression and point mutations share common pathological features, it has been hypothesized that these phenotypes result from a common pathway being used to cope with different types of PMP22 alterations (Robertson et al., 2002). Although the detailed mechanisms underlying these phenotypes are not known, they apparently involve a toxic gain of function of the point mutated or duplicated PMP22. Indeed, the disease is more severe in the duplication and point mutation than the deletion paradigms (Adlkofer et al., 1997; Gabreëls-Festen et al., 1997; Tyson et al., 1997; Boerkoel et al., 2002). The nature of the toxic gain of function has not been elucidated; however, impaired intracellular trafficking and failure of PMP22 to incorporate into myelin have been proposed.

Quality Control Mechanism for PMP22

Based on studies of the wild type PMP22 (Wt-PMP22), two checkpoints in the synthesis and processing of the protein have been outlined: the endoplasmic reticulum (ER) and the Golgi apparatus or post-Golgi compartments (Snipes et al., 1999). The newly synthesized Wt-PMP22 is first subjected to a quality control in the ER, where approximately 80% is targeted for degradation before reaching medial-Golgi (Pareek et al., 1997). The short half-life of PMP22 may result from the inability of such a highly hydrophobic protein to fold correctly in the ER membrane, although it cannot be excluded that an intracellular function of PMP22 requires this rapid turnover (Naef and Suter, 1998). Additionally, proteins forming part of oligomeric complexes are degraded very quickly in the absence of cofactors or subunits (Goldberg, 2003), but whether this is the case for PMP22 has not been determined. Only a small fraction of the newly

synthesized PMP22 traffics through the Golgi and acquires its correct N-glycosylation pattern. Once in the Golgi, upon an unidentified signal derived from Schwann cell-axonal contact, the protein translocates to the plasma membrane and incorporates into myelin (Pareek et al., 1997).

Despite the knowledge concerning the trafficking of Wt-PMP22, several features about the mutant protein and its relationship with diseases remain unsolved. Different in vitro studies have suggested that a variety of point-mutated PMP22s, including the Tr and TrJ, are retained within the cell and are not incorporated into plasma membrane (D'Urso et al., 1998; Tobler et al., 1999; Naef and Suter, 1999; Colby et al., 2000; Sanders et al., 2001). Thus, impaired intracellular trafficking has been proposed as a common disease mechanism to explain peripheral neuropathies associated with PMP22 mutations. The retention in the ER could be explained by extended association with ER chaperones. Indeed, the TrJ mutant interacts with calnexin for a longer time than the normal protein (Dickson et al., 2002) in a glycan-independent manner and this correlates with a reduced diffusion rate within the ER membrane (Fontanini et al., 2005).

The point mutated PMP22s hetero-oligomerize with the Wt protein, which could potentially interfere with the trafficking of the normal PMP22 to myelin, contributing to a loss of its normal function (Tobler et al., 1999; 2002). Thus, the absence of the normal protein in myelin is common for the three types of PMP22-associated neuropathies: deletion, duplication and point mutations. Nonetheless, reduced levels of normal PMP22 in myelin are not enough to explain the increase in phenotype severity observed in neuropathies associated with PMP22 point mutations or duplication, compared to the milder disease resulting from the absence of the protein. This issue was addressed in a

cross-breeding study between the Tr and PMP22-deficient mice, models of CMT1A and HNPP, respectively (Adlkofer et al., 1997). The authors demonstrated that myelin deficiencies were more pronounced when the Tr allele was present in a null (Tr/-) or the Tr (Tr/Tr) background, as compared to the absence of PMP22, both in the null homozygous (-/-) and heterozygous (-/+), or the presence of the normal allele (+/Tr). Thus, it has been proposed that the pathogenesis of these types of neuropathies result from a combination of a dominant negative effect on the trafficking of the normal PMP22 to myelin (loss of function), and a toxic gain of function of the mutated copy that accumulates along the secretory pathway (Boerkoel et al., 2002).

Generally, prolonged retention of misfolded proteins in the ER leads to their degradation by the 26S proteasome. The 26S proteasome is composed of an assembly of proteases in a multicatalytic complex (the 20S), bound to one or two regulatory subunits (19S or 11S) (Groll and Clausen, 2003). This pathway implies that the proteins are exported out of the ER and then are presented to the proteasome, where they are degraded to small peptides inside the catalytic chamber (Goldberg, 2003). Indeed, the proteasome is the main degradation pathway for the newly synthesized PMP22, both the Wt and the Tr or TrJ mutants (Ryan et al., 2002). Furthermore, the half-lives of the Tr and TrJ mutants are increased, as compared to the rapidly turned-over Wt-PMP22 (Ryan et al., 2002). The mutated PMP22s accumulated before reaching medial Golgi; thus, the reduced turnover rate is most likely due to diminished proteasomal degradation rather than escaping quality control mechanisms and targeting to plasma membrane.

Protein Aggregates

Cells in culture respond to pharmacological inhibition of the proteasome by accumulating misfolded proteasomal substrates in aggregates, which are then transported

along the microtubules towards the centrosome to form an inclusion, termed the aggresome (Kopito, 2000). The main characteristics of aggresomes are as follows; assembly at the centrosome in a microtubule-dependent fashion, membrane free, vimentin encaged, excluded from ER and Golgi (Johnson et al., 1998). These inclusions are proposed to form when the cell's capacity to degrade misfolded protein is exceeded, and have been associated with the pathogenesis of different diseases, although their causal relationship remains debated (Kopito, 2000; Goldberg, 2003). In nonmyelinating SC, PMP22 accumulates in aggresomes after treatment for 16h with a proteasome inhibitor agent (Notterpek et al., 1999). Similar to the Wt-, the Tr- and TrJ- PMP22s also form aggresomes in response to proteasome inhibition in vitro (Ryan et al., 2002).

The formation of aggresomes is not unique to the inhibition of the proteasome by a pharmacological agent. In this regard, when the normal PMP22 is overexpressed in nonmyelinating SC, the protein forms spontaneous aggresomes (Notterpek et al., 1999). Moreover, abnormal cytoplasmic accumulation of PMP22 has been detected in human patients diagnosed with CMT1A due to gene duplication (Nishimura et al., 1996). The expression of the L16P mutation also results in cytoplasmic mislocalization of PMP22, both in SC of the TrJ mice (Ryan et al., 2002), as well as CMT1A patients (Hanemann et al., 2000). Moreover, disease-associated dominant mutants, including the Tr and TrJ, when overexpressed in vitro, have a higher propensity to spontaneously form high molecular weight oligomers, when compared to Wt- or polymorphisms in PMP22 (Tobler et al., 2002; Ryan et al., 2002; Liu et al., 2004).

The spontaneous presence of such aggregates suggests that the proteasome pathway might be compromised, either due to the overexpression of the normal protein or the

presence of the mutated PMP22s. The possibility of proteasomal overwhelming is feasible. According to estimates in Hela cells, there are about $3x10^6$ proteins synthesized per minute and from this pool, about 33% are defective ribosomal particles and 50% are short lived proteins that are degraded by the proteasome within 24h after synthesis (Yewdell, 2001). However, the exact amount of abnormal misfolded proteins targeted for degradation is controversial and difficult to measure (Goldberg, 2003). During myelination, the synthesis of myelin proteins, such as PMP22, is increased about 200-fold (Snipes et al., 1992; Bosse et al., 1994; Suter et al., 1994). The presence of mutations in PMP22 that compromise the folding of the protein and/or the trafficking to Golgi, will target more PMP22 for proteasomal degradation. Based on all the above, the $\sim 5x10^5$ proteasomes estimated to exist in an average cell (Yewdell, 2001) would need to work very efficiently to cope with the excess of protein being targeted for degradation or otherwise such proteins will accumulate.

The regulatory subunits of the proteasome recognize, unfold and thread the substrates into the catalytic chamber (Groll and Clausen, 2003). The rate-limiting step in proteasomal degradation is likely the unfolding of proteins or threading the extended polypeptides into the catalytic barrel of the proteasome, failure of which will result in overall proteolysis inhibition (Yewdell, 2001; Navon and Goldberg, 2001). Impairment of proteasomal function in the absence of pharmacological inhibitors has been associated with the presence of protein aggregates in different neurodegenerative conditions, such as Alzheimer's, Parkinson's and polyglutamine diseases (Keller et al., 2000; Waelter et al., 2001; McNaught et al., 2003; Kabashi et al., 2004). Furthermore, the proteasome is directly inhibited by the presence of aggregates (Bence et al., 2001), residues inside the

20S chamber that cannot be degraded, such as polyglutamine repeats (Ventrakaman et al., 2004), or endogenous inhibitors of the proteasomes, such as the enzyme O-GlcNAc transferase (Zhang et al., 2003).

Putative Effects of Aggresome Formation on Schwann Cells

The intracellular aggregation of PMP22 could affect the biology of the Schwann cell by several mechanisms. For example, aggregates formed under a variety of conditions recruit essential proteins, such as components of the ubiquitin-proteasomal system (Sherman and Goldberg, 2001). The implications of components of the ubiquitin-proteasomal pathway being recruited to aggregates might be a double-edge sword. On one hand, it might represent an initial attempt to eliminate such aggregates (Martin-Aparicio et al., 2001; Puttaparthi et al., 2003). Yet, the proteasome within the aggregates might be trapped in nonfunctional complexes, depleting the capacity of the cell for protein turnover (Sherman and Goldberg, 2001). The main signal for proteasome degradation is ubiquitination. A study with polyglutamine aggregates indicated that proteins containing ubiquitin-binding motifs are sequestered within the aggregates through specific interaction with ubiquitin (Donaldson et al., 2003). This might represent a common mechanism contributing to the pathogenesis of disease associated with aggregates, given that most of them contain ubiquitinated substrates (Donaldson et al., 2003; Goldberg, 2003). Similarly, aggregates could also recruit myelin proteins, affecting the stoichiometry of these molecules in peripheral myelin. Because of this, myelin stability could be compromised, favoring the demyelinating phenotype. Overall, the co-aggregation of essential SC components within the aggregates could lead to cell dysfunction by depleting the pool of such proteins from their normal location and role.

Alternatively, the formation of aggresomes could represent a protective response from the cell by which the misfolded proteins are concentrated in a central location to increase the efficiency of degradation (Kopito, 2000). In this regard, chaperones and lysosomes associate with PMP22 aggresomes in vitro (Notterpek et al., 1999; Ryan et al., 2002) and may play a role in their removal. Molecular chaperones might prevent toxicity by at least three ways: blocking inappropriate protein interactions, facilitating disease protein degradation or sequestration, and blocking downstream signaling events that lead to cellular dysfunction and death (Muchowski and Wacker, 2005). Lysosomes could be involved in the degradation of the aggregated proteins, most likely through the activity of the autophagic-lysosomal pathway (Kopito, 2000). Autophagy is a constitutive event by which a cytosolic cargo is engulfed in at least double membrane structures called autophagosomes. After maturation, autophagosomes fuse with the lysosomes to assure degradation of the cargo by the lysosomal enzymes (Klionsky and Emr, 2000).

Recent studies have provided some insight into the mechanisms underlying PMP22-associated neuropathies. However, there are still many questions that remain to be answered. A better comprehension of the subcellular events in the response of SCs to the L16P point mutation will be useful in the identification of targets for pharmacological therapies. The results presented here demonstrate that, first, PMP22 aggregates are present in a TrJ mouse model of CMT1A, which correlate with reduced proteasomal activity and the recruitment of essential SC components to the aggregates. Second, such aggregates are not stable structures and, given the right conditions, can be cleared from the SCs. Furthermore, at least in vitro, the accumulation of PMP22 in aggregates is hindered by enhancement of autophagy and the expression of molecular chaperones.

CHAPTER 2
EMERGING ROLE FOR AUTOPHAGY IN THE REMOVAL OF AGGRESOMES IN SCHWANN CELLS

Note

The work presented in this chapter was published in *The Journal of Neuroscience* 23 (33): 10672-10680 (2003). Shale Joy and Jie Li contributed with the preparation of teased fibers and immunostaining. Dr. William Dunn assisted with the electron microscopy procedure and data interpretation.

Introduction

Intracellular protein aggregates are a common feature of numerous central (CNS) and peripheral nervous system (PNS) disorders (Berke and Paulson, 2003). The mechanism by which aggregates are formed is not fully understood, but in many conditions it involves the misfolding of a protein into a state favoring its aggregation (Sherman and Goldberg, 2001; Kopito and Ron, 2000). A shared characteristic among cytoplasmic aggregates is the presence of molecular chaperones and components of the ubiquitin-proteasome pathway (Sherman and Goldberg, 2001; Garcia-Mata et al., 2002). One type of inclusion, the aggresome, is an assembly of protein aggregates that forms when the activity of the proteasome is inhibited (Johnston et al., 1998). A growing number of disease-associated proteins have been found to accumulate in aggresomes, including peripheral myelin protein 22 (PMP22) (Notterpek et al., 1999; Ryan et al., 2002), huntingtin (Waelter et al., 2001), parkin and α-synuclein (Junn et al., 2002). The aggregation of these proteins is thought to be involved in the pathogenesis of peripheral

neuropathies, Huntington's and Parkinson's diseases, respectively, and both protective and toxic roles have been proposed (Kopito, 2000).

PMP22 is a hydrophobic Schwann cell (SC) glycoprotein whose precise role in PNS myelin is unknown (Naef and Suter, 1998). Duplication of or point mutations within the *PMP22* gene are associated with various demyelinating peripheral neuropathies, including Charcot-Marie-Tooth disease type 1A (CMT1A) (Lupski et al., 1991). One of these point mutations (Leu16Pro), carried by the Trembler J (TrJ) mouse, accurately reproduces the pathological findings of CMT1A nerves (Suter et al., 1992; Notterpek and Tolwani, 1999). Since in normal SCs the majority of the newly synthesized PMP22 is rapidly turned over, presumably by the proteasome (Pareek et al., 1997), we hypothesized that overproduction or misfolding of mutated PMP22 might overwhelm the protein degradative pathway. Indeed, *in vitro* studies indicate that overproduced wild type (Wt) and mutated TrJ and Trembler (Tr) PMP22s form aggresomes when the proteasome is inhibited (Notterpek et al., 1999, Ryan et al., 2002). Comparison of the Tr (Gly150Asp) and TrJ mutations suggests that the tendency of mutant PMP22s to aggregate may correlate with disease severity (Tobler et al., 2002). Furthermore, an unbiased study of three non-naturally occurring PMP22 point mutations shows that the accumulation of mutant PMP22s in large perinuclear aggregates might be protective (Isaacs et al., 2002). Therefore, *in vivo* and *in vitro* studies support the involvement of PMP22 aggregates in the pathogenesis of CMT1A neuropathies. Nevertheless, the presence or the potential role of PMP22 aggregates in neuropathy nerves has not been examined.

Here we show that in TrJ nerves, PMP22 has an extended half-life and accumulates in the perinuclear region of the SCs. These cytosolic PMP22 aggresome-like structures

frequently associate with molecular chaperones, including Hsc70, and recruit lysosomes, suggesting that these systems may be involved in the clearance of aggresomes. Indeed, SCs are able to eliminate PMP22 aggresomes by an autophagy-mediated mechanism. These studies provide further evidence for the involvement of the proteasome in PMP22 neuropathies and support the idea that aggresomes are transitory structures linking the ubiquitin-proteasome and lysosomal pathways.

Materials and Methods

Mouse Colonies

Trembler J (TrJ) (Jackson laboratories, Bar Harbor, ME) and PMP22-deficient (Adlkofer et al., 1995) mouse breeding colonies were housed under SPF conditions at the McKnight Brain Institute animal facility. The use of animals for these studies has been approved by the University of Florida IACUC. Genomic DNA was isolated from tail biopsies of younger than 10 day-old mice and litters were genotyped by PCR followed by Ban*I* enzymatic digestion (TrJ), or Southern blots (PMP22-deficient) (Notterpek et al., 1997; Adlkofer et al., 1995). For all experiments, unless otherwise specified, age-matched, one year-old heterozygous TrJ and wild type (Wt) mice were used.

Metabolic Labeling

Freshly isolated sciatic nerves from 18 day-old Wt, TrJ and heterozygous PMP22-deficient (-/+) mice were metabolically labeled with 0.4 mCi/ml *trans*^{35}S (ICN Biochemicals, Costa Mesa, CA) (Pareek et al., 1997). For the chase experiments, samples were incubated with an excess of cold methionine and cysteine for 0h, 1h, 2h, 4h, 6h, 8h and 24h. Nerve pieces were then lysed for 45 minutes at 4°C with radioimmunoprecipitation (RIPA) buffer (50 mM Tris-HCl, pH 8.0, 150 mM NaCl, 1% deoxycholate, 0.5 % Nonidet P-40 and 0.1% SDS) supplemented with a mixture of

protease inhibitors (Complete™; Roche, Indianapolis, IN). PMP22 was immunoprecipitated with a rabbit polyclonal anti-PMP22 antibody, as described (Pareek et al., 1997). Treatment with endo H (New England Biolabs, Beverly, MA) was performed according to the manufacturer's instructions. Samples were separated on 4-15% acrylamide gradient gels (Biorad, Hercules, CA) and the gels were fixed and treated with AMPLIFY (Amersham Life Science Inc., Arlington Heights, IL). Dried gels were exposed to Kodak XAR film (Kodak, Rochester, NY) at -80°C. The half-lives of Wt and mutant PMP22s were determined quantitatively by densitometry using Scion Image software (Scion Corporation, MD) in three separate experiments. The decay curve was plotted as the percentage of total *trans* ^{35}S-labeled PMP22 remaining at the different time intervals ($\pm$ SEM).

Western Blot Analyses

The detergent partitioning procedure for aggresome characterization has been described elsewhere (Johnston et al., 1998; Ryan et al., 2002). Briefly, frozen sciatic nerves were crushed under liquid nitrogen, lysed in immunoprecipitation buffer (IPB) (10 mM Tris-HCl, pH 7.5, 5 mM EDTA, 1% NP-40, 0.5% deoxycholate and 150 mM NaCl) supplemented with protease inhibitors. The lysates were microcentrifuged, the supernatant removed and the insoluble material incubated with 10 mM Tris-HCl, 1 % sodium dodecylsulfate (SDS) for 10 min. Following the addition of 150 µl of IPB buffer, the pellets were briefly sonicated and total protein was determined. Samples were separated on 12.5 % SDS gels and transferred onto nitrocellulose membranes. Blots were blocked and incubated with the indicated primary antibodies. After incubation with anti-rabbit or anti-mouse horseradish peroxidase (HRP) conjugated secondary antibodies (Sigma, St. Louis, MO), membranes were reacted with an enhanced chemiluminescent

substrate (Perkin Elmer, Boston, MA). Films were digitally imaged using a GS-710 densitometer (Bio-Rad Laboratories).

Primary Antibodies

To detect PMP22 in the studied samples, rabbit polyclonal (for the mouse nerves) (Pareek et al., 1997) and mouse monoclonal (for rat SCs) (Chemicon, Temencula, CA) antibodies were used. Polyclonal rabbit anti-Gsa7 (Dorn et al., 2001) and monoclonal rat FITC conjugated anti-transferrin receptor (Chemicon) antibodies were utilized to label early autophagosomes and early endosomes, respectively. Protein chaperone antibodies utilized, included αB-crystallin, calreticulin, heat shock protein 70 (Hsp 70) and heat shock cognate protein 70 (Hsc 70) (all from Stressgen, Victoria British Columbia, Canada). Antibodies against the 11S and 19S proteasome subunits (Affinity Research Products Ltd., Exeter, United Kingdom), the lysosomal associated membrane protein 1 (LAMP1) (clone 1D4B, Developmental Studies Hybridoma Bank, Iowa City, IA), glyceraldehyde-3-phosphate dehydrogenase (GAPDH) (loading control) (clone 1D4, EnCor Biotechnology Inc., Alachua, FL) and ubiquitin (Dako, Carpinteria, CA) were obtained from the indicated commercial suppliers.

Immunostaining of Teased Fibers

Sciatic nerves from 1-year old Wt and TrJ mice were fixed in 4% para-formaldehyde and teased into single fibers (Arroyo et al., 1999). After drying, samples for aggresome detection were permeabilized with methanol (5 min, -20°C), or with 0.2% Triton X-100 (20 min, room temperature) for the transferrin receptor (endosome marker). Twenty-percent normal goat serum in PBS was used to block nonspecific binding sites. Due to the high levels of endogenous mouse Igs in TrJ nerves, only rat origin monoclonal and rabbit polyclonal antibodies were used for the double immunolabeling studies

(Notterpek et al., 1997). After an overnight incubation at 4°C, bound primary antibodies were detected with goat anti-rabbit Texas red and goat anti-rat FITC-conjugated Alexa dyes (Molecular Probes, Eugene, OR). Hoechst dye was included with the secondary antibodies. Cover slips were mounted using the Prolong Antifade kit (Molecular Probes) and images were acquired with a SPOT digital camera attached to a Nikon Eclipse 1000 microscope or an Olympus MRC-1024 confocal microscope. Images were processed for printing by using Adobe Photoshop 5.0.

Ultrastructural Studies

In parallel with the biochemical studies, nerve samples were fixed in 2 % para-formaldehyde and 1 % glutaraldehyde in Tyrode's buffer (pH 7.4) for 60 min. The specimens were then treated with 2 % OsO_4 in 0.1 M sodium cacodylate (pH 7.5), dehydrated and embedded in Taab. The samples were then sectioned, post-stained with lead citrate and uranyl acetate, and examined on a JEOL 100CX transmission electron microscope.

Aggresome Formation and Removal

Primary rat SC cultures were established and maintained as described (Notterpek et al., 1999). Mouse L fibroblasts were purchased from American Type Culture Collection (ATCC, Rockville, MD) and maintained in Dulbecco's Modified Eagle's Medium (DMEM) with 10% fetal calf serum (FCS) (HyClone, Logan, UT). SCs or L fibroblasts on glass coverslips were treated with 10 μM lactacystin (Calbiochem) to inhibit the proteasome, or dimethlysulfoxide (DMSO) (Sigma) as a control. After 16h incubation, a subset of lactacystin treated cells was immediately processed for immunostaining to visualize aggresomes (Notterpek et al., 1999), while the rest were allowed to recover for 8h or 24h washout periods. During the 8h washout period, parallel samples were

incubated with starvation medium (amino acid- and serum-free) to stimulate autophagy (Aplin et al., 1992), or 3-methyladenine (10 mM) (Sigma) to block autophagy (Dorn et al., 2001). After each paradigm, cells were immunolabeled to evaluate the presence of PMP22 aggresomes (Notterpek et al., 1999). Cell viability was monitored by Trypan blue exclusion after each pharmacological treatment (Stefanis et al., 2001). BrdU incorporation during the wash out periods was performed using a BrdU labeling and detection kit (Roche, Indianapolis, IN). Cells with PMP22 aggresomes were counted and expressed as percent of total number of cells evaluated by nuclear staining with Hoechst #33258 (Molecular Probes, Eugene, OR). Statistically significant differences between the various paradigms were determined using a Student's t-test.

Results

PMP22 Accumulates in Cytoplasmic Aggregates in TrJ Nerves

In normal nerves, the majority of newly synthesized Wt-PMP22 is rapidly degraded from the ER, likely due to inefficient folding (Pareek et al., 1997). In agreement, in proteasome-inhibited rat SCs, PMP22 accumulates in cytoplasmic, perinuclear, membrane-free structures termed aggresomes (Notterpek et al., 1999). Similarly, overexpressed Wt- and mutated-PMP22 also form aggresomes (Ryan et al., 2002). Based on these *in vitro* observations, we hypothesized that disease-associated mutations in PMP22 will further interfere with the correct folding of the newly synthesized protein and potentially saturate the proteasomal pathway, resulting in aggresome formation. To explore this idea, pulse-chase analyses in sciatic nerves from Wt, heterozygous PMP22-deficient (-/+) and TrJ mutant (TrJ) mice (Fig. 2-1A, 1B) were performed.

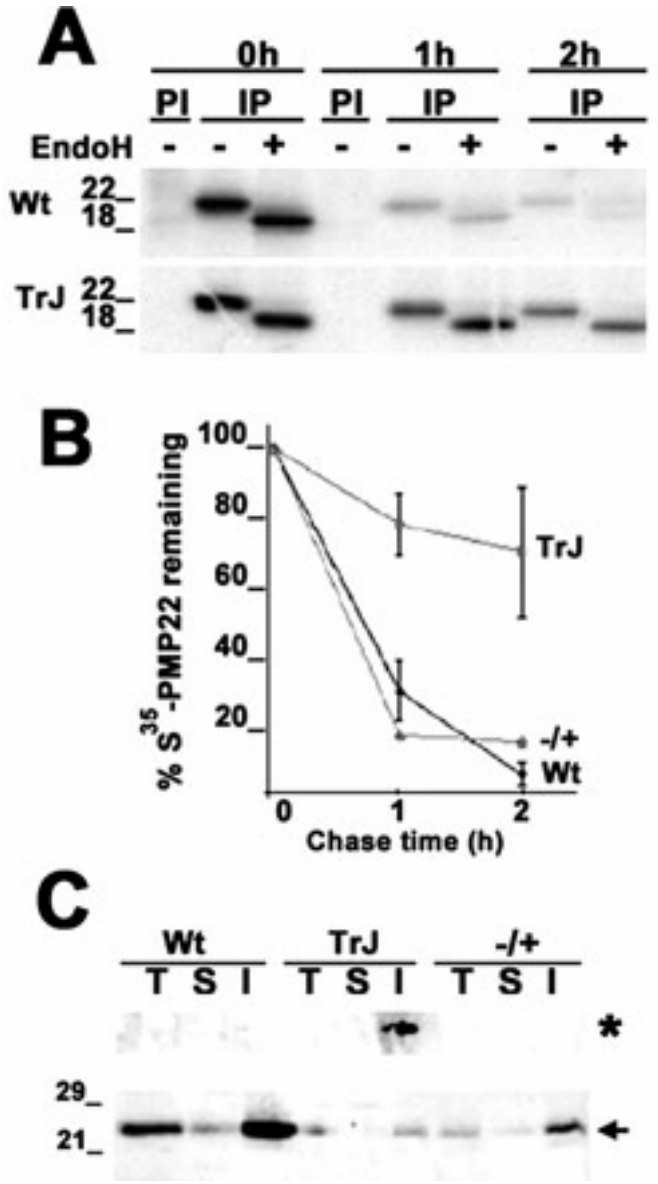

Figure 2-1: Accumulation of PMP22 in TrJ sciatic nerves. Sciatic nerves from wild type (Wt), heterozygous TrJ and heterozygous PMP22-deficient (-/+; autoradiograph not shown) mice were metabolically labeled with ^{35}S-Translabel and PMP22 was immunoprecipitated from pulse (0h) and chase (1h, 2h) time points (A, B). PMP22 immunoprecipitates (IP) were incubated with (+) or without (-) EndoH and separated on a 4-15% acrylamide gradient gel. PI: pre-immune. The decay curve was plotted as the percentage of total ^{35}S-PMP22 remaining at the different chase intervals (n=3; +/-SEM) (B). Total (T), IPB-soluble (S) and -insoluble (I) fractions (20 µg/lane) of nerve lysates were immunoblotted with a polyclonal anti-PMP22 antibody (C). The high molecular weight aggregates (asterisk, top of the gel) and the 22 kD monomer (arrow) of PMP22 are indicated. Molecular mass in kilodaltons.

In Wt mouse nerves, the newly synthesized PMP22 has a short half-life (~ 45 min) and is mostly sensitive to endoglycosidase H (endoH) digestion (Fig. 2-1A, B) (Pareek et al., 1997). In comparison, the turnover rate of PMP22 in TrJ nerves is reduced by about 8-fold, with nearly 75% of the newly synthesized protein remaining at the 2h chase time point (Fig. 2-1A, 1B). These data are in agreement with our previous findings in rat SCs, in which overexpressed TrJ-PMP22 had an increased half-life compared to Wt-PMP22 (Ryan et al., 2002). Extended chase time points reveal that in TrJ nerves the half-life of PMP22 is ~4 h (not shown). Endoglycosidase treatments of the immunoprecipitated PMP22 at the early (1-2h) (Fig. 2-1A), as well as late, chase time points (4-8h) (not shown) demonstrate that in affected nerves the majority of the newly synthesized endo H sensitive PMP22 accumulates before the medial-Golgi compartment (Fig. 2-1A). PMP22 from sciatic nerves of PMP22 +/- mice behaves as in Wt nerves (Fig. 2-1B), suggesting that the effects on PMP22 turnover were due to the presence of the TrJ allele rather than the absence of a Wt allele.

The finding that the newly synthesized, endo H sensitive PMP22 has an extended half-life in TrJ nerves (Fig. 2-1A) suggests that the protein may accumulate in aggresomes. To investigate the occurrence of PMP22 aggregates at the biochemical level, Wt and TrJ sciatic nerves were homogenized (T) and separated into detergent soluble (S) and detergent insoluble (I) fractions, followed by Western blot analyses (Fig. 2-1C) (Ryan et al., 2002). Due to demyelination in the TrJ nerves, the overall steady state levels of the 22 kD PMP22 are reduced (Fig. 2-1C, arrow) (Notterpek et al., 1997). Nevertheless, slow migrating anti-PMP22 antibody reactive aggregates are detected at the top of the gel in the detergent-insoluble fraction of adult TrJ nerves, but not in Wt or

PMP22 -/+ samples (Fig. 2-1C, asterisk). In addition, although most PMP22 is detergent-insoluble in all three genotypes, this insolubility is further increased (~4-fold) in TrJ, compared to Wt (Fig. 2-1C).

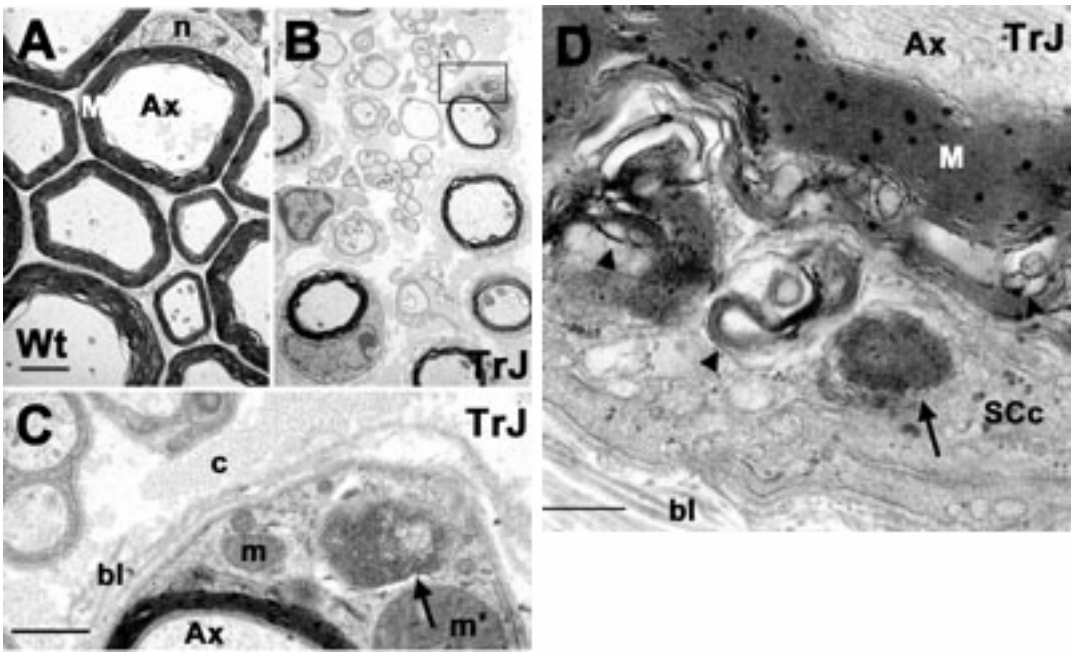

Figure 2-2: Aggresome-like structures are present in TrJ nerves. The ultrastructure of Wt (A) and TrJ (B-D) sciatic nerves are shown. A higher magnification of the area boxed in B is shown in C. Aggresome-like structures (C and D, arrows) and lamellar myelin debris (D, arrowhead) are visible in a transverse section of a TrJ nerve. Scale bars: A-B, 1µm; C, 0.2µm; D, 0.5µm. Ax: axon, bl: basal lamina, c: collagen, m: mitochondria; m': enlarged mitochondria, M: myelin, n: nucleus.

Compared to other cellular inclusions, a unique characteristic of aggresomes is that they are membrane-free (Johnston et al., 1998). To visualize aggresomes at the subcellular level in TrJ neuropathy samples, sciatic nerves from control and affected mice were processed for transmission electron microscopy (Fig. 2-2). As described previously, the majority of axons are well-myelinated in the adult Wt sciatic nerve (Fig. 2-2A) (Notterpek et al., 1997). In comparison, unmyelinated small caliber fibers, supernumerary SC profiles and excessive extracellular matrix are common findings in TrJ samples (Fig.

2-2B) (Henry et al., 1983; Notterpek et al., 1997). A higher magnification view of the boxed area in Fig. 2-2B reveals that a fraction of TrJ SCs contains cytoplasmic, membrane-free granular protein aggregates (Fig. 2-2C, arrow). Similarly, amorphous protein aggregates are detected in a transverse section of a TrJ nerve fiber (Fig. 2-2D, arrow). These aggregates are distinct from previously described "lamellar debris" seen within areas of uncompacted myelin and the cytoplasm of some of TrJ SCs (Fig. 2-2D, arrowheads) (Henry et al., 1983), and resemble aggresomes composed of misfolded cystic fibrosis transmembrane regulator (CFTR) protein (arrows in Fig. 2-2C and 2D) (Johnston et al., 1998).

PMP22 Aggregates Recruit Molecular Chaperones

The formation of PMP22 aggresomes *in vitro* results in the upregulation of heat shock proteins (Hsps) and their association with aggresomes (Ryan et al., 2002). To examine the levels and localization of Hsps in TrJ neuropathy nerves, teased fibers were processed for double immunolabeling with rabbit anti-PMP22 and rat anti-Hsp70 antibodies (Fig. 2-3). As described previously, in normal sciatic nerves, PMP22 is found in the compact portion of myelin and is absent from the nodes of Ranvier (Fig. 2-3A, inset) (Notterpek et al., 1997). In nerve fibers of TrJ mice, a fraction of PMP22 is detected in perinuclear aggregates (Fig. 2-3A, arrows) that are reminiscent of PMP22 aggresomes formed *in vitro* (Notterpek et al., 1999; Ryan et al., 2002). Less frequently, PMP22 can also be seen concentrated in distal, possibly membrane-associated structures (Fig. 2-3A, arrowheads). Compared to the normal nerve (Fig. 2-3B, inset), Hsc70-like immunoreactivity is readily detected in the TrJ sample (Fig. 2-3B) and Hsc70 seems to surround the perinuclear (Fig. 2-3B, arrows), but not the peripheral (Fig. 2-3B,

arrowheads), PMP22-positive structures. The merged image of the PMP22- and Hsc70-stained panels shows that the two molecules do not exclusively overlap (Fig. 2-3C).

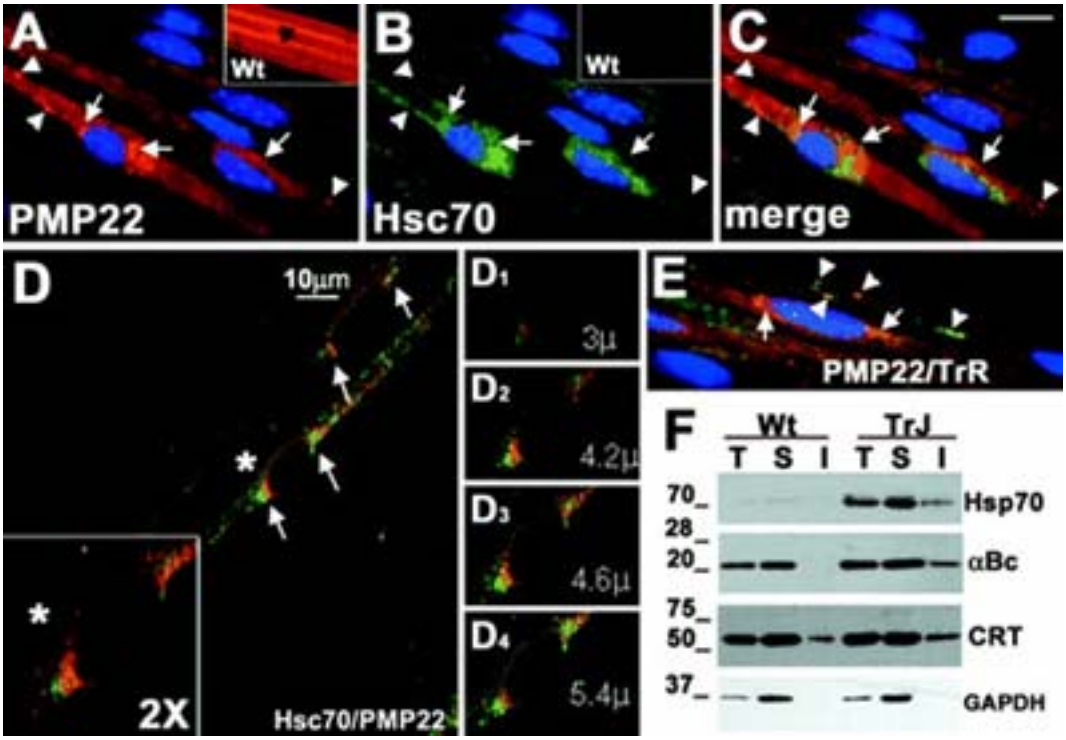

Figure 2-3: Recruitment of cytosolic chaperones to PMP22 aggresomes.Teased sciatic nerves from Wt (insets in A and B) and TrJ (A-E) mice were double immunostained with anti-PMP22 (A, C, D, E, red) and anti-Hsc70 (B, C, D, green) or anti-transferrin receptor (E, green) antibodies. Nuclei are stained with Hoechst dye (A-C, E). In A-E, arrows indicate PMP22 aggresome-like structures, whereas arrowheads point at distal PMP22 positive structures. Scale bar (A-C, E), 10µm. A confocal image of teased TrJ nerve fiber immunostained with anti-PMP22 (D, red) and anti-Hsc70 (D, green) antibodies is shown (D). A magnification (2x) of the perinuclear region of a TrJ SC (D, asterisk) is shown in the lower left corner (D, box). Representative planes (D_1-D_4) of the composite image shown in D illustrate the spatial relationship between PMP22 and Hsc70. Distal PMP22 containing structures (E, arrowheads) costain with transferrin receptor (green in E), but not with Hsc70 (A-C). Total (T), IPB-soluble (S) and -insoluble (I) fractions of Wt and TrJ sciatic nerve lysates (40 µg/lane) were analyzed by Western blots using anti-Hsp70, -αB-crystallin (αBc), -calreticulin (CRT) and -GAPDH (loading control) antibodies (F). Molecular mass in kilodaltons.

To better define the relationship between PMP22 containing aggresome-like structures and Hsc70, teased fibers from TrJ mice were examined by confocal

microscopy (Fig. 2-3D). In a composed image, Hsc70 is present in close proximity to the perinuclear PMP22 aggregate (arrows in Fig. 2-3D), as seen in the conventional light micrograph (Fig. 2-3A-C). Images collected at specific planes (Fig. 2-3D_{1-4}), however reveal that the PMP22 positive aggregates and Hsc70 do not strictly colocalize, but instead Hsc70 appears to surround the aggregates. Therefore, Hsc70 associates with PMP22 aggresomes *in vitro* (Ryan et al, 2002) and PMP22 aggresome-like structures in TrJ neuropathy nerves (Fig. 2-3). Similar to Hsc70, the small chaperone αB-crystallin is also recruited to these perinuclear PMP22 aggregates (not shown). To better define the identity of the Hsc70-negative, PMP22 containing distal structures (Fig. 2-3A, C, arrowheads), TrJ nerve fibers were reacted with anti-PMP22 and anti-transferrin receptor antibodies (Fig. 2-3E). As the merged image reveals, a fraction of the PMP22-containing structures co-stains with the transferrin receptor antibody (Fig. 2-3E, arrowheads). Therefore, these structures most likely represent endocytosed myelin, which are also visible on the electron micrographs (Fig. 2-2D, arrowheads) and have been described previously (Henry et al., 1983; Notterpek et al., 1997).

To corroborate the observed prominent immunoreactivity of cytoplasmic chaperone antibodies in TrJ neuropathy samples, nerve lysates were analyzed by Western blots (Fig. 2-3F). Compared to Wt samples, the levels of Hsp70 (inducible form of Hsc70) and αB-crystallin are elevated in TrJ nerves (Fig. 2-3F). Furthermore, in agreement with our previous *in vitro* studies (Ryan et al, 2002), the detergent-insolubility of these chaperones is increased, which likely reflects their association with PMP22 aggregates. In contrast to cytoplasmic chaperones, only a modest increase in the levels of the ER chaperones,

calreticulin (Fig. 2-3F) and calnexin (not shown) were observed. The levels of GAPDH (protein loading control) remained largely unaffected (Fig. 2-3F).

Alterations in Protein Degradation Pathways

Lysosomes often surround PMP22 aggresomes formed *in vitro*, suggesting that the aggregates may serve as a staging ground for lysosomal degradation (Notterpek et al., 1999; Kopito, 2000). Coincidently, elevated lysosomal proteolysis has been implicated in the pathogenesis of TrJ neuropathy (Notterpek et al., 1997). To investigate the spatial relationship of *in vivo* PMP22 aggresomes with lysosomes, teased TrJ nerve fibers were double immunolabeled with anti-PMP22 and anti-LAMP1 antibodies (Fig. 2-4). As shown above, PMP22 accumulates in perinuclear regions in a fraction of TrJ SCs (Fig. 2-4A, arrows). Compared to Wt, the overall levels of LAMP1 are elevated in TrJ nerves (Notterpek et al., 1997), and LAMP1-like immunoreactivity is detected near the perinuclear PMP22 aggresome-like structures (Fig. 2-4B and C, arrows). When the images are merged and enlarged (Fig. 2-4C, inset), it becomes evident that the LAMP1 immunoreactive lysosomal vesicles are in close proximity to the PMP22 aggregates.

Aggresomes assemble when the proteasome is impaired or overwhelmed leading to the accumulation of polyubiquitinated protein substrates (Johnston et al., 1998). In agreement, elevated ubiquitin-like immunoreactivity (Ryan et al., 2002) and aggresome-like structures (Figs. 2, 3 and 4) are detected in TrJ nerves. Western analysis of nerve lysates also revealed an accumulation of slow-migrating, polyubiquitinated protein complexes in affected nerves (Fig. 2-4D). Furthermore, a significant elevation in detergent-insolubility of polyubiquitinated proteins is detected, likely reflecting their association with the aggregates (Fig. 2-4D). Polyubiquitination is the main targeting signal for degradation by the 26S proteasome, which is composed of a 20S catalytic core

and the regulatory complexes 11S or 19S (Hirsch and Ploegh, 2000). The levels of the 11S proteasome subunit were increased in TrJ nerves, while the levels of the 19S remained largely unaltered (Fig. 2-4D). Since the maximal reaction velocity of the 20S proteasome is enhanced when bound to the 11S subunit (Ma et al., 1992), the elevated levels of 11S in TrJ nerves may represent an attempt of the cell to increase the degradation efficiency of newly synthesized misfolded proteins.

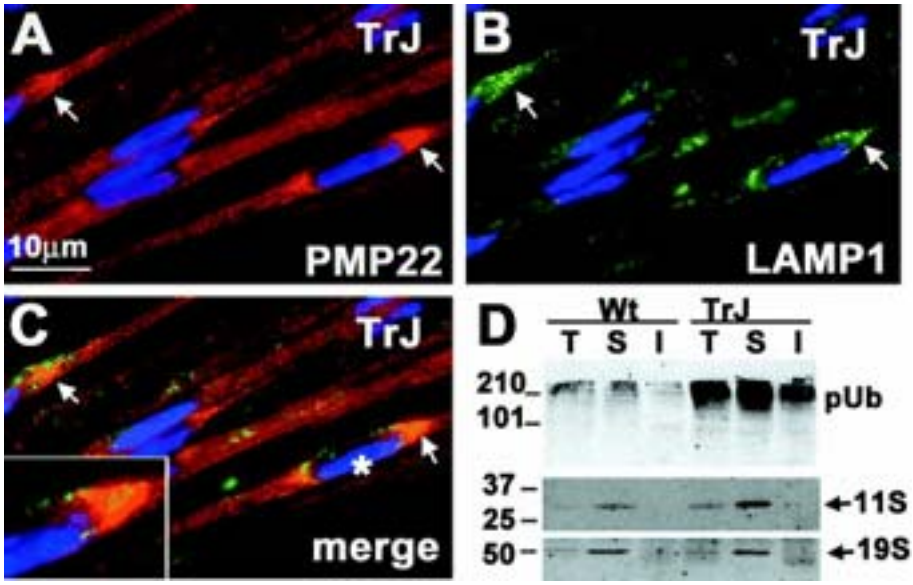

Figure 2-4: Alterations in protein degradation pathways in TrJ nerves. Teased sciatic nerve fibers from TrJ mice were double immunostained for PMP22 (A and C, red) and LAMP1 (B and C, green). PMP22 aggresome-like structures (A and C, arrows) are surrounded by LAMP-1 immunoreactive lysosomes (B and C, arrows). An enlargement of a PMP22 aggresome like structure and its spatial relationship with LAMP1 (C, asterisk) is shown (box, C). Scale bar as indicated. Total (T), IPB-soluble (S) and -insoluble (I) fractions of Wt and TrJ nerve lysates (40 μg/lane) were analyzed for ubiquitin, and the proteasomal subunits 11S and 19S (D). pUb: polyubiquitinated substrates. Molecular mass in kilodaltons.

Implications of Autophagy in the Removal of TrJ Aggresomes

The presence of lysosomes juxtaposed to the aggresomes (Fig. 2-4A-C) suggests that these degradative organelles may have a role in their removal. Since the primary avenue for the delivery of cytosolic proteins to lysosomes is autophagy (Dunn 1990), it is

probable that the aggresomes in TrJ SCs are eliminated by this mechanism. Autophagy is a vital process by which cytoplasmic cargo is engulfed by autophagosomes, which subsequently fuse with lysosomes to ensure degradation (Ohsumi, 2001). A morphological evidence of active autophagy is the presence of autophagosomes, which are characterized by being double membrane bound (Dunn, 1990). Therefore, we investigated the occurrence of autophagosomes in TrJ sciatic nerves (Fig. 2-5).

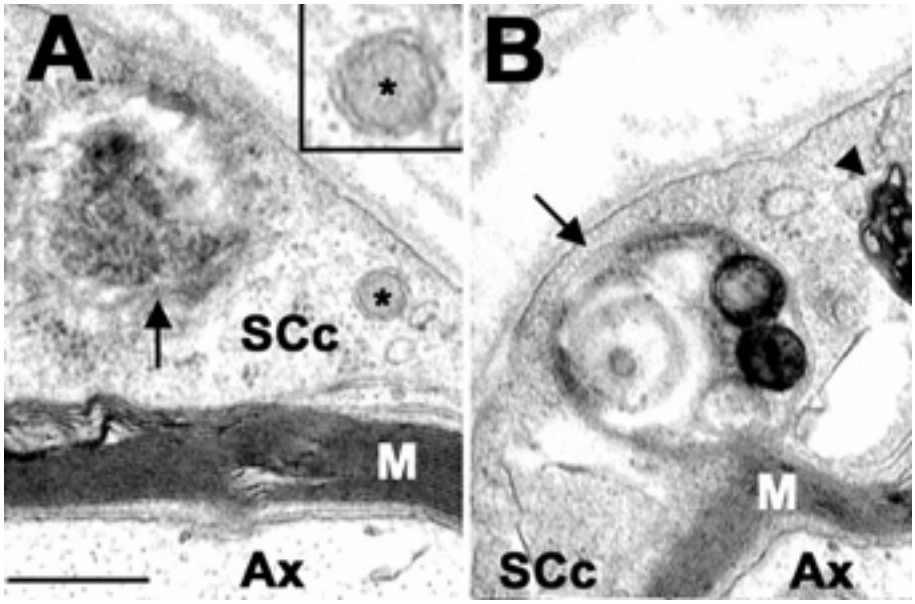

Figure 2-5: Autophagosomes in TrJ nerves. Ultrastructural analyses of TrJ sciatic nerve cross-sections reveal the presence of autophagosomes (arrows) in SC cytoplasm (SCc) (A, B). An enlargement of a double-membrane autophagosome (asterisk) is shown (box, A). A late stage autophagosome/autolysosome (arrow) and lamellar, myelin debri (arrowhead) are visible in the cytoplasm of a TrJ SC (B). Scale bar, 0.25 μm. Ax: axon; M: myelin.

Various autophagic profiles are detected in the cytoplasm of TrJ SCs (Fig. 2-5A and 5B), but are noticeably absent from Wt SCs (Fig. 2-2A). A small autophagosome with the characteristic double membrane border is visible (Fig. 2-5A, box). In the same SC cytoplasm, an amorphous electron-dense aggregate is found within an autophagosome (Fig. 2-5A, arrow). As autophagosomes mature, they fuse with lysosomes and give rise to

the autolysosomes (Dunn 2000). A late stage autophagosome/autolysosome, with concentric arrays of membranes and electron-dense inclusions, is visible in the cytoplasm of a TrJ SC (Fig. 2-5B, arrow).

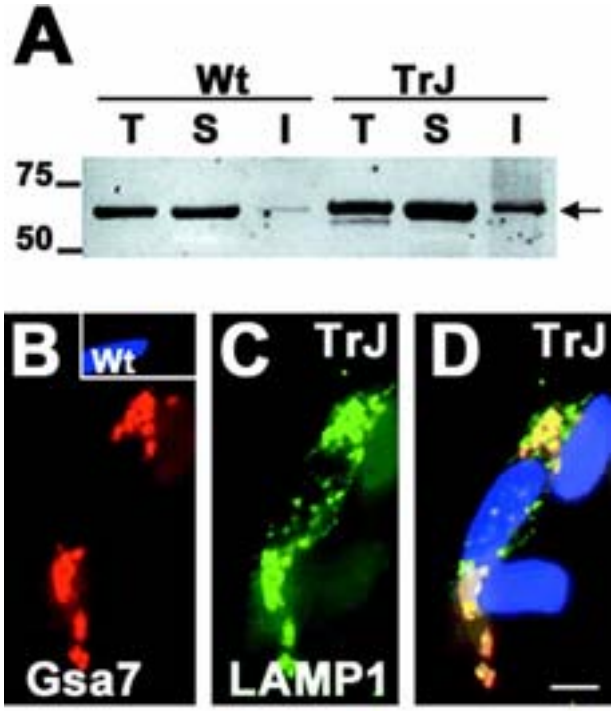

Figure 2-6: Autophagic constituents are present at perinuclear locations. Western blot analysis of a Gsa7 antibody on total (T), IPB-soluble (S) and -insoluble (I) fractions of Wt and TrJ nerve lysates (40 µg/lane) (A). The levels of Gsa7 (kD) are elevated in the IPB-insoluble fraction of the TrJ nerve. Molecular mass in kilodaltons. Teased nerve fibers from Wt (B, inset) and TrJ (B-D) mice were double immunolabeled with the same polyclonal anti-Gsa7 (B, D, red) and a monoclonal anti-LAMP-1 (C and D, green) antibodies. Nuclei are visualized by Hoechst dye (D). Scale bar, 5µm (D).

To obtain further evidence for the involvement of autophagy in TrJ neuropathy, parallel nerve samples were reacted with a polyclonal anti-Gsa7 antibody (Fig. 2-6) (Dorn et al., 2002). Gsa7/Atg7 is an enzyme required for two protein conjugation events that are essential for the formation of autophagosomes (Ohsumi, 2001). The first is the conjugation of Atg5 to Atg12, while the second is the amide linkage of MAP-LC3/Atg8 to the amino group of phosphatidyl-ethanolamine, located at the surface of

autophagosomes. On Western blots, we detected an increase in the steady-state levels of Atg7 in TrJ nerve lysates, as compared to Wt (Fig. 2-6A). The elevated levels of Atg7 in the detergent-insoluble fraction of the TrJ nerve lysate could represent a transient association with the aggregates. Indeed, immunolabeling of teased TrJ nerve fibers with the Atg7 antibody reveals bright Gsa7-like immunoreactivity in the perinuclear regions of affected SCs (Fig. 2-6B). In normal nerves, the levels of Atg7 are low and the protein is diffuse (Fig. 2-6A, inset). The lysosomal marker LAMP1 associates with the majority of the Atg7-positive vesicular structures (Fig. 2-6C, D), which likely represent early events in the fusion of autophagosomes and lysosomes. Together, these findings indicate that autophagy is activated in TrJ nerves, most likely to facilitate the removal of PMP22 aggresomes (see below).

Aggresomes Are Reversible and Can Be Cleared by Autophagy

The consequences of aggresome formation are unknown, although it has been hypothesized they might result in cellular toxicity (Kopito, 2000). Nonetheless, the lack of abnormal nuclear profiles on Hoechst-stained, as well as ultrastructural, TrJ samples indicates that cell death is not a prominent feature of TrJ neuropathy (Notterpek et al., 1997). Furthermore, as shown above (Figs. 2-4), at a given time, only a subset of TrJ SCs contains aggresomes. Therefore, we hypothesized that aggresomes are transient structures, which under permissive conditions can be removed by cells. To test this, normal rat SCs were treated with the proteasome inhibitor lactacystin for 16h, which results in aggresome formation in nearly all of the cells (Fig. 2-7A) (Notterpek et al., 1999). Subsequently, lactacystin was removed and the cells were allowed to recover in normal growth medium for 24h (Fig. 2-7B). Following the 24h washout period, only ~20% of the cells contained aggresomes (Fig. 2-7B, 7C). Utilizing a bromodeoxy-uridine

incorporation assay during the washout period, cell proliferation was ruled out as a possible reason for the reduction in the number of aggresome-containing cells (data not shown). In addition, based on a Trypan blue viability assay (Stefanis et al., 2001), there was no significant difference in cell death between lactacystin-treated cells and those allowed to washout for 24h (not shown). Thus, these results demonstrate for the first time that aggresomes are reversible structures once the conditions that favor their formation are eliminated. SCs possess remarkable reparatory properties and are able to phagocytose and degrade large quantities of myelin proteins during Wallarian degeneration (Hirata and Kawabuchi, 2002). To investigate if aggresome removal was unique to SCs, mouse L fibroblasts were subjected to the same experimental paradigm of lactacystin treatment and subsequent washout (Fig. 2-7D). After a 16 h lactacystin treatment, over ~80% of the SCs and L fibroblasts contained aggresomes (Fig. 2-7D). Following an 8h washout period, only about half of these cells had aggresomes (Fig. 2-7D). These data indicate that L fibroblasts are able to eliminate aggresomes at approximately the same rate observed in SCs. Thus, this clearance event is not unique to peripheral glia.

The most likely mechanism by which cells can remove aggresomes is by their sequestration into autophagosomes for lysosomal degradation (Kopito, 2000). Indeed, our studies show that autophagy is an ongoing process in TrJ SCs (Figs. 5 and 6). To determine if autophagy is involved in the elimination of aggresomes, subsequent to the lactacystin treatment, pharmacologic modulators of autophagy were included in the washout medium. For these experiments, a washout period of 8h was chosen, at which time point ~57% of the SCs still contain aggresomes (Fig. 2-7E). To stimulate autophagy during the 8h washout period, cells were incubated with amino acid/serum deprived

medium (Aplin et al., 1992), which resulted in a significant reduction in the number of cells with aggresomes (~36%) (Fig. 2-7F, 7H).

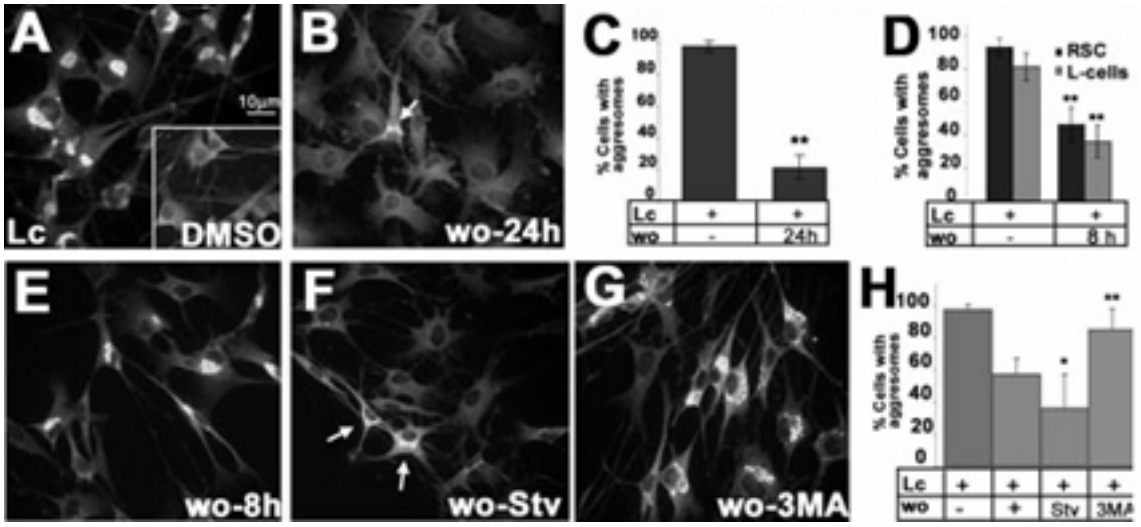

Figure 2-7: Reversibility of aggresomes in cultured SCs. SCs were treated with lactacystin (Lc) (A), or DMSO (inset in A) for 16h, after which the drug was removed and the cells were cultured for an additional 24h (B), followed by anti-PMP22 immunolabeling (A, B). A SC with a remaining PMP22 aggregate is visible (B, arrow). Scale bar, 10 μm. For each condition, cells with aggresomes were counted. The results from eight independent counts were graphed (C) (**$p<0.005$). Rat SCs (RSC) and L cells were treated with Lc for 16h in parallel and the percent of cells with PMP22 aggresomes after an 8h washout was determined and graphed in D (**$p<0.005$). RSCs treated with Lc (16h) (E-H) were subsequently incubated for 8h under the specified conditions: washout with normal media (E, wo-8h); starvation conditions (F, wo-Stv); or 3-methyladenine (G, wo-3MA). Arrows in F indicate two cells with remaining aggregates. Cells with aggresomes in eight independent fields were counted and graphed as a percent of total (Hoechst dye) cells (H), (* $p<0.05$; **$p<0.005$).

Conversely, when autophagy was inhibited with 3-methyladenine (3-MA) (Dorn et al., 2001), the clearance of aggresomes was suppressed (Fig. 2-7G). The differences in the number of aggresome-containing cells between washout alone and autophagy modulators are statistically significant (Fig. 2-7H). There were no significant differences in cell death or cell proliferation between the cells undergoing the various 8h washout

paradigms (not shown). Together, these results indicate that autophagy has a substantial role in the removal of PMP22 aggresomes in SCs.

Discussion

The formation of aggresomes in neurons has been linked to several neurodegenerative disorders of the CNS (Waelter et al., 2001; Junn et al., 2002), but much less is known about protein aggregation in glial cells. PMP22 is a demyelinating peripheral neuropathy-associated SC protein that accumulates in aggresomes when the proteasome is impaired or the protein is misfolded (Notterpek et al., 1999; Ryan et al., 2002). In this report we show that in TrJ-PMP22 neuropathy SCs, PMP22 forms perinuclear aggregates, which share characteristics of PMP22 aggresomes described *in vitro* (Notterpek et al., 1999, Ryan et al., 2002; Isaacs et al., 2002). Concurrently with the presence of aggresomes, TrJ nerves upregulate the lysosomal pathway (Notterpek et al., 1997) and contain autophagosomes, which are likely involved in the removal of the aggresomes. SCs in culture indeed have a remarkable capacity to clear PMP22 aggresomes by an autophagy-dependent mechanism. These results provide *in vivo* evidence for the involvement of aggresomes in PMP22 neuropathy nerves and for the role of autophagy in the removal of glial aggresomes.

If aggresomes are present in PMP22 neuropathy nerves, why have they have not been described previously? One reason might be that, as our studies indicate, aggresomes are transitory and are only present in a fraction of the SCs at a given time. Review of the literature, however suggests that aggresomes have been seen previously in PMP22 neuropathy specimens, but they were not identified as such. In the original studies of the Tr and TrJ mice, Henry and colleagues comment on the presence of non-lamellar electron-dense debris in the cytoplasm of some of the SCs (Henry et al., 1983). In nerve

biopsies of neuropathy patients with *PMP22* gene duplication, cytosolic accumulation of PMP22 was noted and confirmed by double immunolabeling with PMP22 and S100 antibodies (Nishimura et al., 1996). Studies of nerve biopsies from patients with PMP22 point mutations also revealed the retention of PMP22 in the SC cytoplasm with only partial overlap with the ER marker, Bip (Hanemann et al., 2000). In agreement, while TrJ-PMP22 has a prolonged association with the ER chaperone calnexin, likely as an attempt of correct folding, the unfolded protein response is not activated in TrJ nerves (Dickson et al., 2002). This finding points to a post-ER accumulation for the mutated PMP22. Indeed, since PMP22 is destined for degradation by the proteasome (Pareek et al., 1997, Notterpek et al., 1999), when the capacity of the proteasome is overwhelmed the pr7otein will accumulate in the cytoplasm (Berke and Paulsen, 2003).

Aggresome formation is thought to be a protective response to the accumulation of abnormal, likely misfolded proteins (Kopito 2000; Garcia-Mata et al., 2002). Aggresomes form near the centrosome, a site enriched in proteasomal components and cell stress chaperones (Wigley et al., 1999). These aggresomes then sequester misfolded proteins in a central location, thereby increasing the efficiency of their degradation (Kopito 2000). Indeed, preventing aggresome formation results in reduced turnover of expanded polyglutamine repeats and exacerbates cell death (Taylor et al., 2003). Similarly, the presence of large aggregates/aggresomes correlates with a less severe phenotype in three genetically engineered PMP22 mutants (Isaacs et al., 2002). Since aggresomes can further inhibit protein degradation via the proteasome, the extended presence of aggregated protein near the centrosomes is likely to induce cellular dysregulation and cell death (Bence et al., 2001).

While SCs and L fibroblasts can effectively clear aggresomes under permissive conditions, it is unclear if CNS glia and/or neurons share this ability. For example, while parkin and α-synuclein are widely expressed in the CNS and PNS, including SCs (Hase et al., 2002; Mori et al., 2002), the presence of these proteins in aggregates is associated with the selective loss of dopaminergic neurons in the substantia nigra without apparent peripheral nerve dysfunction (Tanaka et al., 2001; Giasson and Lee, 2001). Thus, it is possible that SCs, but not striatal neurons, employ autophagy to clear these aggresomes. Nonetheless, it was previously shown that activation of autophagy reduced the presence of polyglutamine aggregates and ameliorated cell death in PC12 cells (Ravikumar et al., 2002). Therefore, this pathway could be pharmacologically enhanced in neurons in an attempt to reduce the toxicity of these inclusions. Alternatively, dopaminergic neurons may utilize autophagy, but the levels of parkin and α-synuclein may differ among cell types.

Morphological and biochemical studies indicate that autophagy is an active pathway in one-year old TrJ mouse neuropathy nerves. Furthermore, the *in vitro* pharmacologic experiments show that SCs effectively utilize this pathway to remove aggregates. Why then does this pathway fail to prevent the disease progression in PMP22-mutant mice? We believe that in aged animals this pathway might be less efficient allowing it to become saturated. An age-related decline in macroautophagy and chaperone-mediated autophagy has been previously suggested (Cuervo and Dice, 2000; Ward 2002). Given the progressive nature of peripheral neuropathies, and other protein aggregation disorders, it is possible that aggresomes are not prominent during the initial stages of the disease because they are continuously disposed of through autophagy.

However, over time, the autophagy-lysosomal pathway gets saturated, resulting in the accumulation of protein aggregates that may become toxic if not eliminated. The prevalence of aggresomes with disease progression could explain the gain-of-function behavior of some PMP22 point mutations (Adlkofer et al., 1997; Gabreels-Festen and Wetering, 1999).

While autophagy plays a central role in the removal of aggresomes in SCs, our studies suggest that this is not the only mechanism involved. For example, when autophagy was inhibited during the 8h washout period, compared to proteasome-inhibited controls, ~15% of the cells still did not contain any type of aggregates ($p=0.01$). These data indicate that either the autophagy blocking agent 3-MA was not entirely effective or autophagy is aided by other cellular events. In support of the latter, we found that the aggregates remaining during the 3-MA washout lost their initial compactness and appeared more diffuse (compare Fig. 2-7A and 7G). This suggests there is a step preceding autophagy, which is responsible for the initial breakdown of the aggresome into less compact aggregates. Since cytosolic chaperones play an important role in the disassembly of molecular aggregates and accelerate the refolding of insoluble molecules (Cummings et al., 1998; Wang and Spector, 2000; Sherman and Goldberg, 2001), it is likely that chaperones are involved in the initial fragmentation of aggresomes. In agreement, cytoplasmic chaperones are recruited to PMP22 aggresomes, both *in vitro* (Ryan et al., 2002) and *in vivo* (Fig. 2-3).

CHAPTER 3
IMPAIRED PROTEASOME ACTIVITY AND ACCUMULATION OF UBIQUITINATED SUBSTRATES IN A HEREDITARY NEUROPATHY MODEL

Note

The work presented in this chapter was published in *The Journal of Neurochemistry* 92:1531-1541 (2005). Jie Li and Jocelyn Go contributed with the immunostaining of sciatic nerves and the isolation of mouse Schwann cells. Ali Fenstermaker helped with the immnoprecipitation procedures. Brad Fletcher assisted with construct design and infection of Schwann cells.

Introduction

Imbalance between protein synthesis/folding and degradation, in concert with accumulation of misfolded proteins in aggregates is a common, but not well-understood feature of various neurodegenerative conditions (Sherman and Goldberg, 2001). A particular type of cytosolic inclusion, termed the aggresome, forms in a microtubule-dependent fashion near the centrosome when the proteasome is inhibited (Wojcik et al., 1996; Johnston et al., 1998). Disease-associated proteins known to accumulate in aggresomes include cystic fibrosis transmembrane conductance regulator (CFTR), peripheral myelin protein 22 (PMP22), huntingtin and α-synuclein (Johnston et al., 1998; Notterpek et al., 1999; Waelter et al., 2001; Tanaka et al., 2004). The contribution of aggresomes to disease is uncertain and remains a subject of controversy. Indeed, the formation of aggresomes has been independently ascribed both toxic (Waelter et al.,

2001) and protective functions (Isaacs et al., 2002; Taylor et al., 2003; Tanaka et al., 2004).

The main degradation pathway for short-lived proteins is the proteasome, which can exist by itself (20S) or bound to the regulatory subunits 19S or 11S (26S) (Groll and Clausen, 2003). The turnover of substrates by the 26S proteasome is generally ensured by the covalent attachment of at least four ubiquitin moieties (Deveraux et al., 1994). Once a protein is tagged with a polyubiquitin chain, it is recognized by the 19S subunit, transferred to the catalytic chamber (20S) and degraded (Goldberg, 2003). The proteasome is a dynamic entity, present mainly in the nucleus and the cytoplasm, but also associated with the ER membrane and centrosomes (Hirsch and Ploegh, 2000). It is hypothesized that the strategic distribution of the proteasome machinery and stress response elements near the centrosome may be essential to attain a balance between protein folding and degradation (Wigley et al., 1999). Indeed, constituents of the ubiquitin-proteasome pathway co-localize with aggregates formed under a variety of conditions (Hirsch and Ploegh, 2000).

PMP22 is a disease-linked hydrophobic Schwann cell (SC) membrane protein that accumulates in aggresomes when the proteasome is inhibited, or the protein is mutated, or overexpressed (Notterpek et al., 1999; Ryan et al., 2002; Isaacs et al., 2002; Fortun et al., 2003). In normal cells, under nonmyelinating as well as myelinating conditions, most of the newly-synthesized PMP22 is rapidly turned-over by the proteasome (Pareek et al., 1997; Ryan et al., 2002). The mechanism by which PMP22 is targeted for proteasomal degradation remains unknown, although the protein contains three potential ubiquitination sites. In murine Trembler J (TrJ) neuropathy SCs and nerves, PMP22

aggresomes form spontaneously (Ryan et al., 2002; Fortun et al., 2003). TrJ mice carry a Leu16Pro mutation in the first transmembrane domain of PMP22 and are a frequently used model of Charcot-Marie-Tooth disease type IA (CMT1A) neuropathy (Suter et al., 1992; Notterpek and Tolwani, 1999). In accordance with our findings in TrJ SCs, cytosolic accumulation of PMP22 has been reported in nerve biopsies of CMT1A patients associated with *PMP22* duplication, or the Leu16Pro mutation (Nishimura, et al., 1996; Hanemann et al., 2000). Intracellular retention of PMP22 will reduce the amount of protein that is incorporated into myelin and possibly contribute to demyelination.

The accumulation of PMP22 in aggregates upon proteasome inhibition, as well as spontaneously in TrJ SCs, suggests that the ubiquitin-proteasome pathway might be involved in the pathogenesis of the neuropathy (Notterpek et al., 1999; Ryan, et al., 2002; Fortun et al., 2003). To date however, it is unknown whether the localization or the activity of the proteasome is altered in neuropathy SCs. Here we show that the degradative capacity of the proteasome is reduced in TrJ samples compared to wild type (Wt), as determined by the ability of the 20S/26S to degrade substrate reporters. Diminished proteasome activity correlates with cytosolic accumulation of ubiquitinated substrates, including PMP22 and myelin basic protein (MBP), and the recruitment of proteasome constituents to the aggregates.

Materials and Methods

Mouse Colony

TrJ (The Jackson Laboratory, Bar Harbor, ME) mouse breeding colony is housed under specific pathogen-free conditions at the University of Florida McKnight Brain Institute animal facility. The use of animals for these studies has been approved by the Institutional Animal Care and Use Committee. For genotyping, genomic DNA isolated

from tail biopsies of younger than 10-day old mice was used (Notterpek et al., 1997). All nerves samples used for these studies were obtained from genotyped wild type (Wt) and heterozygous TrJ mice, from our breeding colony.

SC Cultures

Primary SC cultures from genotyped postnatal day 6 (P6) Wt and TrJ mouse pups, or neonatal normal rat pups, were prepared and maintained as described (Ryan et al., 2002). Cells were grown to ~80% confluency in 10% fetal calf serum (Hyclone, Logan, UT), 2.5 (mouse) or 5 μM (rat) forskolin (Calbiochem, La Jolla, CA) and 10 μg/ml bovine pituitary extract (Biomedical Technologies Inc, Stoughton, MA) containing Dulbeccos' modified eagle's medium. To induce PMP22 aggresome formation in normal cells, samples were treated with lactacystin (10 μM) (Calbiochem), or dimethyl sulfoxide (DMSO) as control, followed by immunostaining (Notterpek et al., 1999).

Primary Antibodies

Rabbit polyclonal antibodies to PMP22 (Pareek et al., 1997), 20S, 11S, 19S, E1A isoform of the ubiquitin-activating enzyme (all from Biomol, Plymouth Meeting, PA), 20Sα, 20Sβ, E1AB (all from Calbiochem), MBP (gift of Dr. Campagnoni, UCLA) and ubiquitin (Dako, Carpinteria, CA) were used. The specificities of the anti-proteasome antibodies were verified by Western blotting purified rabbit proteasome (Calbiochem). Rat anti-MBP monoclonal antibody was purchased from Chemicon (Chemicon, Temencula, CA). Rat anti-lysosomal associated membrane protein 1 (LAMP1) (clone 1D4B) was obtained from the Developmental Studies Hybridoma Bank (University of Iowa, Iowa City, IA). Mouse monoclonal antibodies against ubiquitin (Santa Cruz Biotechnology, Santa Cruz, CA), actin (Sigma), GFP (Sigma, St. Louis, MO),

glyceraldehyde-3-phosphate dehydrogenase (GAPDH) (loading control) (clone 1D4, EnCor Biotechnology Inc., Alachua, FL) and PMP22 (NeoMarkers, Fremont, CA) were purchased from the indicated supplier.

Immunocytochemical Studies

Frozen sections (6μm thickness) from adult (~ 1-year old) genotyped Wt and TrJ sciatic nerves were fixed with 4% paraformaldehyde and permeabilized with 0.5% Triton X-100 (TX-100) (15 min, room temperature, Johnston et al., 1998). When indicated, sciatic nerves were teased into single fibers after fixation and processed for immunostaining (Fortun et al., 2003). SCs on glass coverslips were similarly fixed and permeabilized. After blocking, the samples were incubated with primary antibodies overnight at 4°C. Bound antibodies were detected using Alexa Fluor 594-conjugated (red) anti-rabbit or anti-rat, and Alexa Fluor 488-conjugated (green) anti-mouse antibodies (Molecular Probes, Eugene, OR). Nuclei were visualized with Hoechst dye. After washing in phosphate buffered saline (PBS), samples were mounted using the Prolong Antifade kit (Molecular Probes). Images were acquired with a SPOT digital camera (Diagnostic Instrumentals, Sterling Heights, MI) attached to a Nikon Eclipse E800 (Tokyo, Japan). Images were processed for printing using Adobe Photoshop 5.0 (Adobe Systems, San Jose, CA). The percentage of SCs with PMP22, or MBP aggregates, as well as increased perinuclear 20S-like immunoreactivity, was determined in four random visual fields per nerve section. The standard deviation between the independent counts was calculated and analyzed by Student's t-test.

Immunoprecipitation

To investigate whether PMP22 is ubiquitinated, the protein was immunoprecipitated from rat SCs treated with MG132 (50 μM) (Calbiochem) for 16h,

and from Wt and TrJ mouse (1-year old) sciatic nerve lysates (250 μg/sample). Samples were solubilized in RIPA buffer (150 mM NaCl, 50 mM Tris-HCl, pH 7.4, 0.5% Nonidet P-40, 1% deoxycholate, 0.1% SDS) supplemented with a mixture of protease inhibitors (Complete; Roche Products, Indianapolis, IN). After 30 min of rocking at 4°C, the soluble material was separated by centrifugation and nonspecific binding was removed by incubation with rabbit serum and Protein A sepharose (PAS). Immunoprecipitation of PMP22 was carried out overnight at 4°C with a mixture of anti-PMP22 rabbit polyclonal antibodies (Pareek et al., 1997) and analyzed by Western blotting with monoclonal anti-ubiquitin, or secondary antibody alone (negative control).

Western Blot Analyses

Sciatic nerves and cultured SCs were lysed in Laemmli buffer or immunoprecipitation buffer (IPB) (150 mM NaCl, 10 mM Tris-HCl, pH 7.5, 5 mM EDTA, 1% NP40, 0.5% deoxycholate) supplemented with protease inhibitors (Roche) to generate detergent-soluble and -insoluble fractions (Johnston et al., 1998). Protein concentrations were determined by the BCA method (Pierce, Rockford, IL) and equal amounts of proteins (60 μg/lane for proteasome constituents and 10 μg/lane for MBP analyses) were separated on 12.5% SDS gels. After transfer onto nitrocellulose membranes, blots were blocked and incubated with the indicated antibodies. Bound antibodies were detected using an enhanced chemiluminescent substrate (Perkin Elmer Life Sciences, Boston, MA) and Kodak BIOMAX ML film (Eastman Kodak, Rochester, NY). Films were digitally imaged using a GS-710 densitometer (Bio-Rad Laboratories, Inc., Hercules, CA). When indicated, the intensity of immunoreactive bands was quantified using Scion Images Software (Scion, Frederick, MD).

20S Enzymatic Activity Assay

The chymotrypsin-like activity of the 20S proteasome was measured by changes in fluorescence of amino-methyl coumarin (AMC)-conjugated to the chymotrypsin peptide substrate LLVY, using a commercial activity assay kit (APT280, Chemicon). Freshly-collected 1-year-old Wt and TrJ sciatic nerves were homogenized by repeated cycles of sonication in ice-cold 50 mM Tris-HCl (pH. 7.5) containing 1 mM EDTA. Primary mouse SCs established from Wt and TrJ nerves were lysed similarly. Homogenates were centrifuged at 16,000 g for 10 min at 4°C, supernatants collected, and protein concentrations determined as above. Assays were conducted using equal total proteins from cell and tissue lysates (40 μg). The degradation of LLVY-AMC was determined by fluorescence changes, using an AMC standard curve. To monitor the specificity of the assay, the proteasome inhibitor lactacystin (10 μM) was added to block fluorescence change (data not shown). The chymotrypsin-like activity of the 20S proteasome was calculated as relative fluorescence units divided by the levels of 20Sβ in 40 μg of soluble lysates. Relative proteasome activity in Wt samples was arbitrarily set at 100%, and the activity in TrJ lysates was calculated as percentage of Wt. For each genotype, four independent nerves were assayed in duplicate. Data was analyzed using a Student's t-test.

Measurements of 26S Proteasome Activity

SCs isolated from Wt and TrJ mouse nerves, plated at equal densities, were transfected with an Ub^{G76V}-GFP reporter construct (Dantuma et al., 2000) using the lipofectamine method (Invitrogen, Life Technology, Carlsbad, CA). The attachment of a mutated uncleavable ubiquitin moiety to GFP results in a fusion protein (Ub^{G76V}-GFP) that is rapidly degraded by the proteasome and is hardly detected under normal

conditions (Dantuma et al., 2000). The efficiency of transfection was monitored using the GreenLantern GFP plasmid (Invitrogen) and was ~43%. Thirty-two hours after transfection, Wt cells were treated with Lc (10 μM) for 16h to control for the stabilization of the GFP signal upon proteasome inhibition. Forty-eight hours after the transfection, Lc-treated Wt, and untreated Wt and TrJ, SCs were lysed in Laemmli buffer, protein concentrations were determined and equal amounts (60 μg) analyzed by Western blotting with a monoclonal anti-GFP antibody. Membranes were reprobed with anti-actin antibody as a loading marker. The intensity of bands was quantified using Scion Images Software (Scion, Frederick, MD). The relative levels of Ub^{G76V}-GFP were expressed as the density of the GFP band, after correction for actin. The results from four independent experiments were averaged, graphed and analyzed using a Student's t-test.

Results

The Activity of the Proteasome Is Impaired in Neuropathy Samples

PMP22 has a tendency to aggregate when overexpressed and/or mutated (Tobler et al., 2002; Ryan et al., 2002; Fortun et al., 2003). To determine whether the presence of PMP22 aggregates correlates with changes in proteasome function, we measured the chymotrypsin-like activity of the proteasomes in adult Wt and TrJ nerves, as reflected by the ability to cleave the substrate LLVY (Fig. 3-1A and C). The chymotrypsin-like activity represents the rate-limiting step in protein degradation by the 20S core and its inhibition causes a large decline in polypeptide breakdown (Kisselev et al., 1997). In TrJ sciatic nerves, the chymotrypsin-like activity of the proteasome is diminished by ~60%, as compared to Wt ($p<0.005$) (Fig. 3-1A). The reduced ability of the 20S to degrade an exogenous substrate suggests impairment of the proteasome and corroborates the increase in slow migrating ubiquitinated substrates (Fig. 3-1B, bracket; also see Fortun et al.,

2003). To exclude an axonal contribution to the reduced proteasome activity, cultured mouse SCs from Wt and TrJ nerves were also analyzed (Fig. 3-1C). Similar to the whole nerve lysates (Fig. 3-1A), we found ~50% decline in the chymotrypsin-like activity of the 20S in TrJ SCs ($p<0.05$) (Fig. 3-1C). Likewise, the levels of ubiquitinated substrates are elevated in cultured TrJ cells (data not shown). The larger reduction in 20S activity in TrJ nerves (~60%), in comparison to cultured TrJ SCs (~50%), correlates with a higher number of PMP22 aggregate-containing cells. In adult TrJ sciatic nerves, ~28% of the SCs contain PMP22 aggregates, while ~17% do in culture (Table 3-1).

Table 3-1: Analysis of aggregates in TrJ samples. The percentage of aggregates relative to total number of nuclei in TrJ sciatic nerves (SN) or mouse Schwann cells (MSC) was counted in random visual fields (SN, n=4; MSC, n=16). Aggregates were assessed by immunofluoresence. Data is presented as the mean ± standard deviation (SD). *$p<0.05$; **$p<0.01$.

	% of Total (Mean ± SD)	
	SN (perinuclear)	MSC (perinuclear + processes)
PMP22	28 ± 11	17 ± 6
20S	6 ± 3**	17 ± 6
MBP	8 ± 4*	n.d.

Although the reduced degradation of LLVY substrate in TrJ samples suggests proteasome impairment, this assay only takes into account the Tris-HCl/EDTA-soluble 20S activity and disregards the contribution of the regulatory subunits. Therefore, we also determined the ability of the 26S to degrade a short-lived GFP reporter substrate (Ub^{G76V}-GFP) (Dantuma et al., 2000) (Fig. 3-1D). Attachment of an uncleavable ubiquitin (Ub^{G76V}) to GFP converts the otherwise stable protein to a rapidly degraded proteasome substrate and thus, GFP levels are rarely detected unless the 26S is inhibited (Dantuma et al., 2000).

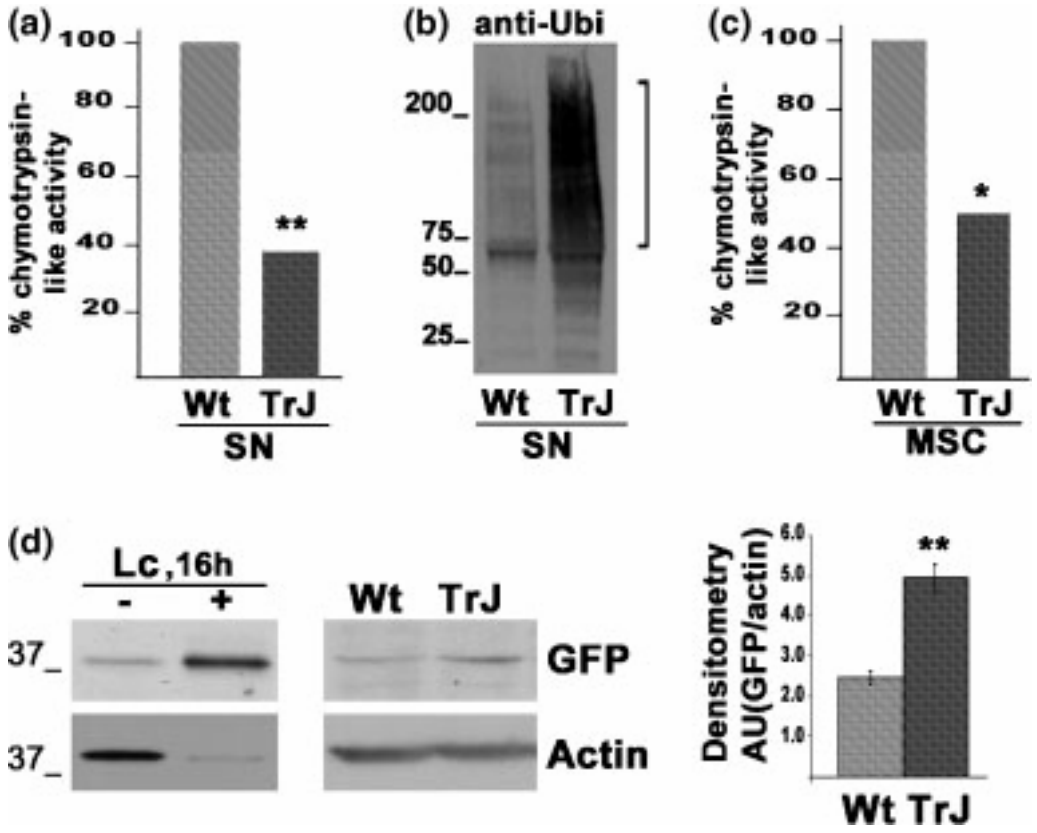

Figure 3-1. The degradative capacity of the proteasome is reduced in TrJ samples. Lysates of sciatic nerves (SN) (a) and mouse SCs (MSC) (c) from Wt and TrJ animals were assayed for the 20S chymotrypsin-like activity. The 20S activity was standardized to 20Sβ levels and arbitrarily set at 100% for Wt samples. The activity in TrJ samples was expressed as percentage of Wt (a, c), (*, $p<0.05$; **, $p<0.005$). The presence of ubiquitinated substrates in Wt and TrJ SN was determined by a Western blot with an anti-ubiquitin (Ubi) antibody (b). The bracket marks the increase in slow migrating ubiquitinated substrates in the TrJ sample (b). To assay the 26S overall activity, SCs from Wt and TrJ/+ mice were transiently transfected with Ub^{G76V}-GFP and the relative levels of GFP were evaluated by Western blot with an anti-GFP antibody (d). In normal MSC (d, left panel), the levels of Ub^{G76V}-GFP are increased upon 16h treatment (+) with the proteasome inhibitor lactacystin (Lc, 10 μM), as compared to untreated (-) cells. In TrJ MSC, Ub^{G76V}-GFP accumulates compared to Wt (d, middle panel). Actin was used as a loading control (d). The levels of GFP, corrected for actin, in four independent experiments were quantified by densitometry and graphed, corroborating the significant (**$p<0.005$) stabilization of Ub^{G76V}-GFP in TrJ MSC (d, graph). Molecular mass at the left, in kDa.

As expected, in normal SCs, transiently transfected with the Ub^{G76V}-GFP plasmid, a 16h treatment with lactacystin leads to a pronounced accumulation of GFP (Fig. 3-1D, left panel). When SCs isolated from Wt and TrJ nerves were transfected with the same plasmid and analyzed by Western blotting with an anti-GFP antibody, in TrJ samples GFP levels were elevated, as compared to Wt (Fig. 3-1D). After correction for actin (loading control), quantification of four independent experiments revealed ~2-fold relative increase of Ub^{G76V}-GFP levels in TrJ samples ($p<0.005$). Conversely, we did not detect impairment of proteasome activity or the accumulation of ubiquitinated substrates in samples from PMP22-deficient mice (data not shown).

The Subunits of the 26S Proteasome Are Recruited to PMP22 Aggresomes

The recruitment of proteasome subunits to disease-linked protein aggregates may contribute to compromised proteasome function (Lindsten and Dantuma, 2003; Hernandez et al., 2004). Therefore, we examined the relationship between PMP22 aggregates and constituents of the proteasome machinery in TrJ nerves (Fig. 3-2) and cultured SCs (Fig. 3-3). Sciatic nerves from ~1-year old Wt and heterozygous TrJ mice were stained with polyclonal anti-PMP22 or 20S antibodies (Fig. 3-2). In comparison to the myelin-like staining observed in Wt samples (Fig. 3-2A) (also see Notterpek et al., 1997), in ~28% of TrJ fibers PMP22 accumulates in perinuclear aggregates (Fig. 3-2B, arrows) (Table 1) (also see Fortun et al., 2003). In normal nerves, 20S-like immunoreactivity is diffuse, with discernible staining at paranodal regions (Fig. 3-2C, arrowheads), where lysosomes are also detected (Fig. 3-2C, inset, lower left) (Notterpek et al., 1997). Nonspecific rabbit serum does not label the nerves sections (Fig. 3-2C, inset, upper right). In neuropathy samples, 20S is prominent at perinuclear regions (Fig. 3-2D, arrows), an area where PMP22 aggregates accumulate (Fig. 3-2B).

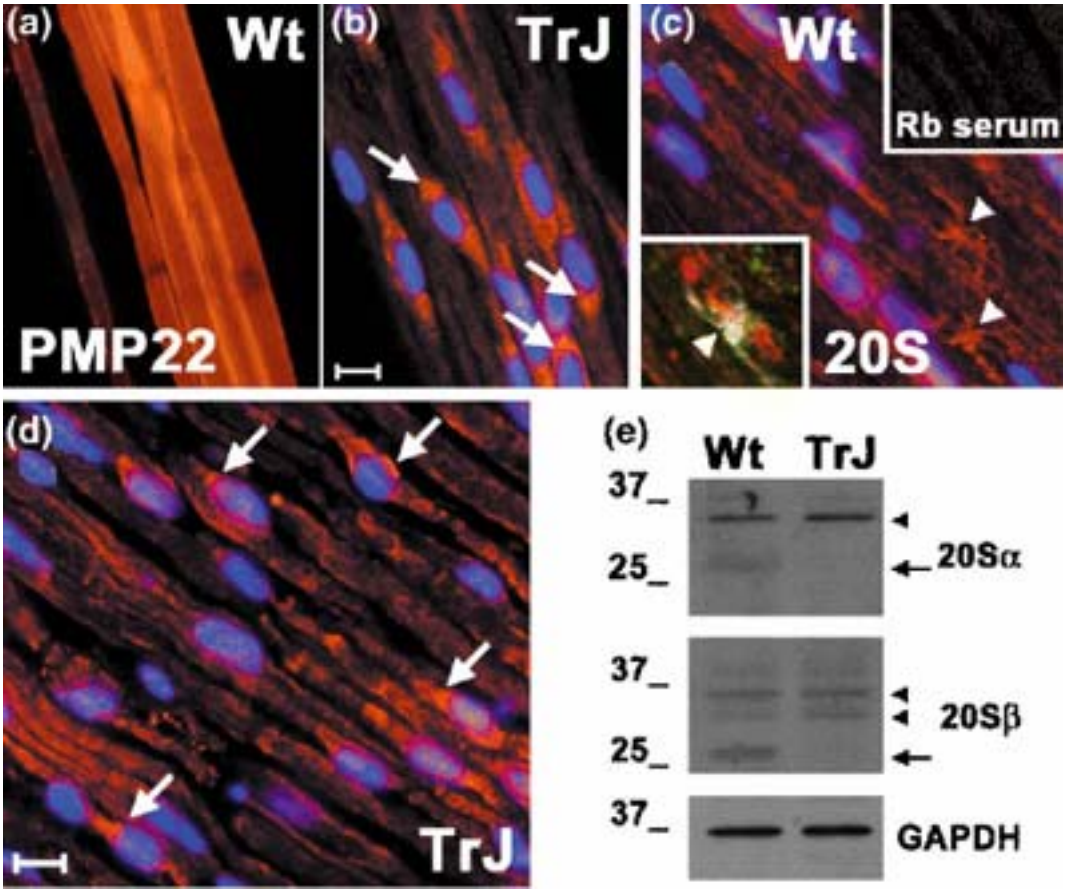

Figure 3-2: Levels and subcellular localization of the 20S proteasome in TrJ nerves. Sciatic nerve sections from Wt (a, c) and TrJ (b, d) mice were stained for PMP22 (red, a, b), 20S (red, c, d) and LAMP1 (green, c, inset). Compared to the normal myelin staining in Wt nerves (a), in TrJ nerves PMP22 accumulates at perinuclear regions in aggresome-like structures (b, arrows). In Wt nerves, the 20S localizes to paranodal regions (c, arrowhead), where LAMP1 is present (c, lower left inset, arrowhead), as well as in and around the nucleus of a subpopulation of SCs. Nonspecific rabbit (Rb) serum does not stain the nerves (c, upper right inset). In TrJ nerves, the 20S immunoreactivity is enlarged at perinuclear regions (d, arrows). Nuclei are visualized by Hoechst dye (blue, b-d). Scale bar, 10 μm (a-d). Western blot analysis (e) reveal that while the ~30 kDa subunits remains unchanged (arrowheads), the levels of the ~25 kDa 20Sα and 20Sβ subunits (arrows) are reduced in the TrJ, as compared to Wt. GAPDH is shown as a constitutive marker. Molecular mass at the left, in kDa.

The percentage of fibers with increased perinuclear 20S-like immunoreactivity is significantly lower ($p<0.01$) as compared to fibers with PMP22 aggregates (Table 3-1), indicating that not all PMP22 aggregates associate with proteasomes. A similar staining

pattern was detected when 20Sα or 20Sβ subunit-specific antibodies were used (data not shown). Despite the altered localization of the 20S in TrJ nerves, overall 20S protein levels are not dramatically altered (Fig. 3-2C-E). Western blot analysis of nerve lysates with the 20Sα and 20Sβ subunit-specific antibodies reveal that while the ~30 kDa subunits remain unchanged (arrowheads), the levels of the ~25 kDa subunits (arrows) are reduced in the TrJ sample, as compared to Wt. The same blot was reprobed with anti-GAPDH, as a loading control.

To further examine the relationship of the proteasome and PMP22 aggregates, proteasome-inhibited Wt and untreated TrJ SCs were immunostained with anti-PMP22 and anti-20Sα or 20Sβ antibodies (Fig. 3-3). As previously described in rat SCs (Lafarga et al., 2002), in DMSO-treated Wt mouse SCs, the 20Sα subunit concentrates at perinuclear regions, presumably the centrosome (Fig. 3-3A, arrows), with less intense nuclear and diffuse cytoplasmic staining. Within the same cells, PMP22-like immunoreactivity is low and diffuse (Fig. 3-3B), without apparent co-localization with 20Sα on overlay (Fig. 3-3C, arrows).

To promote the accumulation of endogenous Wt-PMP22 in aggresomes, parallel samples were incubated for 16h with lactacystin (Notterpek et al., 1999; Fig. 3-3D-F). In proteasome-inhibited cells, the localization of 20Sα does not change, but appears enlarged due to the recruitment of additional proteins to the centrosome (Wigley et al., 1999) (Fig. 3-3D, arrows).

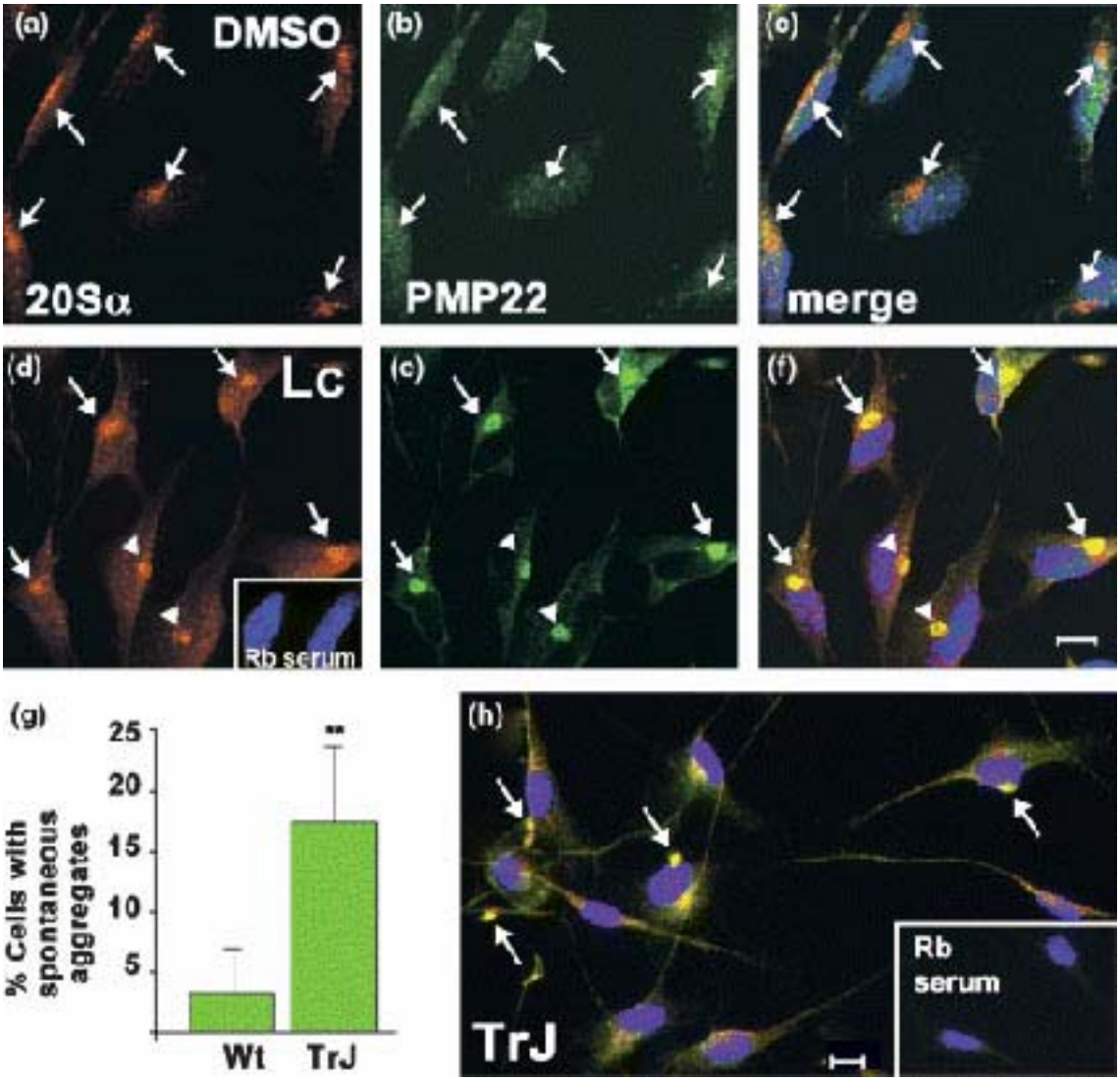

Figure 3-3: PMP22 aggresomes are immunoreactive for the 20Sα and β proteasome subunits. Normal mouse SCs treated with DMSO (a-c) or lactacystin (Lc) (d-f) were stained with anti-20Sα (red, A, C, D, F) and anti-PMP22 (green, b, c, e, f) antibodies. In DMSO-treated cells, the localization of 20Sα is perinuclear (a, arrows) and is distinct from PMP22 (b, arrows), as shown in the merged image (c). In proteasome-inhibited cells, the 20Sα (d) is found adjacent to (arrowheads) or co-localizing with (arrows) PMP22 aggresomes (e, f). Quantification of spontaneous PMP22 aggresomes in TrJ and Wt mouse SCs is shown (**$p<0.005$) (g). As with Lc-induced aggresomes (d-f), spontaneous TrJ-PMP22 aggresomes (green) colocalize with 20Sα (red) (h, arrows). The insets represent the binding of nonspecific rabbit serum to Wt (d) or TrJ (h) cells. Nuclei are visualized by Hoechst dye (blue). Scale bars, 10 μm (a-f, h).

In response to lactacystin treatment, most of PMP22 aggresomes (Fig. 3-3E) are immunoreactive for 20Sα, as revealed in the merged image (Fig. 3-3F, arrows). In a

subset of cells, the 20Sα is adjacent to the aggresomes (Fig. 3-3F, arrowheads). A similar pattern of colocalization with PMP22 aggresomes was seen when we used an anti-20Sβ subunit-specific antibody (not shown).

Next, we investigated whether spontaneous TrJ-PMP22 aggresomes formed in the absence of proteasome inhibition associate with the 20S subunits. In culture, ~17% of TrJ SCs contain spontaneous PMP22 aggregates, as compared to 3% in Wt (Fig. 3-3G, also see Table 3-1). The percentage of SCs with PMP22 aggregates is even higher in cultures from homozygous TrJ animals (Ryan et al., 2002). As seen in the merged image, spontaneous PMP22 aggregates are immunoreactive for the 20Sα (Fig. 3-3H, arrows), and 20Sβ subunits (not shown). Nonspecific rabbit serum does not label the cultured SCs (Fig. 3-3D, H, insets). Together, these results indicate that the proteasome associate with PMP22 aggregates formed under various conditions.

The 20S proteasome can be found alone or in association with the 19S and/or the 11S regulatory subunits (Hirsch and Ploegh, 2000). We previously detected an increase in the levels of the 11S regulatory subunit in TrJ nerves; however, protein localization was not assessed (Fortun et al., 2003). To examine the relationship of 11S with PMP22 aggregates, sciatic nerves from Wt and TrJ mice were studied (Fig. 3-4). In Wt samples, 11S-like immunoreactivity is low and diffuse throughout the fibers, with occasional bright staining near the nucleus (Fig. 3-4A, arrowheads). In comparison, distinct perinuclear 11S immunoreactivity is seen in many of the SCs in TrJ nerves (Fig. 3-4B, arrows). The relationship between 11S and PMP22 aggresomes in proteasome-inhibited SCs was also evaluated (Fig. 3-4C, D). In control cells, the 11S is detected in (asterisks) and around (arrows) the nucleus (Fig. 3-4C), with less intense, diffuse cytoplasmic

staining. When the proteasome is inhibited, the 11S forms ring-like structures around PMP22 aggresomes (Fig. 3-4D, arrows), in addition to remaining in the nucleus (asterisks). A similar 11S-like staining pattern was observed for spontaneous TrJ-PMP22 aggresomes seen in cultured SCs (data not shown).

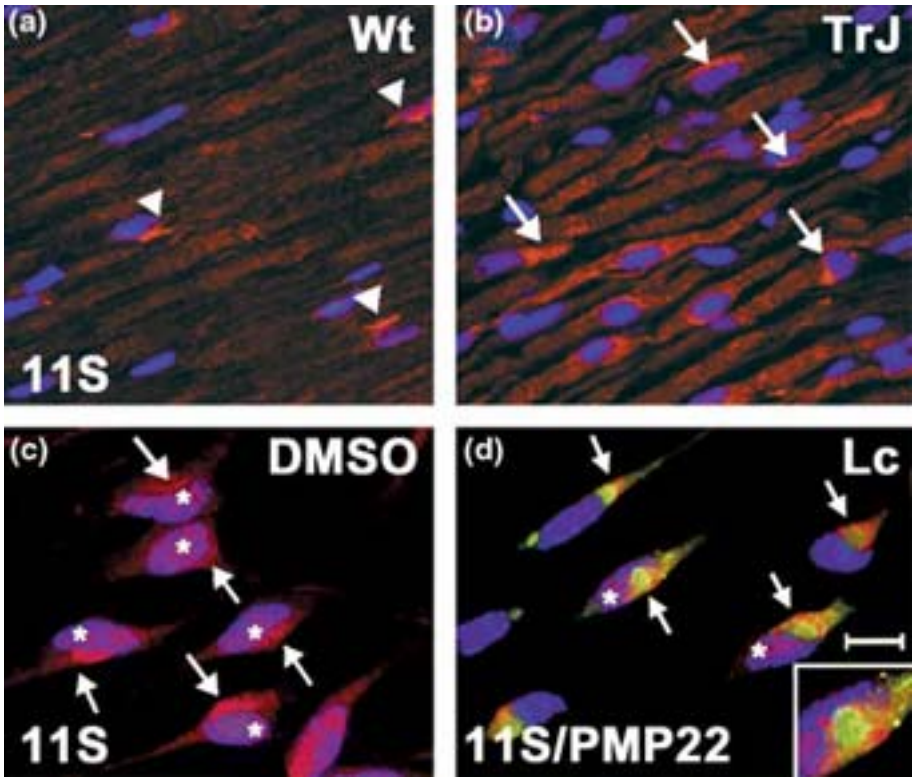

Figure 3-4: The 11S regulatory subunit closely associates with PMP22 aggresomes. Sciatic nerves from Wt (a) and TrJ (b) mice were stained with polyclonal anti-11S antibody. In Wt samples, 11S-like immunoreactivity is diffuse, occasionally bright next to the nucleus (a, arrowheads). In TrJ nerves, 11S perinuclear staining is enlarged and more prominent (b, arrows). Normal mouse SCs were treated with DMSO (c), or lactacystin (Lc) (d), and stained with anti-11S (red) and -PMP22 (green) antibodies. The 11S localizes to the nucleus (asterisks) and the perinuclear area (arrows). Upon proteasome inhibition (d), the 11S (red) forms ring-like structures surrounding PMP22 aggresomes (green, arrows). This relationship is denoted in the enlarged area (d, inset). Nuclei are visualized by Hoechst dye (blue, a-d). Scale bars, 10 μm (a-d).

Polyubiquitinated PMP22 Accumulates when the Proteasome Is Compromised

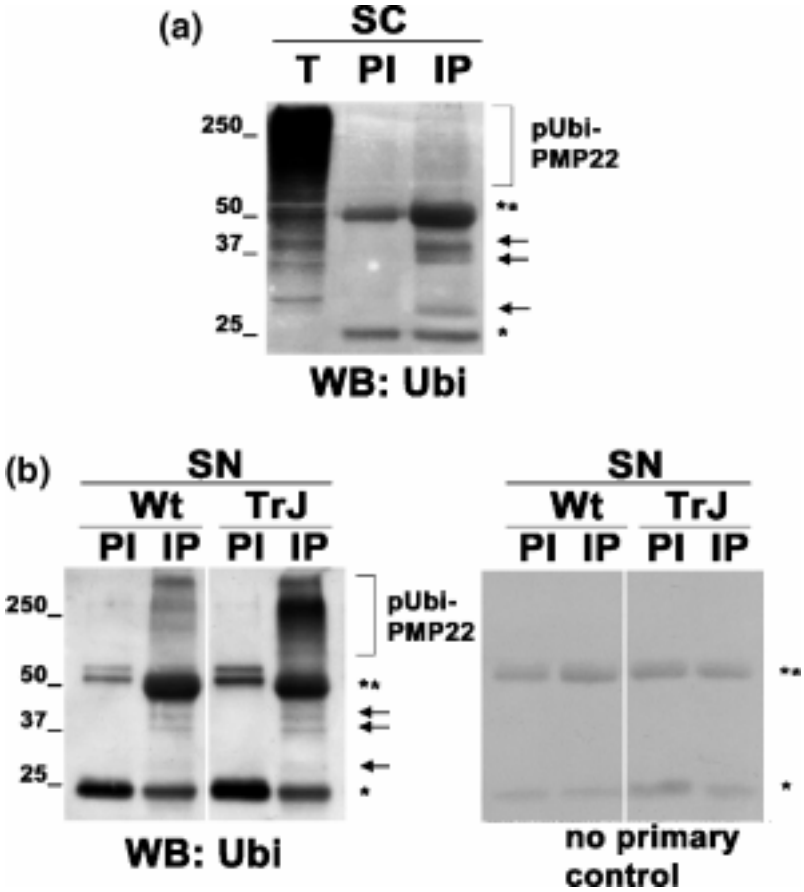

Figure 3-5: PMP22 is polyubiquitinated. PMP22 was immunoprecipitated (IP) from proteasome-inhibited rat SCs (a), or equal amounts (250 μg of soluble lysate) of Wt and TrJ sciatic nerve (SN) RIPA lysates (T) and the presence of ubiquitinated PMP22 was determined by Western blot with an anti-ubiquitin (Ubi) antibody (b). Nonspecific proteins were depleted by previous incubation with preimmune (PI) serum. As a control, blots were incubated with secondary antibody alone (b, no primary control). The light (*) and heavy (**) immunoglobulin chains are indicated. Brackets denote the slow migrating smear of ubiquitinated PMP22 (pUbi-PMP22) whereas arrows indicate smaller forms of ubiquitinated PMP22 (a, b). The levels of pUbi-PMP22 appear increased in TrJ, as compared to Wt nerves (b, bracket). Molecular mass at the left, in kDa.

Degradation of Wt and mutated-PMP22 *in vitro* is carried out mainly by the proteasome (Ryan et al., 2002). Since proteasomal degradation usually requires polyubiquitination and recognition by the 19S particle (Goldberg, 2003), we examined whether PMP22 is ubiquitinated (Fig. 3-5). PMP22 was immunoprecipitated (IP) from

total RIPA lysates (T) of proteasome-inhibited rat SCs (Fig. 3-5A), or equal amounts of Wt and TrJ sciatic nerves (Fig. 3-5B). The presence of ubiquitinated-PMP22 was then assessed by Western blotting the immunoprecipitates with a monoclonal anti-ubiquitin antibody. The heavy ~55 kDa (**) and light ~25 kDa (*) immunoglobulin chains are present in the preimmune (PI) and the IP lanes (Fig. 3-5A, B) and are recognized by the secondary antibody alone (Fig. 3-5B, no primary control). Both IP fractions however, contain specific bands at ~29, ~37 and ~43 kDa that most likely represent the mono-, bi- and tri-ubiquitinated PMP22, respectively (arrows). Because the intensity of the 55 kDa band (**) is higher in both IP fractions (compared to PI), whereas the 25 kDa Ig light chain (*) is not, and this is only observed with the anti-ubiquitin antibody but not in the no primary control, it is possible that a form of ubiquitinated PMP22 runs at ~50 kDa (the approximate molecular mass for tetra-ubiquitinated PMP22).

Significantly, a slow migrating smear of a polyubiquitinated-PMP22 is present in the IP (Fig. 3-5A, B, brackets), but not in the pre-immune fractions. Notably, when PMP22 was immunoprecipitated from equal amounts of Wt and TrJ nerve lysates, the intensity of these slow migrating bands (brackets) is elevated, as compared to Wt (Fig. 3-5B). Similar pattern is observed when the blot was incubated with the anti-PMP22 antibody (data not shown; also see Fortun et al., 2003), corroborating that the indicated bands represent polyubiquitinated PMP22. In agreement with the reduced proteasome activity in TrJ samples (Fig. 3-1), and the reduced turnover of the protein (Fortun et al., 2003), this result indicates that in affected nerves the pool of ubiquitinated PMP22 is elevated.

The Cytoplasmic Ubiquitin-Activating Enzyme E1, Associates with PMP22 Aggregates

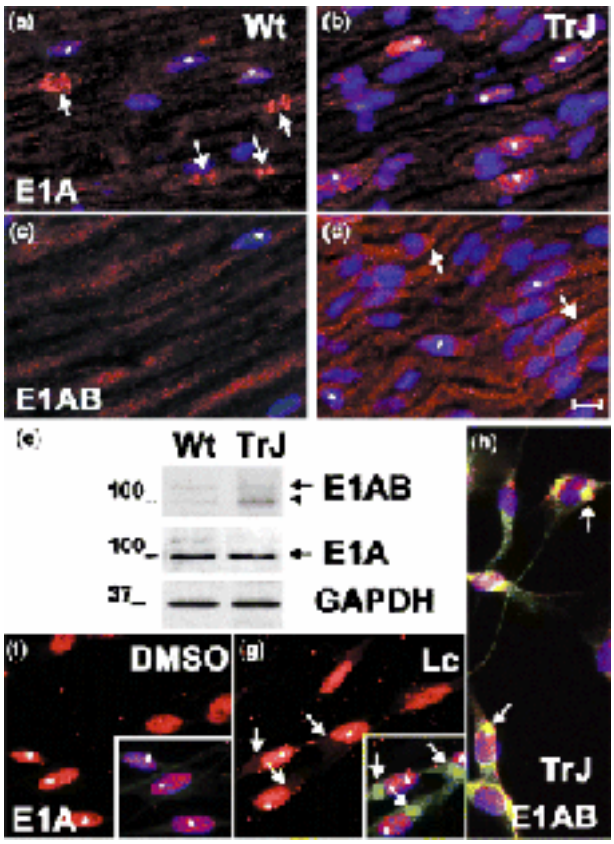

Figure 3-6: Selective recruitment of the ubiquitin-activating enzyme E1B to PMP22 aggregates. Sciatic nerves from Wt (a, c) and TrJ (b, d) mice were stained with anti-E1A (red, a, b) or E1AB (red, c, d) antibodies. In Wt nerves (a), the E1A isoform is detected at paranodal regions (arrows) and in the nucleus (asterisks). The nuclear localization of E1A in TrJ nerves is unchanged (b, asterisks). Using an antibody that recognizes both E1A and E1B isoforms (E1AB, c, d), we detected low and diffuse E1AB-like immunoreactivity in normal nerves (c). As with the E1A antibody, some nuclear staining (asterisks) is also observed in Wt (c) and TrJ (d) nerves. In TrJ fibers, the E1AB staining is concentrated at perinuclear areas (d, arrows). Western blots analysis of Wt and TrJ nerve lysates confirms the increase in E1B levels in TrJ (arrowhead), whereas the E1A is unchanged (arrows). GAPDH is shown as a constitutive marker. Molecular mass at the left, in kDa. Mouse SC from Wt (f, g) and TrJ (h) mice were stained for PMP22 (green, f-h) and E1A (red, f, g) or E1AB (h). Similar to nerves (a, b), E1A is exclusively nuclear (asterisks) and does not change despite the formation of PMP22 aggresomes (green in the inset, arrows) in Lc-treated cells (g). Spontaneous TrJ-PMP22 aggresomes (green, h, arrows) are immunoreactive for the E1AB antibody (red, h, arrows). Nuclei are visualized by Hoechst dye (blue, a-d, f-h). Scale bars, 10 μm (a-d, f-h).

Next, we examined if components of the ubiquitination machinery associate with MP22 aggregates. Currently, it is unknown which E2-E3 combination is responsible for recognizing and ubiquitinating PMP22. Therefore, the localization of the ubiquitin-activating enzyme E1, the only common enzyme in the ubiquitin pathway, was determined (Hernandez et al., 2004) (Fig. 3-6). Utilizing an E1A isoform-specific antibody, E1A is mainly seen in the nuclei (asterisks) of the SCs in both Wt (Fig. 3-6A) and TrJ (Fig. 3-6B) nerves. In Wt nerves, E1A is also found at paranodal regions (Fig. 3-6A, arrows), where the 20S and LAMP-1 are seen (Fig. 3-2C). To assess whether the E1B isoform is also excluded from the perinuclear region, another anti-E1AB antibody, directed to the common carboxyl-termini of both E1A and E1B isoforms was used (Fig. 3-6C, D).

Compared to Wt nerves (Fig. 3-6C), TrJ SCs exhibit increased immunoreactivity toward the E1AB antibody, mostly at perinuclear regions (Fig. 3-6D, arrows), where PMP22 aggregates accumulate (Fig. 3-2B). Similar to the E1A antibody (Fig. 3-6A, B), some nuclear staining is also visible (Fig. 3-6C, D, asterisks). Western blots analysis of Wt and TrJ nerve lysates confirms the elevated levels of E1B (Fig. 3-6E, arrowhead), but not E1A (Fig. 3-6E, arrows), in TrJ samples.

To exclude the possibility that poor epitope accessibility by the E1A antibody in the nerves is responsible for the lack of its association with aggregates, PMP22 aggresomes formed upon proteasome inhibition were studied (Fig. 3-6F, G). In control (Fig. 3-6F), as well as in proteasome-inhibited cells (Fig. 3-6G), E1A remains nuclear (asterisks), despite the formation of PMP22 aggresomes (Fig. 3-6G, arrows in inset). In comparison, lactacystin-induced (data not shown), as well as spontaneous TrJ-PMP22

aggresomes are immunoreactive for the E1AB antibody (Fig. 3-6H, arrows). Because of the distinct isoform specificity of the two antibodies, we attribute the differences in the E1-like immunoreactivity pattern to the recruitment of the cytoplasmic E1B, but not the nuclear E1A isoform, to perinuclear PMP22 aggregates.

MBP Is Recruited to PMP22 Aggregates in TrJ Nerves

Impairment of the 20S/26S in TrJ nerves will lead to the accumulation and potential aggregation of proteasomal substrate molecules. Therefore, we investigated the localization and detergent-solubility of the proteasome substrate MBP (Akaishi et al., 1996), which is an essential component of myelin (Fig. 3-7). In neuropathy samples, MBP-like immunoreactivity is uneven, and MBP aggregates are seen in ~8% of SCs (Fig. 3-7A, arrows) (also see Table 3-1). The percentage of TrJ fibers with MBP aggregates is significantly lower ($p<0.05$) than fibers with PMP22 aggregates, which together with the 20S pattern (Fig. 3-2) corroborates the heterogeneity of these aggregates (Table 3-1). For comparison, the uniform MBP staining along myelin internodes in Wt nerves is shown (Fig. 3-7B, inset). Teased fibers, coimmunostained for MBP (Fig. 3-7B) and PMP22 (Fig. 3-7C) demonstrate the misslocalization of these two myelin proteins to perinuclear aggregates (Fig. 3-7D, arrows).

Since a characteristic of aggregated proteins is detergent-insolubility (Johnston et al., 1999), nerves of Wt and TrJ mice were lysed in IPB buffer and analyzed by Western blotting with anti-MBP antibody (Fig. 3-7E). Due to demyelination, the total (T) levels of the four MBP isoforms are reduced in the TrJ sample, compared to Wt (Fig. 3-7E) (Notterpek et al., 1997). In Wt nerves, MBP partitions into both fractions, with a preference for the detergent-soluble pool (Fig. 3-7E). In TrJ nerves, the detergent-solubility of the ~14 kDa isoform (arrowhead) remains unaltered, while the larger

isoforms become more insoluble (Fig. 3-7E, arrows). Quantification of five independent experiments demonstrate a ~2-fold increase in the detergent-insolubility of MBP in TrJ nerves, as compared to Wt ($p<0.05$).

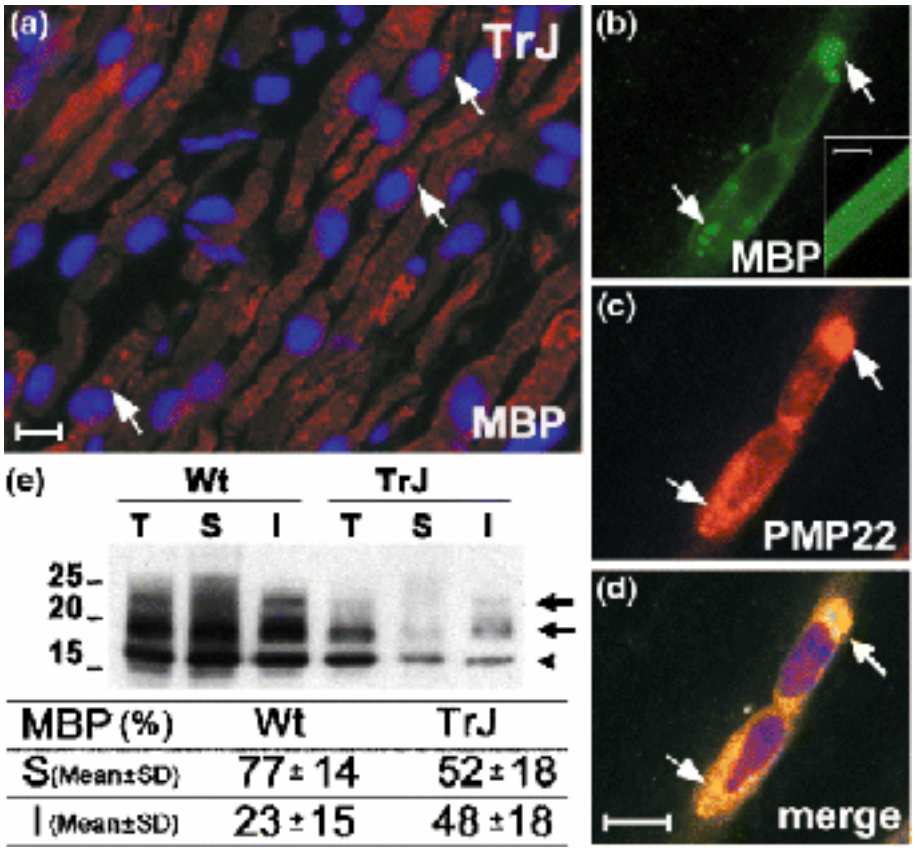

Figure 3-7: Localization of MBP to PMP22 aggregates in TrJ nerves. Sections (a) and teased fibers from TrJ (b-d) and Wt (b, inset) mouse nerves were stained for MBP (red, a, green, b, d) and PMP22 (red, c, d). In TrJ nerves, MBP-like immunoreactivity is irregular, localizing at perinuclear regions in a subset of fibers (a, arrows). Compared to the uniform myelin staining in Wt (b, inset), a close association between perinuclear MBP (b) and aggregated PMP22 (c) is visible in TrJ fibers (b-d, arrows). The total levels (T) and detergent-solubility (S: soluble, I: insoluble) of MBP were determined by anti-MBP Western blot of IPB-lysates from Wt and TrJ nerves (e). In the TrJ sample, the detergent-solubility (S) of the higher molecular weight MBPs are decreased (e, arrows), whereas the solubility of the 14 kDa isoform is unaltered (e, arrowhead). Soluble (S) and insoluble (I) MBP was quantified as percentage of total in five independent experiments, and is shown in a table as the mean ± standard deviation (SD). The partition of MBP to the insoluble fraction is significantly increased in TrJ compared to Wt nerves ($p<0.05$). Molecular mass at the left, in kDa.

Discussion

The studies described here show that similar to CNS neurodegenerative disorders, the presence of protein aggregates correlates with reduced activity of the proteasome in TrJ neuropathy nerves, as compared to Wt. Coincidently, ubiquitinated proteasome substrates, including PMP22 and MBP, accumulate in cytosolic aggregates that recruit components of the ubiquitin-proteasomal pathway. These results indicate a commonality among cytosolic aggregates formed in different cell types and under a variety of conditions with regards to changes in the activity and localization of the proteasome (Keller et al., 2000; Waelter et al., 2001; McNaught et al., 2003; Kabashi et al., 2004).

The degradative capacity of the proteasome can become compromised due to oxidative stress, age, expression of mutated/damaged proteins or the presence of protein aggregates (Carrard et al., 2002). The degree of proteasome impairment appears to be tissue specific and in some instances correlates with neurodegeneration (Keller et al., 2000; McNaught et al., 2003; Zhou, et al., 2003). Although the mechanism of proteasome impairment in TrJ neuropathy is yet unknown, increased targeting of the mutated TrJ-PMP22 for degradation during attempts of remyelination might be a key factor. In normal myelinating SCs, ~80% of the newly-synthesized PMP22 is rapidly degraded, possibly due to misfolding (Pareek et al., 1997). The inability of the TrJ protein to fold correctly, as demonstrated *in vitro* by the α-helix-to-β-sheet transition in the first transmembrane domain of the mutated protein (Yamada, et al., 2003), would further increase the amount of PMP22 destined for degradation. Displacement of the equilibrium between TrJ-PMP22 synthesis/folding and degradation is likely to play a role in the subcellular pathogenesis of the neuropathy.

Reduced levels of proteasomal subunits are known to influence proteasome activity (Carrard et al., 2002). In our model, the levels of the 25 kDa 20S proteasome subunit are slightly reduced (Figure 2), similar to the tissue-specific decrease found in Parkinson's disease (McNaught et al., 2003). Additional factors however, such as the assembly of functional proteasomes, or the localization of the subunits may have also contributed to the observed alterations (Fig. 3-1). For example, the accumulation of precursor proteasomes in a hepatoma H6 cell line has been shown, suggesting that the formation of catalytically active proteasomes is inefficient in rapidly-dividing cells (Nandi et al, 1997). Since the SCs in TrJ nerves are known to hyperproliferate (Notterpek et al., 1997; Robertson et al., 1997), their ability to assemble fully active proteasomes may be compromised and contribute to impaired activity. With regards to the localization of subunits, the 20S proteasome, and its regulatory subunits, associate with spontaneous and pharmacologically-induced PMP22 aggresomes (Figures 2-4), which if trapped in nonfunctional complexes could have also contributed to the reduced activity. Components of the ubiquitin-proteasomal machinery frequently associate with different protein aggregates (Waelter et al, 2001; Schmidt et al., 2002; Ardley et al., 2003; Kabashi et al., 2003; Tanaka et al., 2004). This strategic localization of proteasome subunits at sites of aggregation might represent an attempt to clear misfolded proteins, as suggested by the proteasome-dependent clearance of mutated huntingtin and Cu, Zn superoxide dismutase inclusions (Martin-Aparicio et al., 2001; Puttaparthi et al., 2003). Conversely, the 20S may be trapped within aggregates and become non-functional further compromising the activity of the proteasome and thus leading to a positive feedback mechanism (Hernandez et al., 2004). Moreover, failure of substrates to translocate into

the catalytic chamber can lead to their stable association with the proteasome and inhibition of overall proteolysis (Navon and Goldberg, 2001). In agreement, expression of an aggregation-prone poly-Q-containing polypeptide led to a general inhibition of proteasomal degradation (Bence et al., 2001; Venkatraman et al., 2004).

In addition to the 26 proteasome, the cytoplasmic isoform of the ubiquitin-activating enzyme E1B is also recruited to PMP22 aggregates, whereas the E1A isoform is not. Therefore, components of the ubiquitination machinery are selectively recruited to PMP22 aggregates, likely preserving the compartmentalization between cytoplasmic and nuclear constituents. The higher levels of ubiquitinated substrates in TrJ nerves illustrate that the process of ubiquitination is functional. The possibility of aberrant tagging and thus escape of proteasome recognition, however, has not been ruled out. Additionally, the increase in the levels the 11S (Fortun et al., 2003) and the E1B isoform in TrJ nerves might represent an autoregulatory feedback loop to compensate for the reduced proteasome activity (Meiners et al., 2003).

The accumulation of PMP22 in cytosolic aggregates likely represents an intermediate stage between the inability of the proteasome to degrade its substrates and the removal of misfolded proteins by the autophagy/lysosomal pathway (Fortun et al., 2003). Previous studies with pharmacological inhibitors of the proteasome revealed an association between chronic proteasome malfunctioning and activation of autophagy (Ding et al., 2003). However, it appears that the autophagic/lysosomal pathway in adult neuropathy nerves is unable to clear all of the aggregates, which then accumulate (Fortun et al., 2003). A putative toxicity associated with aggresomes is the recruitment of essential proteins to the site of aggregation and their entrapment in nonfunctional

complexes (Hernandez et al., 2004). In our model, MBP is found at ~30% of perinuclear PMP22 aggregates, which correlates with an increase in detergent-insolubility (Fig. 7). The misslocalization of MBP together with PMP22 at perinuclear aggregates is likely to alter the stability of myelin and contribute to demyelination. Altered disposition of MBP to aggregates has been reported previously, in peripheral nerves of leukodystrophy patients (Vaurs-Barriere et al., 2003).

In summary, our data indicates that in TrJ nerves, slowed turnover rate of PMP22 and its accumulation in cytoplasmic aggregates (Fortun et al., 2003) correlates with reduced activity of the proteasome. A redistribution of proteasomal components to sites of protein aggregation accompanies the compromised proteasome activity. Future studies will reveal if the proteasome machinery is similarly affected in other PMP22-associated neuropathies and whether additional myelin constituents are trapped in nonfunctional complexes.

CHAPTER 4
ENHANCEMENT OF AUTOPHAGY AND EXPRESSION OF CHAPERONES HINDERS THE FORMATION OF PMP22 AGGRESOMES

Note

The results presented in this chapter are being prepared for submission to the Journal of Cell Science. Drs. Lucia Notterpek and William Jr. Dunn contributed to this work. Ms. Debbie Akin helped with the electron microcopy studies.

Introduction

Peripheral myelin protein 22 (PMP22) is a highly hydrophobic, transmembrane glycoprotein expressed mainly in myelinating Schwann cells (SCs) (Snipes et al., 1992). Mutations in PMP22 have been associated with hereditary demyelinating neuropathies among which, Charcot Marie Tooth type 1A (CMT1A) is the most common form (Young and Suter, 2001). Although the molecular mechanisms underlying CMT1A are not well understood, halted intracellular trafficking and formation of protein aggregates are believed to play a role (D'Urso *et al.*, 1998; Tobler *et al.*, 1999; Naef and Suter, 1999; Colby *et al.*, 2000; Fortun et al., 2003; 2005). We previously demonstrated that PMP22 accumulates in spontaneous aggregates in SCs of a CMT1A model, the Trembler J (TrJ) mouse (Ryan et al., 2002; Fortun et al., 2003). Protein aggregates are thought to form as a result of an imbalance between synthesis/folding and degradation, and are the pathological hallmark of several neurodegenerative conditions (Ciechanover and Brundin, 2003). Indeed, PMP22 aggregates in the TrJ model recruit proteasomal constituents and correlate with impaired proteasome activity, which could contribute to

cellular dysfunction by interfering with overall degradation of proteasome substrates (Fortun et al., 2005). On the other hand, PMP22 aggregates associate with molecular chaperones and autophagic-lysosomal components, which could be involved in the dissolution of the inclusions (Fortun et al., 2003).

Given the biological importance of protein aggregates, a better understating of their formation is of great interest (Goldberg, 2003). The events influencing the assembly of new aggregates are difficult to follow or manipulate in vivo; therefore, we used an in vitro approach entailing pharmacological inhibition of the proteasome (Notterpek et al., 1999). In cultured cells, proteasome inhibitors are widely used to study the degradation and aggregation of proteins associated with different diseases, including cystic fibrosis, Parkinson's disease, polyglutamine and polyananine expanded disorders, among others (Johnston et al., 1998; Waelter et al., 2001; Martin-Aparicio et al., 2001; Abu-Baker et al., 2003; Rideout et al., 2004; Goldbaum and Richter-Landsberg, 2004). In SCs, proteasome inhibition results in the formation of PMP22 aggresomes (Notterpek et al., 1999) that are similar to the spontaneous aggregates detected in the TrJ model (Ryan et al., 2002; Fortun et al., 2003). Aggresomes are cytoplasmic membrane-free aggregates that form in a central location (centrosome) and are excluded from the main organelles (Johnston et al., 1998).

In this study, we examine whether the formation of PMP22 aggresomes upon proteasome inhibition can be influenced by the activation of macroautophagy and molecular chaperones. Macroautophagy is a constitutive event by which, substrates or even entire organelles are engulfed within autophagosomes that are delivered for lysosomal degradation (Klionsky and Emr, 2000). We previously demonstrated that

macroautophagy is involved in the removal of pre-existing PMP22 aggregates (Fortun et al., 2003). However, it is yet unknown if modulation of autophagy could influence the assembly of new aggresomes. Similarly, heat shock proteins (HSPs) are molecular chaperones known to interfere with the formation of aggregates, either by aiding protein degradation or (re)folding (Muchowski and Wacker, 2005). Notably, HSPs and autophagic components are recruited to PMP22 aggregates (Ryan et al., 2002; Fortun et al., 2003).

Here we show that the formation of PMP22 aggresomes is hindered by enhancement of autophagy and elevated expression of HSPs. Moreover, proteasome inhibition and subsequent formation of aggresomes results in the activation of autophagy. These results suggest a cross-talk between cellular pathways and open the possibility for different therapeutic approaches to prevent the accumulation of PMP22 in aggregates that could interfere with normal SC biology.

Materials and Methods

Aggresome Formation

Primary rat SC cultures were established and maintained as described (Notterpek et al., 1999). Cells were grown to ~80% confluency in 10% fetal calf serum (Hyclone, Logan, UT), 5 μM forskolin (Calbiochem, La Jolla, CA) and 10 μg/ml bovine pituitary extract (Biomedical Technologies Inc, Stoughton, MA) containing Dulbeccos' modified eagle's medium. SCs were treated with the proteasome inhibitor lactacystin (10 μM) (Biomol Research Laboratories, PA) to accumulate PMP22 in aggresomes, or its vehicle, dimethlysulfoxide (DMSO) (Sigma), as a control (Notterpek et al., 1999). Treatments were preformed for 12h or 16h, as indicated in the text. The proteasome inhibitors epoxomicin (5μM) and MG-132 (20μM) (both from Biomol) were also used to exclude

the effects were unique to lactacystin. After each treatment paradigm, SCs were immediately processed for immunostaining to visualize the aggresomes, or for Western blotting to evaluate the accumulation of ubiquitinated proteins (Notterpek et al., 1999).

Modulation of Aggresome Formation by Autophagy and Molecular Chaperones

To determine the effects of macroautophagy (from this point on referred to as autophagy) and molecular chaperones on the formation of aggresomes, the proteasome inhibition was carried out in the absence or the presence of the following modulators. To stimulate autophagy, SCs were incubated in media deprived of amino acids and serum (starvation medium) (Fortun et al., 2003), or treated with rapamycin (200nM) (Calbiochem) (Ravikumar et al., 2004), alone or with proteasome inhibitors. To block autophagy, 3-methyladenine (3MA) (10 mM) (Sigma) was included, without or during proteasome inhibition, in normal or starvation medium (Fortun et al., 2003). To evaluate the effects of elevated HSPs levels, two approaches were taken, with and without Lc. In the first paradigm, cells were treated with geldanamycin (125 nM-2 μM) (McLean et al., 2004) for 16h. Alternatively, cells were incubated at 45°C for 20min (heat shock) followed by a chase for 0-16h (Allen et al., 2004). Cells with aggresomes were visualized by immunostaining with anti-PMP22 and anti-ubiquitin antibodies.

Immunostaining Procedures and Aggresome Quantification

SCs on glass coverslips were fixed with 4% paraformaldehyde for 10 min and permeabilized with 0.2% Triton Tx100 for 15 min at room temperature. After blocking with 10% goat serum, the samples were incubated with the indicated primary antibodies overnight at 4°C. Bound antibodies were detected using Alexa Fluor 594-conjugated (red) anti-rabbit and Alexa Fluor 488-conjugated (green) anti-mouse antibodies (Molecular Probes, Eugene, OR). Samples were then mounted using the Prolong Antifade

kit (Molecular Probes). Images were acquired with a SPOT digital camera (Diagnostic Instrumentals, Sterling Heights, MI) attached to a Nikon Eclipse E800 (Tokyo, Japan) or an Olympus MRC-1024 confocal microscope. The number of cells with aggresomes was counted and expressed as a percent of total cells, as detected by nuclear staining with Hoechst #33258 (Molecular Probes, Eugene, OR). All experiments were repeated independently three times, and in each one, cells in eight different visual fields (0.277μm^2 area) were counted. The criteria for aggresome counting included: 1) immunoreactivity for ubiquitin and PMP22; 2) assembly at perinuclear region 3) exclusion from ER and Golgi 4) diameter larger than 1μm. Statistical significance between the various paradigms was evaluated using a Student's t-test. Images were processed for printing using Adobe Photoshop 5.0 (Adobe Systems, San Jose, CA).

Primary Antibodies

To detect PMP22 in the studied samples, a mouse monoclonal antibody was used (Chemicon, Temencula, CA). A polyclonal rabbit anti-LC3 antibody was utilized to monitor autophagy (gift form Dr. Dunn). Antibodies for protein chaperones used included calnexin and heat shock protein 70 (Hsp 70) (both from Stressgen, Victoria British Columbia, Canada). Monoclonal anti-actin, -tubulin (both from Sigma), -ubiquitin (Santa Cruz Biotechnology, CA) and polyclonal anti-GFP (gift form Dr. Shaw), -ubiquitin (Dako, Carpinteria, CA), cathepsin D (Cortex Biochem, San Leandro, CA), mTor (Cell Signaling Technology, MA) were obtained from the indicated suppliers.

Western Blot Analyses

After exposure to the specified conditions, SCs treated were lysed with 3% sodium dodecylsulfate (SDS) Laemmli buffer supplemented with protease inhibitors (Fortun et al., 2005). Protein lysates were separated on SDS gels and transferred onto

nitrocellulose or PVDF membranes (for ubiquitin and LC3). Blots were blocked and incubated with the indicated primary antibodies. After incubation with anti-rabbit or anti-mouse horseradish peroxidase (HRP) conjugated secondary antibodies (Sigma, St. Louis, MO), membranes were reacted with an enhanced chemiluminescent substrate (Perkin Elmer, Boston, MA). Films were digitally imaged using a GS-710 densitometer (Bio-Rad Laboratories).

Evaluation of Ub^{G76V}-GFP Levels

SCs plated at equal densities were transfected with an Ub^{G76V}-GFP reporter construct (Dantuma et al., 2000) using the lipofectamine method (Invitrogen, Life Technology, Carlsbad, CA). The attachment of a mutated uncleavable ubiquitin moiety to GFP results in a fusion protein (Ub^{G76V}-GFP) that is rapidly degraded by the proteasome and is hardly detected under normal conditions (Dantuma et al., 2000). The efficiency of transfection was monitored using the GreenLantern GFP plasmid (Invitrogen) and was ~43% (Fortun et al., 2003). Twenty-four hours after transfection, the cells were treated with Lc (10 μM) with or without autophagy modulation, as explained in the text. Sixteen hours later, cells were imaged for GFP expression and phase contrast using a T1-SM inverted microscope equipped with a Nikon DS-L1 camera. To quantify the levels of GFP, samples were processed for Western blot using anti-GFP and anti-tubulin (loading control) antibodies. The intensity of bands was quantified using Scion Images Software (Scion, Frederick, MD). The relative levels of Ub^{G76V}-GFP were expressed as the absorbance units of the GFP band, after correction for tubulin. The results from duplicates of three independent experiments were averaged, graphed and analyzed using a Student's t-test.

Ultrastructural Studies

SCs treated with or without proteasome inhibitors for 12h or 16h were fixed in 2 % para-formaldehyde and 2.5 % glutaraldehyde in 0.1 M sodium cacodylate buffer (pH 7.5) 7% sucrose at 4°C for 60 min. The specimens were then treated with 2 % OsO_4, stained with uranyl acetate, dehydrated and embedded in Epon resin. For localization of acid phosphatase (AP) activity, samples after fixation were treated with cytidine 5'-monophosphate and cerium chloride (Lenk et al., 1992). The product of this reaction labels lysosomes and autolysosomes. The sections were examined on a JEOL 100CX transmission electron microscope. Representative electron-micrographs were scanned and process for printing in Adobe Photoshop. The volume of autophagosomes divided by the volume of cytoplasm was determined in 8 independent samples of proteasome inhibited or control cells. The results are presented as percent, and statistical differences evaluated using a Student's t test.

Results

The Formation of PMP22 Aggresomes Is Hindered by Enhancement of Autophagy and Promoted by Its Inhibition

PMP22 accumulates in aggresomes after treatment with the proteasome inhibitor, lactacystin (Lc) (Notterpek et al., 1999). To determine the effect of autophagy on the assembly of new PMP22 aggresomes, the proteasome was inhibited in SCs, with and without modulation of autophagy (Fortun et al., 2003). The experiments were carried out for 12h and 16h. We choose 16h as the end point because is the time at which, mostly all SCs contain PMP22 aggresomes (Fig. 4-1A) (Notterpek et al., 1999), as compared to DMSO-treated control cells (Fig. 4-1A, inset), without inducing cell death, as previously shown (Fortun et al., 2003). When simultaneous to proteasome inhibition, autophagy is

stimulated by depriving the cells from amino acid and serum (starvation, Stv), fewer cells contain PMP22 aggresomes (Fig. 4-1B). To confirm the specificity of this approach, the effect of starvation on autophagy activation was blocked with 3MA (Fortun et al., 2003). When 3MA is included (Fig. 4-1C), most of the cells still contain PMP22 aggregates, indicating that the reduction in the number of aggresomes by starvation was indeed autophagy-dependent (compare B and C). The aggregates formed however, are not as compact as the ones after proteasome inhibition alone (compare 1C with 1A) or in combination with 3MA (compare 1C with its inset), suggesting that the blockage of the autophagic response is only partial and/or other cellular events might be involved. The levels or the localization of PMP22 are not affected in cells incubated independently with starvation media or 3MA alone (not shown). In proteasome inhibited cells, fed with amino acid and serum, inclusion of 3MA did not have any significant effect at 16h (Fig. 4-1C, inset), as compared to Lc alone (Fig. 4-1A).

The percent of cells with aggregates in independent experiments was determined, confirming that during a 16h proteasome inhibition, enhancement of autophagy results in a significant reduction in the formation of aggregates (Fig. 4-1D, solid bars). Similar results were obtained when autophagy was stimulated by rapamycin treatment (not shown; 27%±4; p=0.32).We then examined the effect of autophagy on the number of cells with aggregates after a shorter proteasome inhibition (12h, Fig. 4-1D, diagonal bars) and compare this with the 16h period. We choose the 12h middle point because is the time at which, about half of the cells contain aggresomes, as compared to 16h (Fig. 4-1D). Similar to 16h, when autophagy is enhanced by starvation, significantly lower number of cells forms aggresomes after 12h of proteasome inhibition. Note there are no

statistical differences between these two points, suggesting that the enhancement of autophagy halts the formation of aggresomes. Even after 24h of Lc and starvation, the percent of cells with aggregates (33.75%±12.39) remains the same ($p=0.97$). Inclusion of 3MA in Lc-treated starved SCs significantly increases the number of cells with aggregates, confirming that the effect of starvation is autophagic-dependent. Yet, the blockage of starvation-induced autophagy by 3MA, although complete at 12h, is only partial at 16h since the number of cells with aggregates is still reduced, as compared to Lc alone.

So far, the results presented indicate that enhancement of autophagy hinders aggresome formation. Next, we examined if inhibition of autophagy has the opposite effect. For this, the number of cells containing aggregates was determined in fed cells treated with 3MA and Lc to inhibit simultaneously autophagy and the proteasome, respectively (Fig. 4-1D). The formation of aggresomes during simultaneous inhibition of autophagy and proteasome for 12h is increased compared to Lc-12h alone, but statistically similar than Lc-16h alone (Fig. 4-1D), suggesting that blocking autophagy accelerate the accumulation of proteins in aggresome. Autophagy inhibition alone by 3MA does not result in the formation of aggresomes (not shown). Similar results (not shown) were obtained using another proteasome inhibitor, epoxomicin (Webb et al., 2003). The following experimental designs were performed at 16h of proteasome inhibition because this point is the minimum time required to induce aggresome formation in the majority of cells without affecting cell death.

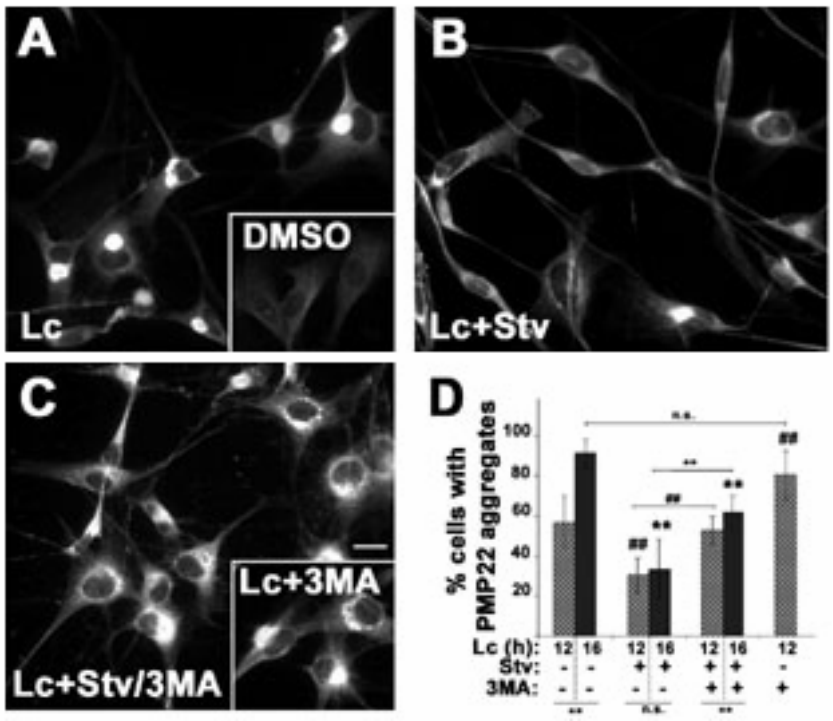

Figure 4-1: Formation of aggresomes is modulated by autophagy. The formation of aggresomes upon 16h of proteasome inhibition in the absence (A) or the presence of autophagic modulators (B, C) was monitored by immunostaining with anti-PMP22 antibody (A-C). SCs were treated with the proteasome inhibitor lactacystin (Lc, A-C) or DMSO (A, inset) in normal (A), or amino acid and serum deprived (B, C, Stv) media. The inhibitor of autophagy 3-methyladenine (3MA) was included in proteasome inhibited cells with (C) or without (C, inset) autophagy stimulation. Scale bar, 10μm (A-C). The percent of cells with aggregates after the indicated paradigms for 12h (diagonal bar) or 16h (solid bar) were counted (D). Differences in the effect of autophagy modulation, compared to Lc alone at 16h (**,$p<0.005$) or 12h (##,$p<0.005$) are denoted. Connecting horizontal lines represent the significance between the corresponding treatments (**,$p<0.005$; n.s., not significance).

Aggresome formation after proteasome inhibition results in the overall accumulation of unrelated proteasomal substrates (Johnston et al., 1998; Bence et al., 2001). Thus, we determined if the effect of starvation-induced autophagy on the reduction in the amount of cells with aggregates correlate with lower levels of proteasome substrates (Fig. 4-2). For this, we used two approaches. First, because ubiquitinated substrates accumulate upon proteasome inhibition (Johnston et al., 1998),

the levels of slow migrating ubiquitinated proteins were evaluated by western blot (Fig. 4-2A). Compared to control cells, Lc alone results in the accumulation of slow migrating ubiquitinated proteins, which is slightly reduced if autophagy is stimulated by starvation (Stv). Ubiquitinated proteins do not accumulate in starved cells alone. The levels of the monomeric ubiquitin (Fig. 4-2A, arrows) are reduced in Lc-treated cells, as compared to control, likely due to its utilization in the assembly of polyubiquitinated chains and conjugation to the substrates, forming the detected slow migrating ubiquitinated forms. Actin is shown as a loading control.

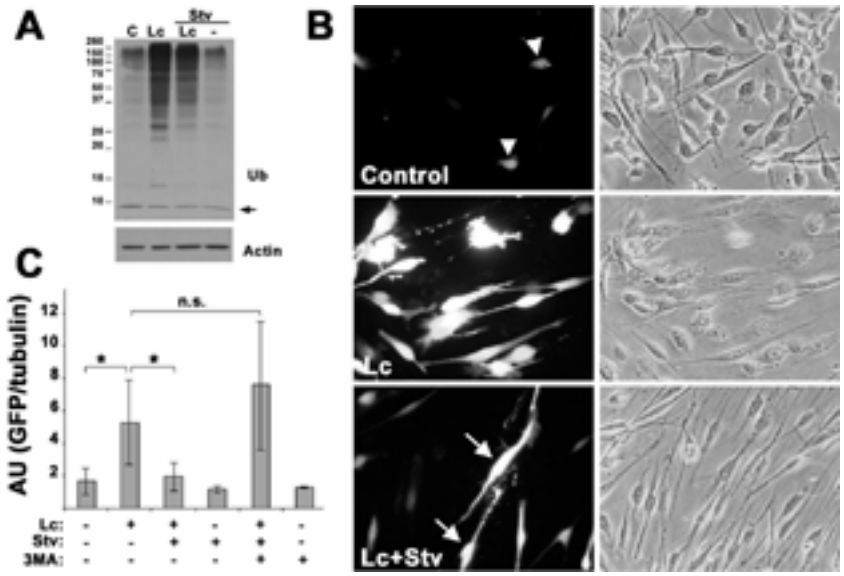

Figure 4-2: Reduced aggresome formation correlate with degradation of proteasomal substrates. Fed and starved cells (Stv) were treated with DMSO control (C) or Lc for 16h and western blotted with anti-ubiquitin (Ub) and –actin antibodies (A). Arrow denotes the monomeric Ub (A). Cells infected with Ub^{G76V}-GFP and treated as indicated were imaged for GFP expression (B, left column) or phase contrast (B, right column). Arrowheads indicate the low levels of GFP expression in control cells. Arrows point at a small percent of higher expressing cells in starved cells incubated with Lc (B). The stabilization of GFP signal was evaluated by the levels of GFP corrected for tubulin (C). AU: absorbance units; duplicates of n=3; *, $p<0.05$; n.s., no significant differences.

As an alternative method to evaluate the levels of proteasome substrates, the accumulation of Ub^{G76V}-GFP was determined. Attachment of the uncleavable Ub^{G76V} to

GFP targets this otherwise stable protein for rapid proteasome degradation and thus, the levels are hardly detected unless the proteasome is inhibited (Dantuma et al., 2000). SCs were transiently transfected with Ub^{G76V}-GFP, and following 24h, the proteasomal and autophagic pathways were modulated as indicated (Fig. 4-2B, C). After each treatment, the cells were imaged for fluorescence (Fig. 4-2B, left column) and phase contrast (Fig. 4-2B, right column). Because of the rapid turnover rate of Ub^{G76V}-GFP (Dantuma et al., 2000), GFP levels are very low (arrowheads) or undetectable in most SCs (Fig. 4-2B, control). When the proteasome is inhibited, the Ub^{G76V}-GFP protein accumulates (Fig. 4-2B, Lc). Confocal microscopy indicated that the Ub^{G76V}-GFP is found throughout the cytosol, partially co-localizing with, but not exclusive to, PMP22 aggresomes (not shown). However, when autophagy is simultaneously enhanced by starvation (Fig. 4-2B, Lc+Stv), the number of cells with GFP fluorescence is considerably reduced. This effect correlates with the ability of autophagy to hinder aggresome formation (Fig. 4-1). Thus, degradation of aggregates by macroautophagy likely accounts for the reduction of aggregate formation and the accumulation of proteasomal substrates. In a small percent of these cells however, intense Ub^{G76V}-GFP signal is still detected (Fig. 4-2B, Lc+Stv arrows), likely representing the pool of GFP that is not degraded by autophagy.

To corroborate this result, transfected and treated cells as above were lysed and analyzed by western blot. The levels of GFP, after correction for tubulin, were determined in duplicates from three independent experiments, quantified and graphed (Fig. 4-2C). As expected, there is a significant stabilization of Ub^{G76V}-GFP in proteasome inhibited cells, as compared to control cells. When autophagy is simultaneously enhanced during proteasome inhibition, there is a significant drop in Ub^{G76V}-GFP signal, as

compared to fed cells. As a measure of specificity, this effect is blocked by inclusion of 3MA. Inhibition of autophagy alone by 3MA in control cells did not have any effect on the accumulation of Ub^{G76V}-GFP, confirming that this substrate is originally tagged for proteasomal and not autophagy degradation (Dantuma et al., 2000). Likewise, starvation alone did not affect the levels of Ub^{G76V}-GFP.

Correlation between Aggresome Formation and Autophagy

In a neuropathy mouse model, PMP22 aggregates correlate with proteasome impairment and the formation of autophagosomes (Fortun et al., 2003; 2005). Thus, we then examined the relationship between the formation of Lc-induced aggresomes and autophagosomes, in the absence of exogenous modulators (starvation or 3MA) (Fig. 4-3). We analyzed SCs subjected to 12h and 16h of proteasome inhibition, which resulted in ~57% and 92% of cells containing aggresomes, respectively. Aggregates in SC are electron dense amorphous inclusions that form near the nucleus, as shown in representative electron-micrographs (Fig. 4-3, arrows). Figure 3A depict a representative aggregate after 12h of proteasome inhibition (arrow) that is surrounded by autophagosomes (narrow arrows) containing multiple membranes, as seen better at higher magnification (Fig. 4-3B). Figure 3C shows a micrograph of a SC after 16h of proteasome inhibition (arrow). Comparing panels A and C, it appears that the size of the inclusion at 16h is bigger; yet, smaller and less organized electron dense material were also detected, indicating the heterogeneity of the aggregates. As a general rule however, more autophagosomes were identified at longer times of proteasome inhibition. Autophagosomes are seen within (narrow arrows) and around (arrowheads) the aggresome (Fig. 4-3C, D) at higher frequency, as compared to the 12h proteasome inhibition (Fig. 4-3A, B).

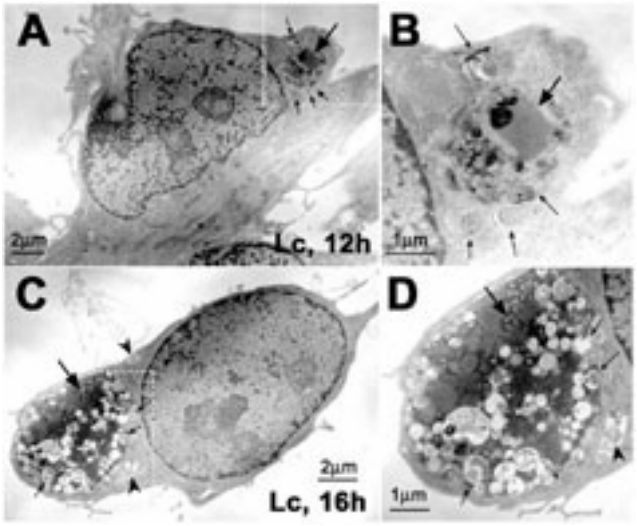

Figure 4-3: Increased autophagosome number and size correlate with aggresome formation. Proteasome inhibited cells (Lc) for 12h (A, B) or 16h (C, D) were processed for electron microscopy. The inclusions formed at the different times are represented by an arrow, and the autophagosomes inside, by thin arrows (A-D). Arrowheads denote autophagic profiles outside the inclusion. B and D are enlargements of A and C, respectively. Scale bars, as indicated.

Table 4-1: Analyses of autophagic markers in proteasome inhibited cells. The fraction of autophagosome (Ap)/cytoplasm volume was calculated as percent in untreated (-) and Lc treated (+) samples (n=8). The levels of LC3 I and II as determined by Western blot of independent treatments (n=5) were quantified and corrected for actin (AU: absorbance units). The values were used to calculate LC3II/I ratio. Data is presented as the mean ± standard deviation (SD).

	(Mean ± SD)			
Lc, 16h	Ap volume (%)	LC3-I/actin (AU)	LC3-II/actin (AU)	Ratio II/I
-	2.43 ± 1.23	226 ± 24.94	69.5 ± 37.85	0.287 ± 0.221
+	16.92 ± 8.84	302.75 ± 23.23	150.5 ± 8.89	0.429 ± 1.385

We then quantified the volume of autophagosomes in relation to the cytoplasmic area, since this is a reliable method to monitor autophagy (Kirkegaard et al., 2004). The volume of autophagosomes is slightly but not significantly increased after 12h of proteasome inhibition (4±3%; p=0.257), compared to control cells. However, this

augment becomes significant after 16h (Table 4-1), when mostly all the cells contain aggresomes, as shown in Figure 4-1.

Autophagosomes mature and fuse with lysosomes to form autolysosomes, where the degradation of the cargo takes place (Klionsky and Emr, 2000). Mature autophagosomes/autolysosomes acquire acid phosphatases (AP) and cathepsins from this fusion event (Kirkegaard et al., 2004). Thus, parallel samples were examined for AP activity to visualized lysosomal vesicles (Fig. 4-4). Lysosomal profiles are detected in electron micrographs of control samples, as revealed by the electron dense products of the AP reaction (Fig. 4-4A). After treatment with Lc, more lysosomes (smaller, round, uniform) and late autophagosomes (larger, less uniform) are noticeable, mainly at perinuclear regions (Fig. 4-4B). Moreover, the volume of some of these lysosomal profiles is higher than in control cells.

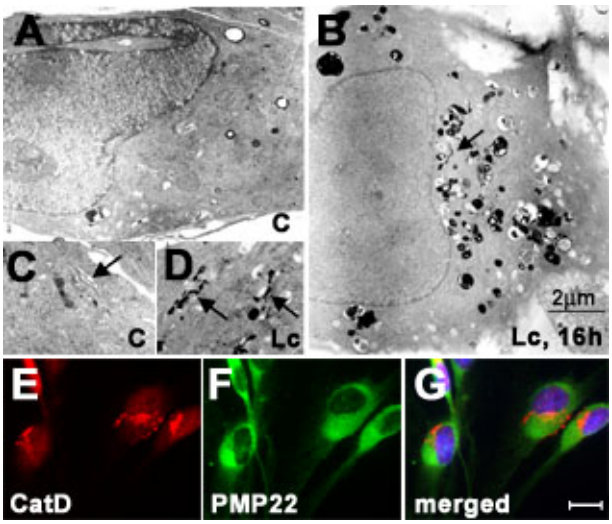

Figure 4-4: Localization of lysosomes upon proteasome inhibition. SCs (A,C) were treated with Lc (B, D-G) for 16h and processed for AP cytochemistry (A-D) or immunostaining (E-G) with anti-cathepsin D (E, G) and PMP22 (F,G) antibodies. Arrows point at Golgi stacks (B, F). Scale bar as indicated (A-D) or 10µm (E-F).

Furthermore, Golgi stacks appears reactive for AP (Fig. 4-4B, arrow). Close examination at the Golgi apparatus (arrows) in control cells does not reveal AP activity (Fig. 4-4C), contrary to Lc-treated samples (Fig. 4-4D), suggesting synthesis and trafficking of AP upon Lc treatment. Moreover, the lysosomal protein cathepsin D (Fig. 4-4E), are found around PMP22 aggregates (Fig. 4-4F), as indicated in the merged images (Fig. 4-4G) of SCs stained after Lc treatment.

Another method to monitor autophagy is the conversion of LC3I to LC3II, which then binds to the autophagosome membrane, a process required for autophagosome formation (Tanida et al., 2004). The induction of aggresomes by pharmacological inhibition of the proteasome results in higher levels of LC3, both I and II forms, when compared to control, as seen in a representative Western blot (Fig. 4-5A, left panel; Table 4-1). Quantification of LC3 levels, after correction for actin, corroborates the significant increase in LC3, both I and II, in proteasome inhibited SC (Fig. 4-5B, n=5; Table 4-1). Indeed, the synthesis of LC3 is necessary for the expansion of the autophagic response (Abeliovich et al., 2004). The above values were used to calculate the ratio of LC3II/I, which is about 2-fold compared to control cells (Table 1; $p=0.05$). Similar results were obtained when using other proteasome inhibitors, specifically epoxomycin and MG132 (not shown). To make sure that increased LC3 ratio was a valid method to monitor autophagy in SCs, independent treatments with rapamycin (Fig. 4-5A, Rp, right panel) or starvation (not shown) were used as controls. The elevated levels of LC3 are also obvious by immunostaining (Fig. 4-5C-F). In control cells, LC3 levels are low and diffuse (Fig. 4C) but increase after 16h of proteasome inhibition (Fig. 4-5D) when the majority of SCs contain PMP22 aggresomes (Fig. 4-5E). A marked LC3 staining in the periphery of

PMP22 aggresomes is noticeable in most cells (Fig. 4-5F, arrow), which likely represent the autophagosomes seen on the electron micrographs (Fig. 4-3).

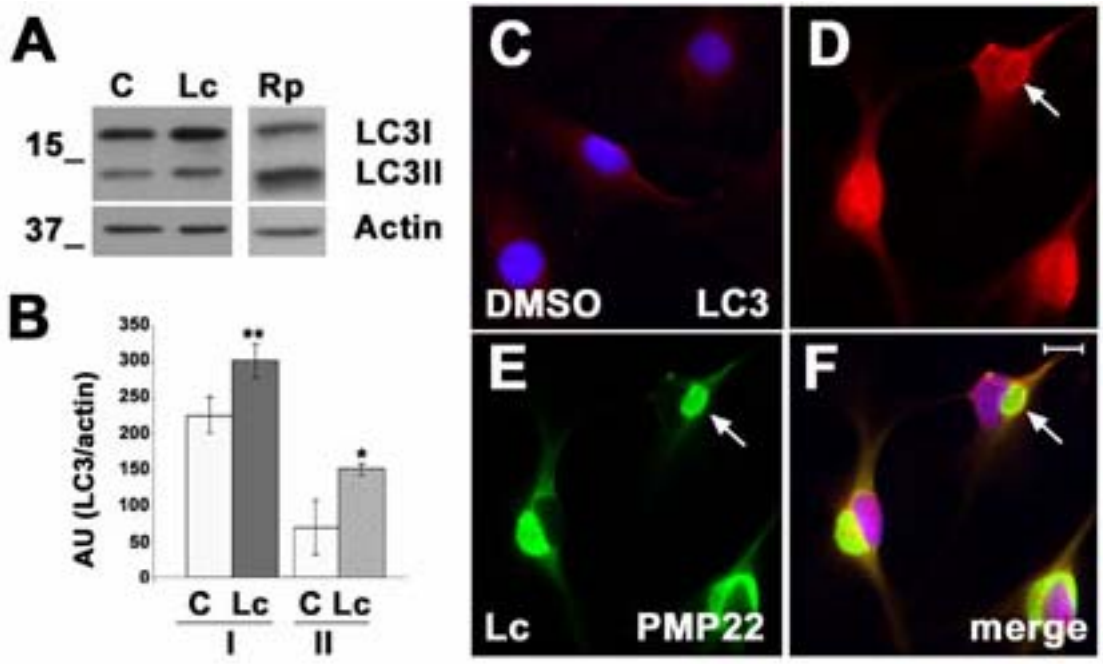

Figure 4-5: Changes in the levels, lipidation and localization of LC3 in aggresome forming cells. The levels of LC3 were determined in DMSO control (C), Lc or rapamycin (Rp) treated cells by Western blot with anti-LC3 antibody (A). Actin is shown as a loading control (A). The levels of LC3I and II, corrected for actin (AU, absorbance units) were quantified (B, n=5; $p<0.05$*; $p<0.005$**). SCs were treated with DMSO (C) or Lc (D-F) and stained for LC3 (C, D, F) or PMP22 (E, F). Arrow exemplifies the relationship between LC3 and PMP22 aggresomes (D-F). Scale bar, 10µm (C-F).

Higher number and volume of autophagosomes and autolysosomes, as well as increased LC3II suggest ongoing autophagy. One mechanism whereby autophagy might be activated upon formation of aggregates is the trapping of the negative regulator of the pathway, mTor, within the inclusion (Ravikumar et al., 2004). In control SCs, mTorP is distributed throughout the cytoplasm and the nucleus (Fig. 4-6A), as expected (Kim and Chen, 2000), without apparent co-localization with PMP22 (Fig. 4-6A, left inset). A

fraction of mTor can be found at the microtubule organizing center, as revealed by its partial co-localization with γ tubulin (Fig. 4-6A, right inset).

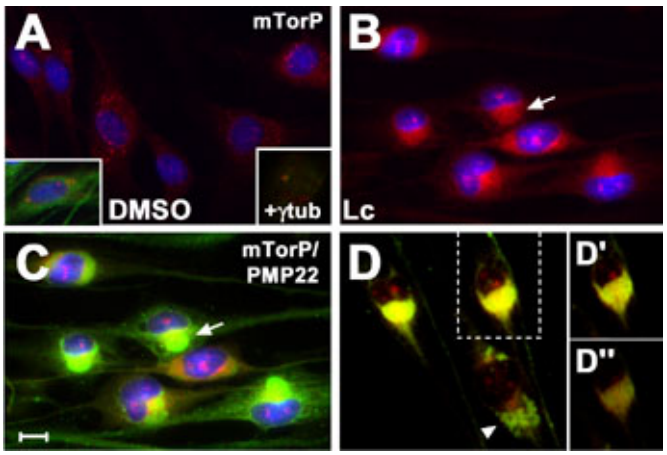

Figure 4-6: mTor is sequestered within PMP22 aggresomes. SCs treated with DMSO (A) or Lc (B-D) were processed for immunostaining with anti-mTorP (A-D) and -PMP22 (A, left inset and C, D) or -γtubulin (A, right inset) antibodies. Scale bar, 10μm (A-C). A representative confocal image of PMP22 and mTorP stained cells is shown (D). The insets represent two planes of the boxed area (D'-D'', top to bottom). The arrow exemplifies the co-localization and the arrowhead denotes the lack of it (B-D).

In proteasome inhibited cells, mTorP levels appear increased at perinuclear regions (Fig. 4-6B), where PMP22 aggresomes form (Fig. 4-6C). The arrow represents an example of the association between an aggresome and mTor (Fig. 4-6B and C). The localization of mTor within PMP22 aggresomes was confirmed by confocal microscopy (Fig. 4-6D). The spatial association of these two proteins within the aggresomes in the boxed cell (Fig. 4-6D) is shown at two different focal planes (Fig. 4-6D'-D''). This pattern differs considerably from LC3 (Fig. 4-5D-F), which is mostly located at the periphery of the aggresomes. In a small percent of cells however, PMP22 aggresomes do not co-localize with mTorP (Fig. 4-6D, arrowhead). Similar results were obtained with an antibody against the non-phosphorylated form of mTor (not shown).

Enhancement of Molecular Chaperones Hinder Aggresome Formation

Because heat shock proteins (HSPs) are known to prevent protein aggregation in other in vitro models (Muchowski and Wacker, 2005) and they are recruited to PMP22 aggresomes (Ryan et al., 2002), we investigated their effect on the formation of aggresomes.

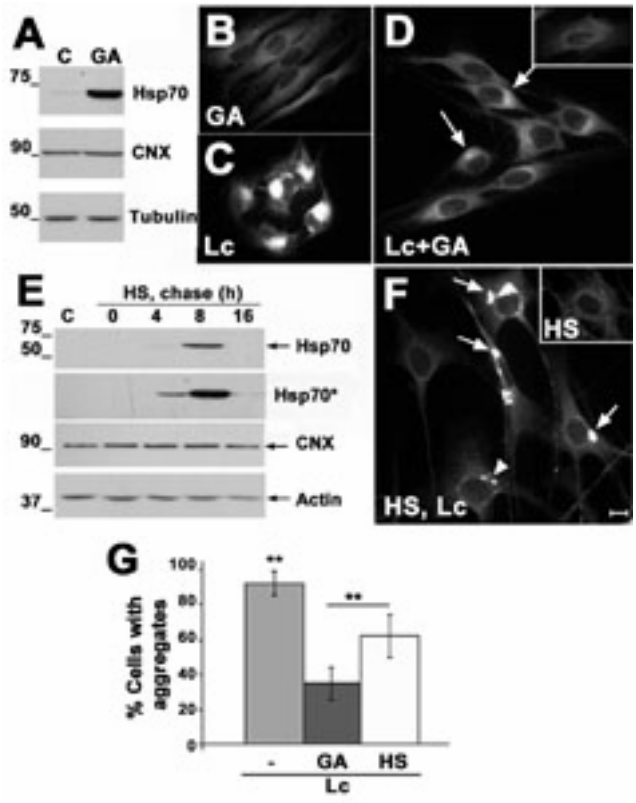

Figure 4-7: Enhancement of HSP expression hinders aggresome formation. Rat SCs were treated for 16h with GA (A, B, D, G), Lc (C, D, F, G), control (A, inset D, E), or subjected to a HS and allowed to recover for the indicated times (E, F, G). The levels of Hsp70, CNX and tubulin were determined by western blot (A, E). Asterisk represents an overexposed blot (Hsp70*). Parallel samples were stained with anti-PMP22 antibody (B-D, F). Arrows point at the Lc-induced aggregates after GA simultaneous treatment (D) or HS (F) preconditioning. Arrowhead indicates a cluster of small aggregates (F). Scale bar, 10μm.The percent of cells with aggregates in Lc-treated cells is significantly higher than cells simultaneously treated with GA or preconditioned with HS (G). Simultaneous GA treatment was more effective than HS in reducing the number of aggregates (G) (**, $p<0.005$).

Two approaches were taken to increase the levels HSPs: treatment with geldanamycin (GA) (McLean et al., 2004) and precondition with heat shock (HS) (Allen et al., 2004) (Fig. 4-7). GA binds to an ATP site on Hsp90 and blocks its interaction with HS transcription factor 1, promoting its activation and the synthesis of HSPs (Muchowski and Wacker, 2005). In SC treated with increasing concentrations of GA (0-2μM) for 16h, the levels of HSPs are progressively increased (not shown). We chose a concentration of 250nM at which, after 16h of treatment, the levels of Hsp70 are increased by ~7-fold, whereas calnexin is not affected (Fig. 4-7A). Furthermore, when SCs are treated with 250nM of GA, no significant cell death, gross morphological changes or alterations in PMP22 levels are observed (Fig. 4-7B). Compared to proteasome inhibition alone (Fig. 4-7C), most SCs do not contain aggregates when GA is included (Fig. 4-7D, arrows) and look similar to control (Fig. 4-1D, inset). The fewer aggregates seen are less defined than the ones formed after proteasome inhibition alone.

As an alternative approach to increase the expression of HSPs, cells were pre-condition with a brief HS (Allen et al., 2004). The time course of Hsp70 expression in SCs at the indicated times after HS was monitored by Western blot (Fig. 4-7E). The levels of Hsp70 in control cells or immediately after HS are nearly undetectable, but increase transiently starting after 4h. The augmentation in the levels of Hsp70 peaks at 8h after HS. At 16h after HS, it is still evident, although to a lesser extent, as indicated on the overexposed blot (Hsp70*). The levels of calnexin (Fig. 4-7E) and other ER chaperones (not shown) appear unaffected. When cells were pre-conditioned with HS and then treated with Lc for 16h (Fig. 4-7F), the formation of aggresomes was reduced, as compared with proteasome inhibition alone. Furthermore, the size of the aggregates

formed (arrows) is reduced ~3-fold when the cells are pre-conditioned with HS (p=8.02E-08). No aggresomes or cell death were seen in cells subjected to HS and allowed to recover for the 16h without proteasome inhibition (Fig. 4-7F, upper inset), similar to control cells (Fig. 4-7D, upper inset).

The influence of GA treatment or HS pre-conditioning on the number of cells with aggregates was determined. Some cells contain a cluster of smaller aggregates (less than 1μm; Fig. 4-7F, arrowhead) and were not included in our quantification. As shown in panel G, aggresome formation is significantly reduced by any of these approaches. Comparing the different methods shown to hinder aggresome formation, stimulation of autophagy by starvation and treatment with GA were equally effective (p=0.8), whereas HS had the mildest effect (p=0.001).

Discussion

Intracellular protein aggregation generally takes place when the quality control mechanisms fail to ensure the folding and/or degradation of a protein (Goldberg, 2003). These aggregates are commonly found in different neurodegenerative diseases and often associate with malfunction of the proteasome (Keller et al., 2000; Waelter et al., 2001; McNaught et al., 2003; Kabashi et al., 2004). PMP22 is a disease-linked, short-lived glycoprotein that accumulates in cytoplasmic aggregates when the proteasome is inhibited or the protein is overexpressed and/or mutated (Notterpek et al., 1999; Ryan et al., 2002; Fortun et al., 2003, 2005). Here we show that in proteasome inhibited SCs, the formation of ubiquitin/PMP22 aggresomes is hindered by enhancement of autophagy or heat shock proteins. In accordance, stimulating autophagy or the expression of molecular chaperones have been independently found to reduce protein aggregation and toxicity in a variety of conditions (Cuervo, 2004; Muchowski and Wacker, 2005).

We previously showed that pre-existing PMP22 aggresomes are removed by an autophagy dependent mechanism (Fortun et al., 2003). Now, we provide evidence for the role of autophagy in the formation of new aggresomes, as well. Enhancement of autophagy hinders the formation of aggresomes upon proteasome inhibition. Correspondingly, blockage of autophagy synergizes with proteasome inhibition, resulting in higher number of cells containing aggresomes. In addition, autophagy enhancement reduces the observed increased in the steady state levels induced by proteasome inhibition. Aggresome assembly is a multi-step process, by which small aggregates throughout the cell are transported along microtubules towards the centrosome, where they stick together and are then enclosed by a vimentin cage (Johnston et al, 1998). It is likely that, upon stimulation of autophagy, the small aggregates are engulfed within autophagosomes, reducing the load of proteins being transported towards the centrosome and therefore, affecting the formation of the final inclusion. In other in vitro models of aggregation-prone proteins, such as α-synuclein, polyalanine and polyglutamine repeats, stimulation of autophagy prevented the accumulation of protein aggregates (Ravikumar et al., 2002; 2004; Rideout et al., 2004). Importantly, enhancement of autophagy protects against neuronal toxicity in a fly model of Huntington disease (Ravikumar et al., 2004). A model has been proposed based on studies with normal α-synuclein and its A53T or A30P mutants whereby, the soluble protein is degraded mainly by the proteasome, whereas the aggregated forms are rerouted to the autophagy-lysosomal pathway for clearance (Tofaris et al., 2001; Webb et al., 2003; Rideout et al., 2004).

In the absence of experimental activation of autophagy, the formation of PMP22 aggresomes correlates with increased number and size of autophagosomes, as well as

higher levels, lipidation and recruitment of LC3 to aggregates, markers commonly used to monitor autophagy (Kirkegaard et al., 2004). Accordingly, autophagosomes have been previously found into or adherent to the surface of unrelated cytoplasmic protein aggregates formed upon proteasome inhibition (Wojcik et al., 1996; Harada et al., 2003; Rideout et al., 2004). Additionally, autophagosome formation and LC3 lipidation have been reported in cells containing ubiquitinated inclusions as a result of oxidative stress (Martinet et al., 2004). In the TrJ neuropathy model, the spontaneous PMP22 aggregates correlate with the presence of autophagosomes (Fortun et al., 2003). Thus, activation of autophagy in cells with inclusions is not unique to proteasome inhibition, but rather a general response of the cell to cellular stress and the formation of cytoplasmic inclusions.

The results outlined above suggest a cellular response by which, autophagy is activated upon degradative failure of the proteasome, likely to keep cellular homeostasis and prevent the accumulation of potentially harmful protein aggregates. Indeed, a relationship between degradation pathways has been reported previously, in which chronic low levels of proteasome inhibition resulted in enhanced macroautophagy (Ding et al., 2003). However, the signal behind this compensation mechanism is uncertain. The formation of protein aggregates could represent this missing link. Recent studies have suggested a mechanism of autophagy activation, based on a depletion of mTor, the negative regulator of autophagy, by trapping within polyglutamine expanded inclusions recent results (Ravikumar et al., 2004). In our model, mTor is also sequestered within PMP22 aggresomes formed upon proteasome inhibition. Although this could explain the initial activation of autophagy, it is unknown how these inclusions are recognized and degraded by the autophagic-lysosomal system? This is an important question that

requires further exploring. Aggresomes are surrounded by a vimentin cage (Johnston et al., 1998; Notterpek et al., 1999), a factor that is poorly studied but might have important consequences aside being a structural constrain. In this regard, previous studies with internalized viral proteins, or microinjected purified proteins, suggested the existence of a sequestration site for protein aggregates in tight association with intermediate filaments at perinuclear regions, as a necessary step preceding autophagy-lysosomal degradation (Earl et al., 1987; Doherty et al., 1987).

A common response to proteasome inhibition and formation of aggresomes is the activation of the heat shock response and expression of molecular chaperones, which may represent an attempt of the cell to refold the inclusions or prevent the addition of new unfolded proteins to it (Muchowski and Wacker, 2005). Proteasome inhibition in SCs results in an augmentation of HSPs levels and their recruitment to PMP22 aggresomes (Ryan et al., 2002). Here we show that the formation of PMP22 aggresomes is hindered by GA treatment or HS preconditioning, likely due to enhancement of cytoplasmic molecular chaperones. In different in vitro models, overexpression of Hsp40 and/or Hsp70 were similarly effective in suppressing the intracellular aggregation of unrelated proteins (Cummings et al., 1998; Stenoien et al., 1999; Dul et al., 2001; Abu-Baker et al., 2003). In our model, GA treatment was more effective than a heat shock pre-conditioning in preventing Lc-induced aggresome formation, likely because of the increased expression of HSPs over time by GA, as compared to the transient effect of HS. Moreover, the aggregates formed when GA is included are less defined than the ones after HS preconditioning (compare 6D and 6F). In previous studies, GA was shown to prevent aggregation of unrelated proteins, including huntingtin and α-synuclein, and

reduced toxicity associated with their expression (Sittler et al., 2001; McLean et al., 2004). The stimulation of a heat shock response and subsequent increased expression of HSPs by GA treatment is dependent on the ability of this benzoquinone ansamycin to bind Hsp90, preventing its physiological function (Kim et al., 1999). The effects of GA on hindering aggresome formation does not correlate with a reduction in the steatdy state levels of ubiquitinated substrates (not shown) suggesting that the action of GA may be based in the physical disassembly of the aggregates by chaperones and/or promoting the trafficking of PMP22 to plasma membrane. Alternatively, the effect of GA may be related to the stabilization of yet unknown factors and their contribution to aggresome formation, given the various Hsp90 substrates and the different processes in which they are involved, such as signal transduction and cell cycle regulation (Neckers, 2002). In any case, the effect of GA does not involve stimulation of autophagy.

Taken together, the data presented suggest that different cellular pathways crosstalk to prevent the accumulation of potential harmful inclusions whereby, if one of the systems (proteasome) is not working properly, is substituted by the analogous function of others (autophagy and/or molecular chaperones).

CHAPTER 5
CONCLUSIONS

Overview of Findings

Mutations in peripheral myelin protein 22 (PMP22) are associated with a variety of demyelinating peripheral neuropathies (Gabreëls-Festen and Wetering, 1999). However, the disease mechanism is not fully understood. For the duplication and point mutation paradigms, impaired intracellular trafficking of PMP22 has been proposed to play a role (Sanders et al., 2001). The results presented in this dissertation suggest that PMP22 aggregation and alterations in protein degradation pathways may also be important factors underlying the pathogenesis of neuropathies associated with duplication of, or point mutations in PMP22.

In normal nerves, the majority of the newly synthesized PMP22 is turned-over by the proteasome (Pareek et al., 1997; Ryan et al., 2002). The results in Chapter 2 indicate that in sciatic nerves of the Trembler J (TrJ) neuropathy mouse, PMP22 is not degraded as quickly as in normal nerves. This reduced turnover rate does not result in increased trafficking to plasma membrane, since the protein does not reach medial Golgi. Notably, cytoplasmic PMP22 aggregates are detected. As indicated in Chapter 3, these aggregates correlate with reduced enzymatic activity of the proteasome, changes in the levels and localization of its components, and accumulation of ubiquitinated substrates, suggestive of proteasome impairment. Similar correlations between formation of aggregates and malfunction of the proteasome have been reported for other disease-linked aggregation

prone proteins (Keller et al., 2000; Waelter et al., 2001; McNaught et al., 2003; Kabashi et al., 2004).

The consequences of the formation of protein aggregates are not well understood, and whether they play a protective or toxic role remains subject of debate (Ciechanover and Brundin, 2003). Generally, cytoplasmic inclusions of ubiquitinated proteins are found at the centrosome, in which case they are usually termed aggresomes (Kopito, 2000). A protective role of aggresomes has been proposed, mainly based on two reasons. First, misfolded and nonfunctional proteins might be concentrated in a central location to increase the efficiency of disposal by the autophagy-lysosomal pathway (Kopito, 2000). Additionally, the segregation of these proteins within the aggresomes likely reduces the threat to cellular homeostasis by limiting abnormal interaction with other cell constituents (Sherman and Goldberg, 2001). In TrJ nerves, the levels and detergent-insolubility of cytoplasmic (but not ER) molecular chaperones, lysosomes and autophagic components are increased, and they are commonly found in the periphery of PMP22 aggregates (Chapter 2). Furthermore, PMP22 aggregates correlate with the presence of autophagosomes in the TrJ SCs, indicative of ongoing autophagy. Enhanced expression of heat shock proteins and formation of autophagosomes could represent a protective response of the cell to fold and degrade, respectively, the aggregated proteins. However, the autophagy and lysosomal systems decline with age and under stress conditions (Cuervo and Dice, 2000; Ward, 2002). Thus, it is possible that these initially protective structures are not cleared efficiently over time, developing into stable aggregates, which in turn could contribute to abnormal SC biology.

A possibility whereby aggresomes could be detrimental for cell biology is through the trapping of essential proteins in non-functional complexes, reducing their availability and functionality (Hernandez et al., 2004). In our model, PMP22 aggregates associate with myelin basic protein (MBP), another myelin component and proteasome substrate (Akaishi et al., 1996). Thus, not only PMP22 is reduced in myelin but also MBP, likely resulting in altered stoichiometry of proteins in the SC membrane, which could further contribute to demyelination (Chapter 3). Additionally, the observed recruitment of components of the ubiquitin-proteasomal pathway to aggregates (Chapter 3) could explain the impaired proteasome activity by nonspecific and nonfunctional trapping within the aggregates, as previously suggested as a general mechanism of proteasome failure (Hernandez et al., 2004). In summary, in the TrJ neuropathy model, PMP22 aggregates are present, which correlate with impaired proteasome activity and the recruitment of essential cellular components.

Using an in vitro system of pharmacological proteasome inhibition, the cellular pathways influencing the formation of PMP22 aggregates and the consequences of their occurrence were examined (Chapter 2 and 4). This approach was taken since aggresomes resemble the PMP22 aggregates detected in the neuropathy model and the observation that proteasome impairment is indeed one of the underlying alterations in the TrJ model (Notterpek et al., 1999; Ryan et al., 2002; Chapter 2 and 3). Cell death was not detected in proteasome inhibited SCs up to 16h, supporting the notion that during its initial stages, aggresomes may be protective. In nonmyelinating SC, enhancement of autophagy prevents the accumulation of PMP22 and ubiquitinated proteins in aggregates, either by hindering their formation and/or aiding their clearance (Chapter 2 and 4). In agreement, a

protective response of autophagy is supported by independent studies based on the overexpression of disease-linked α-synuclein, polyglutamine or polyalanine expanded proteins, in which, the number of inclusions and cellular toxicity were reduced upon pharmacological augmentation of autophagy (Ravikumar et al., 2002; 2004; Rideout et al., 2004). Furthermore, an increase in the number and volume of autophagosomes, as well as lipidation and recruitment of LC3 to aggresomes, are detected after 16h of proteasome inhibition, when nearly all cells contain aggresomes. These results agree with previous studies reporting activation of macroautopahgy as a response of proteasome inhibition and/or overexpression of an aggregation prone protein (Wojcik et al., 1996; Harada et al., 2003; Ding et al., 2003; Rideout et al., 2004). Enhancement of HSPs hindered the accumulation of PMP22 aggregates (Chapter 4), similar to other protein aggregates (Stenoin et al., 1999; Sittler et al., 2001; Dul et al., 2001; McLean et al., 2004).

Taken together, enhancing autophagy and molecular chaperones prevents the accumulation of PMP22 in aggresomes. Moreover, a cross-talk between cellular pathways may exist to ensure the disposal of proteins that do not traffic to their final destination or are not degraded by the proteasome efficiently. Different diseases, known as protein conformational disorders, have as a common theme the accumulation of aggregates that are generally associated with a toxic state (Ciechanover and Brundin, 2003). Therefore, the existence and modulation of intrinsic cellular pathways to prevent toxicity would be useful for the development of therapeutic approaches.

Unresolved Issues and Future Studies

As described in Chapters 2 and 3, the presence of PMP22 aggregates and proteasome impairment are characteristic features of TrJ neuropathy nerves. However, it is important to determine if similar alterations are found in other models of the disease. In our laboratory, preliminary studies with a CMT1A mouse model based on PMP22 overexpression (Huxley et al., 1996) suggest that these results are not specific to the Leu16Pro mutation paradigm, since both neuropathy nerves present common alterations of PMP22 turnover and aggregation. Other animal models, such as the Trembler mouse (Suter et al., 1992b) and the overexpressor rat (Niemann et al., 1999) should also be examined.

Do PMP22 aggregates play an active role in the disease mechanism or are just a feature of these nerves without actual pathology associated to them? This is a complex question, often referred to as "the chicken or the egg" paradigm, not only for PMP22-associated neuropathies but also for a number of diseases linked to the presence of protein aggregates (Ciechanover and Brundin, 2003). Initially, a correlation (or not) of aggregate number and proteasome impairment with markers of neuropathy severity, such as percent of demyelinated fibers, g-ratio, and nerve conduction velocities, could be determined by morphometric and electrophysiological studies, respectively (Gabreels-Festen, 2002; Sereda et al., 2003; Passage et al., 2004). The role of aggregates in the pathogenesis of the disease will be partially supported if the neuropathy is reversed or ameliorated by the removal of aggregates upon activation of autophagy and/or molecular chaperones. Moreover, it will be important to examine how aging influences the formation of aggregates, as well as the response of SCs to their presence. Aging correlates with the progression of the neuropathy (Young and Suter, 2001) and the

impairment of protein degradation pathways (Cuervo and Dice, 2000; Ward, 2002). Preliminary studies from our laboratory indicate that the number of PMP22 aggregates in TrJ nerves increases in older mice, but how this relates to the levels and activity of the degradation pathways have not yet been addressed.

PMP22 aggregates associate with a variety of cellular proteins, but the exact consequences of this are difficult to determine. For example, PMP22 aggregates associate with cytoplasmic molecular chaperones (Chapter 2), which could represent an attempt to (re)fold or to aid degradation, as demonstrated for other protein aggregates (Muchowski and Wacker, 2005). Indeed, the kinetics of association and dissociation of Hsp70 with polyglutamine aggregates is similar to the kinetics reported for the folding of non-aggregated peptides, supporting an active role of molecular chaperones in the breakdown of aggregates (Kim et al., 2002). The subunits of the proteasome also associate with PMP22 aggregates (Chapter 4). Based on the reduced activity of the proteasome, as well as the accumulation of proteasomal substrates, it is feasible to speculate that the proteasome within the aggregates might not be functional. Indeed, it has been shown that the presence of protein aggregates results in failure of the proteasome to degrade unrelated substrates (Bence et al., 2001; Ventrakaman et al., 2004). On the other hand, it has been suggested that the proteasome is actively recruited to sites of aggregation to aid in the removal of protein aggregates (Martin-Aparicio et al., 2001; Puttaparthi et al., 2003). The association/dissociation of the proteasome with intranuclear ataxin-1 inclusions is a dynamic process, as revealed by fluorescence recovery after photobleaching (Stenoien et al., 2002). Using the same technique, it should be determined if this is true for cytoplasmic PMP22 aggregates as well. Additionally, measurement of

the enzymatic activity of the proteasome in a purified population of PMP22 aggresomes could provide clues about the degradative capacity of the proteasomes. However, this is technically challenging, since aggresomes are difficult to solubilize and the detergent concentrations needed inactivate most of the enzymes (Johnston et al., 1998).

In addition to the quality control of newly synthesized proteins, the proteasome is responsible for the degradation of a variety of substrates involved in different cellular functions, including cell cycle, apoptosis, differentiation, transcription regulation, among others (Badano et al., 2005). Thus, it should be examine how the formation of aggregates affects any of these proteasome-mediated events. Moreover, the internalization and further lysosomal degradation of certain membrane proteins is controlled by ubiquitination and therefore, any alterations in this event will lead to altered endocytosis-lysosomal turnover of those proteins (Ciechanover, 2005). Likewise, proteasome activity is required following internalization of another tetraspan membrane protein, connexin 43, before delivery to lysosomes for degradation (Qin et al., 2003). In the TrJ nerves, the lysosomal pathway is altered, and myelin proteins are constantly being delivered to lysosomes for degradation, likely as a result of unstable myelin (Notterpek et al., 1999). Thus, the possibility of demyelination also contributing to the aggregation of myelin constituents needs consideration. Although PMP22 aggregates do not co-localize with transferin receptor-positive vesicles (Chapter 2), other populations of endocytosed vesicles should be examined. At least in vitro, a fraction of PMP22 accumulates in Arf6-recycling vesicles that are not positive for transferin receptor but instead, for PIP_2 and actin (Chies et al., 2002). Furthermore, it remains to be evaluated if other myelin proteins, in addition to myelin basic protein (MBP) (Chapter 3), are recruited to PMP22

aggregates. A good candidate is myelin protein zero (P0), the major protein in peripheral myelin also associated with demyelinating neuropathies, which is known to interact with PMP22 (D'Urso et al., 1999; Hasse et al., 2004).

An interesting possibility based on the results presented in Chapter 4 is that formation of aggresomes results in the activation of macroautophagy to cope with the degradative failure of the proteasome and prevent the abnormal accumulation of its substrates. Because the main signal for macroautophagy activation is deprivation of amino acids, the simplest explanation could be that the available pool of amino acids is reduced due to stalled proteasomal degradation. Additionally, activation of autophagy at the molecular level may be explained based on the trapping of the negative regulator of the pathway, mTor, within PMP22 aggregates, as previously suggested in a model of neurodegeneration associated with polyglutamine expanded proteins (Ravikumar et al., 2004). Although this justifies the initial activation of autophagy as a general response, it does not account for the specific recognition of the aggresome by this system. The signal by which aggresomes are targeted for autophagy-lysosomal degradation is an important issue that requires further investigations. A general understanding of this mechanism will give clues about the relationship between these two protein degradation pathways. In this regard, a possible role of intermediate filaments in the activation of autophagy has been previously suggested (Earl et al., 1987; Doherty et al., 1987). Indeed, the filament network is reorganized after aggresome formation, resulting in a collapse of vimentin around the inclusion; yet, the functionality of this event is still unknown (Johnston et al., 1998; Notterpek et al., 1999). The role of vimentin can be examined using a conditional model in which, the expression of vimentin can be turned off during or after proteasome

inhibition. Assuming aggresomes still form in the absence of vimentin, it could be examined if autophagy is equally activated as a result of its formation and whether autophagy-mediated clearance of aggresomes still occurs in the absence of exogenous stimulation.

The studies presented in Chapter 4 used a proteasome inhibitor to accumulate the endogenous PMP22 in nonmyelinating SCs. However, it is important to examine if autophagy and molecular chaperones could prevent the accumulation of PMP22 aggregates in myelinating SCs, without affecting the stability or integrity of myelin. Myelination can be followed in vitro using a system in which, SCs and dorsal root ganglion (DRG) neurons are co-cultured (Pareek et al., 1997; Notterpek et al., 1999b). In this system, the levels of PMP22 significantly increase during myelination (Pareek et al., 1997; Notterpek et al., 1999b). The SC-DRG co-cultures could be established from TrJ (and other neuropathy mouse models) and for comparison, normal and PMP22-deficient SCs. The experiments will be conducted in the absence of proteasome inhibitors. Preliminary data from our laboratory suggest that spontaneous PMP22 aggregates are present in myelinating SCs from mutant mice. It will be essential to determine whether myelinating SCs are able to remove the aggregates by enhancement of autophagy and molecular chaperones, alone or in combination, and if this correlate with restored myelination. Because prolonged autophagy is also a form of cell death (Cuervo, 2004) it is important to monitor whether this method interferes with normal myelination and axon biology, or promote toxicity. Furthermore, the association of PMP22 aggregates with other myelin proteins, such as P0 and MBP, could also be followed with this approach

(Notterpek et al., 1999b). These studies will lead the way for the development of future therapeutic approaches to be tested in mouse models of the disease.

LIST OF REFERENCES

Abeliovich H, Dunn WAJr, Kim J, Klionsky DJ (2000) Dissection of autophagosome biogenesis into distinct nucleation and expansion steps. J Cell Biol 151:1025-1033.

Abu-Baker A, Messaed C, Laganiere J, Gaspar C, Brais B, Rouleau GA (2003) Involvement of the ubiquitin-proteasome pathway and molecular chaperones in oculopharyngeal muscular dystrophy Hum Mol Genet 12(20):2609-23.

Adlkofer K, Martini R, Aguzzi A, Zielasek J, Toyka KV, Suter U (1995) Hypermyelination and demyelinating peripheral neuropathy in Pmp22- deficient mice. Nat Genet 11:274-280.

Adlkofer K, Naef R, Suter U (1997) Analysis of compound heterozygous mice reveals that the Trembler mutation can behave as a gain-of-function allele. J Neurosci Res 49:671-680.

Akaishi T, Shiomi T, Sawada H., Yokosawa H (1996) Purification and properties of the 26S proteasome from the rat brain: evidence for its degradation of myelin basic protein in a ubiquitin-dependent manner. Brain Res 722:139-44.

Allen TA, Von Kaenel S, Goodrich JA, Kugel JF (2004) The SINE-encoded mouse B2 RNA represses mRNA transcription in response to heat shock. Nat Struct Mol Biol 11(9):816-2.

Aplin A, Jasionowski T, Tuttle DL, Lenk SE, Dunn WA Jr (1992) Cytoskeletal elements are required for the formation and maturation of autophagic vacuoles. J Cell Physiol 152(3):458-66.

Ardley HC, Scott GB, Rose SA, Tan NGS, Markham AF, Robinson PA (2003) Inhibition of proteasomal activity causes inclusion formation in neuronal and non-neuronal cells overexpressing parkin. Mol Biol Cell 14:4541-4556.

Arroyo EJ, Xu YT, Zhou L, Messing A, Peles E, Chiu SY, Scherer SS (1999) Myelinating Schwann cells determine the internodal localization of Kv1.1, Kv1.2, Kvbeta2, and Caspr. J Neurocytol 28(4-5):333-47.

Badano JL, Teslovich TM, Katsanis N (2005) The centrosome in human genetic disease. Nat Rev Genet 6(3):194-205.

Baechner D, Liehr T, Hameister H, Altenberger H, Grehl H, Suter U, Rautenstrauss B (1995) Widespread expression of the peripheral myelin protein-22 gene (PMP22) in neural and non-neural tissues during murine development. J Neurosci Res 42:733-741.

Bence NF, Sampat RM, Kopito RR (2001) Impairment of the ubiquitin-proteasome system by protein aggregation. Science 292:1552-1555.

Berke SJ, Paulson HL (2003) Protein aggregation and the ubiquitin proteasome pathway: gaining the UPPer hand on neurodegeneration.Curr Opin Genet Dev 13(3):253-61.

Boerkoel CF, Takashima H, Garcia CA, Olney RK, Johnson J, Berry K, Russo P, Kennedy S, Teebi AS, Scavina M, Williams LL, Mancias P, Butler IJ, Krajewski K, Shy M, Lupski JR (2002) Charcot-Marie-Tooth disease and related neuropathies: mutation distribution and genotype-phenotype correlation. Ann Neurol. 51(2):190-201.

Bosse F, Zoidl G, Wilms S, Gillen CP, Kuhn HG, Muller HW (1994) Differential expression of two mRNA species indicates a dual function of peripheral myelin protein PMP22 in cell growth and myelination. J Neurosci Res 37:529-537.

Brancolini C, Edomi P, Marzinotto S, Schneider C (2000) Exposure at the cell surface is required for gas3/PMP22 To regulate both cell death and cell spreading: implication for the Charcot-Marie- Tooth type 1A and Dejerine-Sottas diseases. Mol Biol Cell 11:2901-2914.

Carrard G, Bulteau AL, Petropoulos I, Friguet B (2002) Impairment of proteasome structure and function in aging. Int J Biochem Cell Biol 11:1461-74.

Chance PF, Alderson MK, Leppig KA, Lensch MW, Matsunami N, Smith B, Swanson PD, Odelberg SJ, Disteche CM, Bird TD (1993) DNA deletion associated with hereditary neuropathy with liability to pressure palsies. Cell 72(1):143-51.

Chance PF (1999) Overview of hereditary neuropathy with liability to pressure palsies. Ann N Y Acad Sci 883:14-21.

Chies R, Nobbio L, Edomi P, Schenone A, Schneider C, Brancolini C (2003) Alterations in the Arf6-regulated plasma membrane endosomal recycling pathway in cells overexpressing the tetraspan protein Gas3/PMP22. J Cell Sci 116(Pt 6):987-99.

Ciechanover A, Brundin P (2003) The ubiquitin proteasome system in neurodegenerative diseases: sometimes the chicken, sometimes the egg. Neuron 40(2):427-46.

Ciechanover A (2005) Proteolysis: form the lysosome to ubiquitin and the proteasome. Nat Rev Mol Cell Biol 6:79-86.

Colby J, Nicholson R, Dickson KM, Orfali W, Naef R, Suter U, Snipes GJ (2000) PMP22 carrying the trembler or trembler-J mutation is intracellularly retained in myelinating Schwann cells. Neurobiol Dis 7:561-573.

Cuervo AM, Dice JF (2000) Age related decline in chaperone-mediated autophagy. J Biol Chem 275:31505-31513.

Cuervo AM (2004) Autopahagy: in sickness and in health. Trends in Cell Biol 14 (2):70-77.

Cummings CJ, Reinstein E, Sun Y, Antalffy B, Jiang Y, Ciechanover A, Orr HT, Beaudet AL, Zoghbi HY (1998) Chaperone suppression of aggregation altered subcellular proteasome localization implying protein misfolding in SCA1. Nat Genet 19:148-154.

Dantuma N.P, Heessen S, Lindsten K, Jellne M, Masucci MG (2000) Short-lived green fluorescent proteins for quantifying ubiquitin/proteasome-dependent proteolysis in living cells. Nat Biotechnol 18:538-43.

Dejerine J, Sottas J (1893) Sur la nevrite interstitielle hypertrophique et progressive de l'enfance. Comp Rend Soc Biol 45:63-96.

Devaux JJ, Scherer SS (2005) Altered ion channels in an animal model of Charcot-Marie-Tooth disease type IA. J Neurosci 5(6):1470-80.

Deveraux Q, Ustrell V, Pickart C, Rechsteiner M (1994) A 26S protease subunit that binds ubiquitin conjugates. J Biol Chem 269:7059-61.

Ding Q, Dimaguya E, Martin S, Bruce-Keller AJ, Nukula V, Cuervo AM, Keller N (2003) Characterization of chronic low level proteasome inhibition on neuronal homeostasis. J Neurochem 86:489-497.

Dickson KM, Bergeron JJ, Shames I, Colby J, Nguyen DT, Chevet E, Thomas DY, Snipes GJ (2002) Association of calnexin with mutant peripheral myelin protein-22 ex vivo: a basis for "gain-of-function" ER diseases. Proc Natl Acad Sci USA 99(15):9852-7.

Doherty FJ, Wassell JA, Mayer RJ (1987)A putative protein-sequestration site involving intermediate filaments for protein degradation by autophagy. Studies with microinjected purified glycolytic enzymes in 3T3-L1 cells. Biochem J 241(3):793-800.

Dorn BR, Dunn WA Jr, Progulske-Fox A (2001) Porphyromonas gingivalis traffics to autophagosomes in human coronary artery endothelial cells. Infect Immun 69(9):5698-708.

Dul JL, Davis DP, Williamson EK, Stevens FJ, Argon Y (2001) Hsp70 and antifibrillogenic peptides promote the degradation and inhibit intracellular aggregation of amyloidogenic light chains. J Cell Biol 152 (4):705-715.

Dunn Jr WA (1990) Studies on the mechanism of autophagy: formation of the autophagic vacuole. J Cell Biol 110:1923-1933.

D'Urso D, Schmalenbach C, Zoidl G, Prior R, Muller HW (1997) Studies on the effects of altered PMP22 expression during myelination in vitro. J Neurosci Res 48(1):31-42.

D'Urso D, Prior R, Greiner-Petter R, Gabreels-Festen AA, Muller HW (1998) Overloaded endoplasmic reticulum-Golgi compartments, a possible pathomechanism of peripheral neuropathies caused by mutations of the peripheral myelin protein PMP22. J Neurosci 18(2):731-40.

D'Urso D, Ehrhardt P, Muller HW (1999) Peripheral myelin protein 22 and protein zero: a novel association in peripheral nervous system myelin. J Neurosci 19:3396-3403.

Earl RT, Mangiapane EH, Billett EE, Mayer RJ (1987) A putative protein-sequestration site involving intermediate filaments for protein degradation by autophagy. Studies with transplanted Sendai-viral envelope proteins in HTC cells.Biochem J. 1987 Feb 1;241(3):809-15.

Fabbretti E, Edomi P, Brancolini C, Schneider C (1995) Apoptotic phenotype induced by overexpression of wild-type gas3/PMP22: its relation to the demyelinating peripheral neuropathy CMT1A. Genes Dev 9:1846-1856.

Fontanini A, Chies R, Snapp EL, Ferrarini M, Fabrizi GM, Brancolini C (2005) Glycan-independent role of calnexin in the intracellular retention of Charcot-Marie-tooth 1A Gas3/PMP22 mutants. J Biol Chem 280(3):2378-87.

Fortun J, Dunn WA, Jr., Joy S, Li J, Notterpek L (2003) Emerging role for autophagy in the removal of aggresomes in Schwann cells. J Neurosci 23:10672-10680.

Fortun J, Li J, Go J, Fenstermaker A, Fletcher BS, Notterpek L (2005) Impaired proteasome activity and accumulation of ubiquitinated substrates in a hereditary neuropathy model. J Neurochem 92:1531-1541.

Gabreels-Festen A (2002) Dejerine-Sottas syndrome grown to maturity: overview of genetic and morphological heterogeneity and follow-up of 25 patients. J Anat. 200(4):341-56.

Gabreels-Festen A, Bolhuis PA, Hoogendijk JE, Valentijn LJ, Eshuis EJ, Gabreels FJ (1995) Charcot-Marie-Tooth disease type 1A: morphological phenotype of the 17p duplication versus PMP22 point mutations. Acta Neuropathol (Berl) 90 (6):645-9.

Gabreels-Festen A, Wetering RV (1999) Human nerve pathology caused by different mutational mechanisms of the PMP22 gene. Ann NY Acad Sci 883:336-343.

Gabriel JM, Erne B, Pareyson D, Sghirlanzoni A, Taroni F, Steck AJ (1997) Gene dosage effects in hereditary peripheral neuropathy. Expression of peripheral myelin protein 22 in Charcot-Marie-Tooth disease type 1A and hereditary neuropathy with liability to pressure palsies nerve biopsies. Neurology 49:1635-1640.

Garcia CA (1999) A clinical review of Charcot-Marie-Tooth. Ann N Y Acad Sci 883:69-76.

Garcia-Mata R, Gao YS, Sztul E (2002) Hassles with taking out the garbage: aggravating aggresomes. Traffic 3(6):388-96.

Giasson BI, Lee VM (2001) Parkin and the molecular pathways of Parkinson's disease. Neuron 31:885-888.

Goldbaum O, Richter-Landsberg C (2004) Proteolytic stress causes heat shock protein induction, tau ubiquitination, and the recruitment of ubiquitin to tau-positive aggregates in oligodendrocytes in culture. J Neurosci 24(25):5748-57.

Goldberg AL (2003) Protein degradation and protection against misfolded or damaged proteins. Nature 426 (6968):895-9.

Groll M and Clausen T (2003) Molecular shredders: how proteasomes fulfill their role. Curr Opin Struct Biol 13(6):665-73.

Hanemann CO, D'Urso D, Gabreels-Festen AA, Muller HW (2000). Mutation-dependent alteration in cellular distribution of peripheral myelin protein 22 in nerve biopsies from Charcot-Marie-Tooth type 1A. Brain 123 (Pt5): 1001-6.

Haney C, Snipes GJ, Shooter EM, Suter U, Garcia C, Griffin JW, Trapp BD (1996) Ultrastructural distribution of PMP22 in Charcot-Marie-Tooth disease type 1A. J Neuropathol Exp Neurol 55:290-299.

Harada M, Kumemura H, Omary MB, Kawaguchi T, Maeyama N, Hanada S, Taniguchi E, Koga H, Suganuma T, Ueno T, Sata M (2003) Proteasome inhibition induces inclusion bodies associated with intermediate filaments and fragmentation of the Golgi apparatus. Exp Cell Res 288(1):60-9.

Hase A, Yamada H, Arai K, Sunada Y, Shimizu T, Matsumura K (2002) Characterization of parkin in bovine peripheral nerve. Brain Res 930:143-149.

Hasse B, Bosse F, Hanenberg H, Muller HW (2004) Peripheral myelin protein 22 kDa and protein zero: domain specific trans-interactions. Mol Cell Neurosci 27(4):370-8.

Henry EW, Cowen JS, Sidman RL (1983) Comparison of Trembler and Trembler-J mouse phenotypes: varying severity of peripheral hypomyelination. J Neuropathol Exp Neurol 42:688-706.

Henry EW, Sidman RL (1988) Long lives for homozygous trembler mutant mice despite virtual absence of peripheral nerve myelin. Science 241:344-346.

Hernandez F. Diaz-Hernandez M., Avila J. and Lucas J.J. (2004) Testing the ubiquitin-proteasome hypothesis of neurodegeneration in vivo. Trends Neurosci 27:66-68.

Hirata K, Kawabuchi M (2002) Myelin phagocytosis by macrophages and nonmacrophages during Wallerian degeneration. Microsc Res Tech 57(6):541-7.

Hirsch C. and Ploegh H.L. (2000) Intracellular targeting of the proteasome. Trends Cell Biol 10:268-72.

Huxley C, Passage E, Manson A, Putzu G, Figarella-Branger D, Pellissier JF, Fontes M (1996) Construction of a mouse model of Charcot-Marie-Tooth disease type 1A by pronuclear injection of human YAC DNA. Hum Mol Genet 5:563-569.

Huxley C, Passage E, Robertson AM, Youl B, Huston S, Manson A, Saberan-Djoniedi D, Figarella-Branger D, Pellissier JF, Thomas PK, Fontes M (1998) Correlation between varying levels of PMP22 expression and the degree of demyelination and reduction in nerve conduction velocity in transgenic mice. Hum Mol Genet 7(3):449-58.

Ionasescu VV, Searby CC, Ionasescu R, Chatkupt S, Patel N, Koenigsberger R (1997) Dejerine-Sottas neuropathy in mother and son with same point mutation of PMP22 gene. Muscle Nerve 20:97-99.

Isaacs A, Jeans A, Oliver P, Vizor L, Brown S, Hunter A, Davies K (2002) Identification of a new Pmp22 mouse mutant and trafficking analysis of a Pmp22 allelic series suggesting that protein aggregates may be protective in Pmp22-associated peripheral neuropathy. Mol Cell Neurosci 1:114-125.

Johnston JA, Ward CL, Kopito RR (1998) Aggresomes: a cellular response to misfolded proteins. J Cell Biol 143:1883-1898.

Junn E, Lee SS, Suhr UT, Mouradian MM (2002) Parkin accumulation in aggresomes due to proteasome impairment. J Biol Chem 277:47870-47877.

Kabashi E, Agar JN, Taylor DM, Minotti S, Durham HD (2004) Focal dysfunction of the proteasome: a pathogenic factor in a mouse model of amyotrophic lateral sclerosis. J Neurochem 89, 1325-1335.

Keller JN, Hanni KB, Markerbery WR (2000) Impaired proteasome function in Alzheimer's disease. J Neurochem 75:436-439.

Kim HR, Kang HS, Kim HD (1999) Geldanamycin induces heat shock protein expression through activation of HSF1 in K562 erythroleukemic cells. IUBMB Life 48(4):429-33.

Kim JE, Chen J (2000) Cytoplasmic-nuclear shuttling of FKBP12-rapamycin-associated protein is involved in rapamycin-sensitive signaling and translation initiation. Proc Natl Acad Sci USA 97(26):14340-5.

Kim S, Nollen EAA, Kitagawa K, Bindokas VP, Morimoto RI (2002) Polyglutamine aggregates are dynamic. Nat Cell Biol 4:826-831.

Kirkegaard K, Taylor MP, Jackson WT (2004) Cellular autophagy: surrender, avoidance and subversion by microorganisms. Nat Rev 2:301-314.

Kisselev AF, Goldberg AL (1997) Proteasome inhibitors: from research tolls to drug candidates. Chem Biol 8:739-758.

Klionsky DJ, Emr SD (2000) Autophagy as a regulated pathway of cellular degradation. Science 290(5497):1717-21.

Kopito RR (2000) Aggresomes, inclusion bodies and protein aggregation. Trends Cell Biol 10:524-530.

Kopito RR, Ron D (2000) Conformational disease. Nat Cell Biol 2:E207-209.

Laemmli UK (1970) Cleavage of structural proteins during the assembly of the head of bacteriophage T4. Nature 227:680-685.

Lafarga M, Fernandez R, Mayo I, Berciano MT, Castano JG (2002) Proteasome dynamics during cell cycle in rat Schwann cells. Glia 38:313-328.

Lenk SE, Dunn WA Jr, Trausch JS, Ciechanover A, Schwartz AL (1992) Ubiquitin-activating enzyme, E1, is associated with maturation of autophagic vacuoles. J Cell Biol 118(2):301-8.

Lindstein K, Dantuma NP (2003) Monitoring the ubiquitin/proteasome system in conformational diseases. Ageing Res Rev 2(4):433-49.

Liu N, Yamauchi J, Shooter EM. (2004) Recessive, but not dominant, mutations in peripheral myelin protein 22 gene show unique patterns of aggregation and intracellular trafficking. Neurobiol Dis 17(2):300-9.

Lupski JR, de Oca-Luna RM, Slaugenhaupt S, Pentao L, Guzzetta V, Trask BJ, Saucedo-Cardenas O, Barker DF, Killian JM, Garcia CA (1991) Duplication associated with Charcot-Marie-Tooth disease type 1A. Cell 66(2):219-32.

Ma CP, Slaughter CA, DeMartino GN (1992) Identification, purification, and characterization of a protein activator (PA28) of the 20 S proteasome (macropain). J Biol Chem 267:10515-10523.

Maier M, Berger P, Suter U (2002) Understanding Schwann cell-neurone interactions: the key to Charcot-Marie-Tooth disease? J Anat 200(4):357-66.

Martin-Aparicio E, Yamamoto A, Hernandez F, Hen R, Avila J, Lucas JL (2001) Proteasomal-dependent aggregate reversal and absence of cell death in a conditional mouse model of Huntington's disease. J Neurosci 21:8772-8781.

Martinet W, De Bie M, Schrijvers DM, De Meyer GR, Herman AG, Kockx MM (2004) 7-ketocholesterol induces protein ubiquitination, myelin figure formation, and light chain 3 processing in vascular smooth muscle cells. Arterioscler Thromb Vasc Biol 24(12):2296-301.

Matsunami N, Smith B, Ballard L, Lensch MW, Robertson M, Albertsen H, Hanemann CO, Muller HW, Bird TD, White R (1992) Peripheral myelin protein-22 gene maps in the duplication in chromosome 17p11.2 associated with Charcot-Marie-Tooth 1A. Nat Genet 1(3):176-9

Maycox PR, Ortuno D, Burrola P, Kuhn R, Bieri PL, Arrezo JC, Lemke G (1997) A transgenic mouse model for human hereditary neuropathy with liability to pressure palsies. Mol Cell Neurosci 8:405-416.

Mclean PJ, Klucken J, Shin Y, Hyman BT (2004) Geldanamycin induces Hsp70 and prevents α-synuclein aggregation and toxicity in vitro. Biochemical and Biophysical Res Com 321:665-669.

McNaught KSt P, Belizaire R, Isacson O, Jenner P, Olanow CW (2003) Altered proteasome function in sporadic Parkinson's disease. Exp Neurol 179:38-46.

Meekins GD, Emery MJ, Weiss MD (2004) Nerve conduction abnormalities in the trembler-j mouse: a model for Charcot-Marie-Tooth disease type 1A? J Peripher Nerv Syst 9(3):177-82.

Meiners S., Heyken D., Weller A., Ludwing A., Stangl K., Kloetzel P.M. and Kruger E (2003) Inhibition of the proteasome activity induces concerted expression of proteasome genes and de novo formation of mammalian proteasomes. J Biol Chem 278:21517-21525.

Mori F, Hayashi S, Yamagishi S, Yoshimoto M, Yagihashi S, Takahashi H, Wakabayashi K (2002) Pick's disease: alpha- and beta-synuclein-immunoreactive Pick bodies in the dentate gyrus. Acta Neuropathol (Berl) 104:455-461.

Muchowski PJ, Wacker JL (2005) Modulation of neurodegeneration by molecular chaperones.Nat Rev Neurosci 6(1):11-22.

Naef R, Suter U (1998) Many facets of the peripheral myelin protein PMP22 in myelination and disease. Microsc Res Tech 41:359-371.

Naef R, Suter U (1999) Impaired intracellular trafficking is a common disease mechanism of PMP22 point mutations in peripheral neuropathies. Neurobiol Dis 6(1):1-14.

Nandi D, Woodward E, Ginsburg DB, Monaco J (1997) Intermediates in the formation of mouse 20S proteasomes: implications for the assembly of precursors β subunits. Embo J 16:5363-5375.

Navon A, Goldberg AL (2001) Proteins are unfolded on the surface of the ATPase ring before transport into the proteasome. Mol. Cell 8:1339-1349.

Navon R, Seifried B, Gal-On NS, Sadeh M (1996) A new point mutation affecting the fourth transmembrane domain of PMP22 results in severe de novo Charcot-Marie-Tooth disease. Hum Genet 97(5):685-7.

Neckers L (2002) Hsp90 inhibitors as novel cancer chemotherapeutic agents. Trends Mol Med 8(4 Suppl):S55-61.

Niemann S, Sereda MW, Rossner M, Stewart H, Suter U, Meinck HM, Griffiths IR, Nave KA (1999) The "CMT rat": peripheral neuropathy and dysmyelination caused by transgenic overexpression of PMP22. Ann N Y Acad Sci 883:254-61.

Niemann S, Sereda MW, Suter U, Griffiths IR, Nave KA (2000) Uncoupling of myelin assembly and schwann cell differentiation by transgenic overexpression of peripheral myelin protein 22. J Neurosci 20(11):4120-8.

Nishimura T, Yoshikawa H, Fujimura H, Sakoda S, Yanagihara T (1996) Accumulation of peripheral myelin protein 22 in onion bulbs and Schwann cells of biopsied nerves from patients with Charcot-Marie-Tooth disease type1A. Acta Neuropathol 92: 454-460.

Nobbio L, Vigo T, Abbruzzese M, Levi G, Brancolini C, Mantero S, Grandis M, Benedetti L, Mancardi G, Schenone A (2004) Impairment of PMP22 transgenic Schwann cells differentiation in culture: implications for Charcot-Marie-Tooth type 1A disease. Neurobiol Dis 16(1):263-73.

Notterpek L, Shooter EM, Snipes GJ (1997) Upregulation of the endosomal-lysosomal pathway in the trembler-J neuropathy. J Neurosci 17(11):4190-200.

Notterpek L, Ryan MC, Tobler AR, Shooter EM (1999) PMP22 accumulation in aggresomes: implications for CMT1A pathology. Neurobiol Dis 6: 450-460.

Notterpek L, Snipes JG, Shooer EM (1999b) Temporal expression patter of peripheral myelin protein 22 during in vivo and in vitro myelination. Glia 25: 358-369.

Notterpek L, Tolwani RJ (1999) Experimental models of peripheral neuropathies. Lab Anim Sci 49: 588-599.

Notterpek L, Roux KJ, Amici SA, Yazdanpour A, Rahner C, Fletcher BS (2001) Peripheral myelin protein 22 is a constituent of intercellular junctions in epithelia. Proc Natl Acad Sci USA 98:14404-14409.

Ohsumi Y (2001) Molecular dissection of autophagy: two ubiquitin-like systems. Nat Rev Mol Cell Biol 2:211-216.

Pareek S, Notterpek L, Snipes GJ, Naef R, Sossin W, Laliberte J, Iacampo S, Suter U, Shooter EM, Murphy RA (1997) Neurons promote the translocation of peripheral myelin protein 22 into myelin. J Neurosci 17:7754-7762.

Pareyson D, Scaioli V, Taroni F, Botti S, Lorenzetti D, Solari A, Ciano C, Sghirlanzoni A (1996) Phenotypic heterogeneity in hereditary neuropathy with liability to pressure palsies associated with chromosome 17p11.2-12 deletion. Neurology 46:1133-1137.

Parmantier E, Cabon F, Braun C, D'Urso D, Muller HW, Zalc B (1995) Peripheral myelin protein-22 is expressed in rat and mouse brain and spinal cord motoneurons. Eur J Neurosci 7:1080-1088.

Parmantier E, Braun C, Thomas JL, Peyron F, Martinez S, Zalc B (1997) PMP-22 expression in the central nervous system of the embryonic mouse defines potential transverse segments and longitudinal columns. J Comp Neurol 378:159-172.

Passage E, Norreel JC, Noack-Fraissignes P, Sanguedolce V, Pizant J, Thirion X, Robaglia-Schlupp A, Pellissier JF, Fontes M (2004) Ascorbic acid treatment corrects the phenotype of a mouse model of Charcot-Marie-Tooth disease. Nat Med 10:396-401.

Perea J, Robertson A, Tolmachova T, Muddle J, King RH, Ponsford S, Thomas PK, Huxley C (2001) Induced myelination and demyelination in a conditional mouse model of Charcot-Marie-Tooth disease type 1A. Hum Mol Genet. 10(10):1007-18.

Puttaparthi K, Wojcik C, Rajendran B, DeMartino GN, Elliot JL (2003) Aggregate formation in the spinal cord mutant SOD1 transgenic mice is reversible and mediated by proteasome. J Neurochem 87: 851-860.

Qin H, Shao Q, Igdoura SA, Alaoui-Jamali MA, Laird DW (2003)Lysosomal and proteasomal degradation play distinct roles in the life cycle of Cx43 in gap junctional intercellular communication-deficient and -competent breast tumor cells. J Biol Chem 278(32):30005-14.

Ravikumar B, Duden R, Rubinsztein DC (2002) Aggregate-prone proteins with polyglutamine and polyalanine expansions are degraded by autophagy. Hum Mol Genet 11:1107-1117.

Ravikumar B, Vacher C, Berger Z, Davies JE, Luo S, Oroz LG, Scaravilli F, Easton DF, Duden R, O'Kane CJ, Rubinsztein DC (2004) Inhibition of mTOR induces autophagy and reduces toxicity of polyglutamine expansions in fly and mouse models of Huntington disease. Nat Genet 36(6):585-95.

Rideout HJ, Lang-Rollin I, Stefanis L (2004) Involvement of macroautopahgy in the dissolution of neuronal inclusions. Int J Biochem Cell Biol 36(12):2551-62.

Robertson AM, King RH, Muddle JR, Thomas PK (1997) Abnormal Schwann cell/axon interactions in the Trembler-J mouse. J Anat 190:423-32.

Robertson AM, Perea J, McGuigan A, King RH, Muddle JR, Gabreels-Festen AA, Thomas PK, Huxley C (2002) Comparison of a new pmp22 transgenic mouse line with other mouse models and human patients with CMT1A. J Anat 200(4):377-90.

Roux KJ, Amici SA, Notterpek L (2004) The temporospatial expression of peripheral myelin protein 22 at the developing blood-nerve and blood-brain barriers. J Comp Neurol 474:578-588.

Ryan MC, Shooter EM, Notterpek L (2002) Aggresome formation in neuropathy models based on peripheral myelin protein 22 mutations. Neurobiol Dis 10:109-118.

Sancho S, Magyar JP, Aguzzi A, Suter U (1999) Distal axonopathy in peripheral nerves of PMP22-mutant mice. Brain 122 (Pt 8):1563-77.

Sanders CR, Ismail-Beigi F, McEnery MW (2001) Mutations of peripheral myelin protein 22 result in defective trafficking through mechanisms which may be common to diseases involving tetraspan membrane proteins. Biochemistry 40:9453-9459.

Schmidt T, Lindenberg KS, Krebs A, Schols L, Laccone F, Herms J, Rechsteiner M, Riess O, Landwehrmeyer GB (2002) Protein surveillance machinery in brains with spinocerebellar ataxia type 3: redistribution and differential recruitment of 26S proteasome subunits and chaperones to neuronal inclusions. Ann Neurol 51:302-310.

Sereda M, Griffiths I, Puhlhofer A, Stewart H, Rossner MJ, Zimmerman F, Magyar JP, Schneider A, Hund E, Meinck HM, Suter U, Nave KA (1996) A transgenic rat model of Charcot-Marie-Tooth disease. Neuron 16:1049-1060.

Sereda MW, Meyer zu Horste G, Suter U, Uzma N, Nave KA (2003) Therapeutic administration of progesterone antagonist in a model of Charcot-Marie-Tooth disease (CMT-1A). Nat Med 9:1533-1537.

Sherman MY, Goldberg AL (2001) Cellular defenses against unfolded proteins: a cell biologist thinks about neurodegenerative diseases. Neuron 29:15-32.

Sittler A, Lurz R, Lueder G, Priller J, Hayer-Hartl MK, Hartl FU, Lehrach H, Wanker EE (2001) Geldanamycin activates a heat shock response and inhibits huntingtin aggregation in a cell culture model of Huntington's disease. Hum Mol Gen 10(12):1307-1315.

Snipes GJ, Suter U, Welcher AA, Shooter EM (1992) Characterization of a novel peripheral nervous system myelin protein (PMP-22/SR13). J Cell Biol 117:225-238.

Snipes GJ, Orfali W, Fraser A, Dickson K, Colby J (1999) The anatomy and cell biology of peripheral myelin protein-22. Ann N Y Acad Sci 883:143-51.

Stefanis L, Larsen KE, Rideout HJ, Sulzer D, Greene LA (2001) Expression of A53T mutant but not wild-type alpha-synuclein in PC12 cells induces alterations of the ubiquitin-dependent degradation system, loss of dopamine release, and autophagic cell death. J Neurosci 21(24):9549-60.

Stenoien DL, Cummings CJ, Adams HP, Mancini MG, Patel K, DeMartino GN, Marcelli M, Weigel NL, Mancini MA (1999) Polyglutamine-expanded androgen receptors form aggregates that sequester heat shock proteins, proteasome components and SRC-1, and are suppressed by the HDJ-2 chaperone. Hum Mol Genet 8(5):731-41.

Stenoien DL, Mielke M, Mancini MA (2002) Intranuclear ataxin1 inclusions contain both fast- and slow-exchanging components. Nat Cell Biol 4(10):806-10.

Suter U, Moskow JJ, Welcher AA, Snipes GJ, Kosaras B, Sidman RL, Buchberg AM, Shooter EM (1992a) A leucine-to-proline mutation in the putative first transmembrane domain of the 22-kDa peripheral myelin protein in the trembler-J mouse. Proc Natl Acad Sci U S A 89:4382-4386.

Suter U, Welcher AA, Ozcelik T, Snipes GJ, Kosaras B, Francke U, Billings-Gagliardi S, Sidman RL, Shooter EM (1992b). Trembler mouse carries a point mutation in a myelin gene. Nature 356:241-244.

Suter U, Snipes GJ (1995) Peripheral myelin protein 22: facts and hypotheses. J Neurosci Res 40:145-151.

Tanaka K, Suzuki T, Chiba T, Shimura H, Hattori N, Mizuno Y (2001) Parkin is linked to the ubiquitin pathway. J Mol Med 79:482-494.

Tanaka M, Kim YM, Lee G, Junn E, Iwatsubo T, Mouradian MM (2004) Aggresomes formed by alpha-synuclein and synphilin-1 are cytoprotective. J Biol Chem 279(6):4625-31.

Tanida I, Ueno T, Kominami E (2004) LC3 conjugation system un mammalian autophagy Int J Biochem Cell Biol 36:2503-2518.

Taylor JP, Tanaka F, Robitschek J, Sandoval CM, Taye A, Markovic-Plese S, Fischbeck KH (2003) Aggresomes protect cells by enhancing the degradation of toxic polyglutamine-containing protein. Hum Mol Genet 12(7):749-57.

Timmerman V, Nelis E, Van Hul W, Nieuwenhuijsen BW, Chen KL, Wang S, Ben Othman K, Cullen B, Leach RJ, Hanemann CO (1992) The peripheral myelin protein gene PMP-22 is contained within the Charcot-Marie-Tooth disease type 1A duplication. Nat Genet 1(3):171-5.

Tobler AR, Notterpek L, Naef R, Taylor V, Suter U, Shooter EM (1999) Transport of Trembler-J mutant peripheral myelin protein 22 is blocked in the intermediate compartment and affects the transport of the wild- type protein by direct interaction. J Neurosci 19:2027-2036.

Tobler AR, Liu N, Mueller L, Shooter EM (2002) Differential aggregation of the Trembler and Trembler J mutants of peripheral myelin protein 22. Proc Natl Acad Sci USA 99:483-488.

Tofaris GK, Layfield R, Spillantini MG (2001) alpha-synuclein metabolism and aggregation is linked to ubiquitin-independent degradation by the proteasome. FEBS Lett 509(1):22-6.

Tyson J, Ellis D, Fairbrother U, King RH, Muntoni F, Jacobs J, Malcolm S, Harding AE, Thomas PK (1997) Hereditary demyelinating neuropathy of infancy. A genetically complex syndrome. Brain 120 (Pt 1):47-63.

Valentijn LJ, Baas F, Wolterman RA, Hoogendijk JE, van den Bosch NH, Zorn I, Gabreels-Festen AW, de Visser M, Bolhuis PA (1992b) Identical point mutations of PMP-22 in Trembler-J mouse and Charcot-Marie-Tooth disease type 1A. Nat Genet 2:288-291.

Valentijn LJ, Bolhuis PA, Zorn I, Hoogendijk JE, van den Bosch N, Hensels GW, Stanton VP Jr, Housman DE, Fischbeck KH, Ross DA (1992a) The peripheral myelin gene PMP-22/GAS-3 is duplicated in Charcot-Marie-Tooth disease type 1A. Nat Genet 1(3):166-70.

Varus- Barriere C, Wong K, Weibel TD, Abu-Asab M, Weiss MD, Kaneski CR, Mixon TH, Bonavita S, Creveaux I, Heiss JD, Tsokos M, Goldin E, Quarles RH, Boespflug-Tanguy O, Schiffmann R (2003) Insertion of mutant proteolipid protein results in missorting of myelin proteins. Ann Neurol 54(6):769-80.

Venkatraman P, Wetzel R, Tanaka M, Nukina N, Goldberg AL (2004) Eukaryotic proteasomes cannot digest polyglutamine sequences and release them during degradation of polyglutamine-containing proteins. Mol Cell 14(1):95-104.

Waelter S, Boeddrich A, Lurz R, Scherzinger E, Lueder G, Lehrach H, Wanker EE (2001) Accumulation of mutant huntingtin fragments in aggresome-like inclusion bodies as a result of insufficient protein degradation. Mol Biol Cell 12:1393-1407.

Wang K, Spector A (2000) α-Crystallin prevents irreversible protein denaturation and acts cooperatively with other heat shock proteins to renature the stabilized partially denatured protein in an ATP-dependent manner. Eur J Biochem 267:4705-4712.

Ward WF (2002) Protein degradation in the aging organism. Prog Mol Subcell Biol 29:35-42.

Webb JL, Ravikumar B, Atkins J, Skepper JN, Rubinsztein DC (2003) Alpha-Synuclein is degraded by both autophagy and the proteasome. J Biol Chem 278(27):25009-13.

Wigley WC, Fabunmi RP, Lee MG, Marino CR, Muallem S, DeMartino GN, Thomas PJ (1999) Dynamic association of proteasomal machinery with the centrosome. J Cell Biol 145:481-490.

Wojcik C, Scroeter D, Wilk S, Lamprecht J, Paweletz N (1996) Ubiquitin-mediated proteolysis centers in Hela cells: indication from studies of an inhibitor of the chymotrypsin-like activity of the proteasome. European J Cell Biol 71: 311-3187.

Yamada K, Sato J, Oku H, Katakai K (2003) Conformation of the transmembrane domains of peripheral myelin protein 22. Part I. Solution-phase synthesis and circular dichroism study of protected 17-resideu partial peptides in the first putative transmembrane domain. J Peptide Res 62: 78-87.

Yewdell JW (2001) Not such a dismal science: the economics of protein synthesis, folding, degradation and antigen processing. Trends Cell Biol 11(7):294-7.

Young P, Suter U (2001) Disease mechanisms and potential therapeutic strategies in Charcot- Marie-Tooth disease. Brain Res Brain Res Rev 36:213-221.

Zhang F, Su K, Yang X, Bowe DB, Paterson AJ, Kudlow JE (2004) O-GlcNAc modification is an endogenous inhibitor of the proteasome. Cell 115(6):715-25.

Zhou H, Cao F, Wang Z, Yu ZX, Nguyen HP, Evans J, Li SH, Li XJ (2003) Huntingtin forms toxic NH2-terminal fragment complexes that are promoted by the age-dependent decrease in proteasome activity. J Cell Biol 163:109-118.

Zoidl G, Blass-Kampmann S, D'Urso D, Schmalenbach C, Muller HW (1995) Retroviral-mediated gene transfer of the peripheral myelin protein PMP22 in Schwann cells: modulation of cell growth. Embo J 14:1122-1128.

Zoidl G, D'Urso D, Blass-Kampmann S, Schmalenbach C, Kuhn R, Muller HW (1997) Influence of elevated expression of rat wild-type PMP22 and its mutant PMP22Trembler on cell growth of NIH3T3 fibroblasts. Cell Tissue Res 287:459-470.

BIOGRAPHICAL SKETCH

Jenny Fortun was born in Cuba in 1973. She is the daughter of Osmaida Fernandez and Raul Fortun, and she has one brother, Waldo Perez. She earned a Bachelor in Science, in biochemistry, from the University of Havana, Cuba. Jenny conducted her thesis at the Center for Genetic Engineering and Biotechnology in Cuba. After graduation, she continued working for 2 years at the University of Havana. During the next seven months, she worked at the Swiss Federal Institute of Technology in Zurich as an exchange fellow. Following her arrival to the United States, she started her doctorate studies in the College of Medicine at the University of Florida in 2000, and joined the laboratory of Dr. Lucia Notterpek a year later.